

Modeling and Management of Migratory Shorebird Habitat in
Northern Brazil using Remote Sensing

By

Daniel Macy Merchant

A dissertation submitted to the
School of Graduate Studies
Rutgers, The State University of New Jersey

In Partial fulfillment of the requirements
For the degree of
Doctor of Philosophy
Graduate Program in Ecology and Evolution

Written under the direction of

Richard G. Lathrop Jr.

And approved by

New Brunswick, New Jersey

May, 2021

ABSTRACT OF THE DISSERTATION

Modeling and Management of Migratory Shorebird Habitat in Northern Brazil using Remote Sensing

by Daniel Macy Merchant

Dissertation Director:

Richard G. Lathrop Jr.

Migratory shorebirds utilize the intertidal zone as key foraging habitat throughout the Western Americas Flyway, from stopover locations like Delaware Bay in the United States, to overwintering locations like the Gulf Coast, Bahia Lomas in Chile, and the states of Pará and Maranhão on the northern coast of Brazil. Northern Brazil serves as a critical stopover and overwintering location for a number of migratory shorebirds. Characterizing, modeling, and managing the intertidal habitat in northern Brazil is critical for conserving this ecosystem crucial to the Western Americas Flyway. In Chapter 1, intertidal habitat is characterized by evaluating the relationship between the remote sensing metrics of Landsat 8 optical reflectance, Sentinel 1 radar backscatter, and intertidal sediment conditions in northern Brazil and Bahia Lomas, Chile. Consistent patterns are found within each site, indicating that remote sensing effectively characterizes sediment, but the patterns are unique to each location, and distinct from previous research. In Chapter 2, remote sensing, landscape, and climatic metrics are utilized in Maxent distribution models of eight shorebird species of conservation interest. Resulting models effectively distinguished between presence and absence validation data, even though some

models did not have high values of internal model function. Remote sensing metrics contributed significantly to model performance, with models' responses reflecting the relationships between remote sensing and sediment size determined in Chapter 1 and known ecology of each shorebird species. Landscape metrics also contributed significantly, though interpreting how the metric response related to shorebird ecology was less clear. Climatic variables contributed significantly, but their relevance to the underlying biological processes was suspect, considering the equatorial nature of northern Brazil. Finally, in Chapter 3, the models developed in Chapter 2 were applied to a case study of three different conservation prioritization strategies: umbrella species, flagship species, and biodiversity. Semipalmated sandpipers were used as the umbrella species, red knots as the flagship, and areas with high shorebird species richness as biodiversity. The umbrella approach cast the widest net, and protected very species rich habitat, the biodiversity protected similarly rich habitat, but under a much narrower range, and the flagship species protected the least species rich areas, though with greater species richness than the landscape or areas currently protected. Both umbrella and biodiversity approaches did not cover a significant portion of the rarer, red knot habitat. A final hybrid approach, using both biodiversity and flagship species approaches, was proposed to protect both species diversity, and the rarer species of concern. Three areas outside of current protections were identified as potential hot spots for conservation prioritization using the different management regimes, Baía do Cumã, and Baía de São José, and an area west of Extractive Reserve Cururuçu.

ACKNOWLEDGMENTS

Thank you to my wife, Emily Merchant, and our daughter Olivia, as well as my parents and family for their continued support

Without the help, mentorship, and comradery of Jim “Jimbo” Trimble and John “Bigfoot” Bognar, this dissertation would literally have not been possible.

Everyone who, despite some setbacks, kept the field work afloat in Brazil and Chile, including Carlos David Santos, Danielle Paludo, Humphrey Sitters, Joseph Smith, Amanda Dey, Stephanie Feigin, and more.

My graduate committee who provided excellent feedback for improving the manuscript, including Joanna Burger, Julie Lockwood, Larry Niles, and of course, my advisor Richard G. Lathrop Jr.

Several colleagues who have acted as guides, mentors, and sounding boards over the years including Ed Green and Ruth Howison.

This work was funded through a Neotropical Migratory Bird Conservation Act IMPACT Program Grant: F15AP00964, administered by the US. Fish & Wildlife Service.

TABLE OF CONTENTS

ABSTRACT	ii
ACKNOWLEDGEMENTS.....	iv
TABLE OF CONTENTS	v
LIST OF TABLES	vii
LIST OF ILLUSTRATIONS.....	viii
INTRODUCTION	1
CHAPTER 1: REMOTE SENSING OF INTERTIDAL SEDIMENT	6
1.1 INTRODUCTION.....	6
1.2 METHODS	9
1.2a <i>Field data collection</i>	9
1.2b <i>Reflectance data acquisition/preparation</i>	10
1.2c <i>Surface roughness data acquisition/preparation</i>	11
1.2d <i>Intertidal mask</i>	12
1.2e <i>Pixel analysis</i>	12
1.2f <i>Cross-Tidal transects</i>	13
1.2g <i>Intertidal land cover classification</i>	14
1.3 RESULTS.....	15
1.4 DISCUSSION.....	17
1.5 CONCLUSIONS	26
1.6 TABLES AND FIGURES	27
CHAPTER 2: DISTRIBUTION MODELING OF INTERTIDAL SHOREBIRD HABITAT	43
2.1 INTRODUCTION.....	43
2.2 METHODS	47
2.2a <i>Survey methods</i>	47

2.2b Climatic variables	47
2.2c Remote sensing variables	48
2.2d Landscape metrics	49
2.2e Isolating intertidal zone.....	51
2.2f Species distribution modeling	52
2.3 RESULTS.....	55
2.4 DISCUSSION.....	56
2.5 CONCLUSIONS	64
2.6 TABLES AND FIGURES	65
CHAPTER 3: MULTISPECIES CONSERVATION DECISION MAKING.....	78
3.1 INTRODUCTION.....	78
3.2 METHODS	81
3.2a Maxent modeling and thresholding	81
3.2d Comparing conservation strategies.....	83
3.2e Identifying new conservation zones	83
3.3 RESULTS.....	84
3.4 DISCUSSION.....	88
3.5 CONCLUSIONS	95
3.6 TABLES AND FIGURES	96
CONCLUSIONS.....	119
APPENDICES	122
A.1 HOW TO USE MAXENT IN AMAREL	122
REFERENCES	123

LIST OF TABLES

1.1 – ERROR MATRIX, INTERTIDAL COVERAGE IN NORTHERN BRAZIL.....	30
1.2 – TUKEY HSD COMPARING REMOTE SENSING OF MUD, MIXED, AND SAND.....	33
1.3 – WELCH’S T-TEST OF SAND VALUES, NORMALIZED BETWEEN STUDY SITES	36
1.4 – WELCH’S T-TEST OF MUD VALUES, NORMALIZED BETWEEN STUDY SITES	39
1.5 – ERROR MATRIX, INTERTIDAL SEDIMENT SIZE END MEMBERS, BRAZIL	39
1.6 – ERROR MATRIX, INTERTIDAL SEDIMENT SIZE ALL CLASSES, BRAZIL	41
1.7 – ERROR MATRIX, INTERTIDAL SEDIMENT SIZE END MEMBERS, BAHIA LOMAS	41
1.8 – ERROR MATRIX, INTERTIDAL SEDIMENT SIZE ALL CLASSES, BAHIA LOMAS	42
2.1 – LIST OF EIGHT SHOREBIRD SPECIES CONSIDERED	65
2.2 – AUC SCORES AND VALIDATION RESULTS OF ALL MODELS.....	69
2.3A – TOP FOUR VARIABLES, LS ONLY, RS ONLY MODELS.....	70
2.3B – TOP FOUR VARIABLES, WC ONLY, LS AND RS MODELS	71
2.3C – TOP FOUR VARIABLES, LS AND WC, RS AND WC, ALL VARIABLE MODELS	72
3.1 – HABITAT RELATIVE TO MERS FOR ALL MANAGEMENT SCENARIOS	97
3.2 – OVERLAP OF MODELING APPROACH OUTPUTS	98
3.3 – RED KNOT HABITAT PROTECTED UNDER MANAGEMENT SCENARIOS	98
3.4 – SPECIES RICHNESS ACROSS LANDSCAPE, LS AND RS MODELS	102
3.5 – SPECIES RICHNESS ACROSS LANDSCAPE, LS RS AND WC MODELS.....	103
3.6 – COMMON SPECIES ASSEMBLAGES, LS AND RS MODELS	106
3.7 – COMMON SPECIES ASSEMBLAGES, LS RS AND WC MODELS.....	108
3.8 – COMPARISON OF POTENTIAL CONSERVATION ZONES	113
3.9 – PERCENT OF CONSERVATION ZONES DELINEATED BY MANAGEMENT SCENARIOS ..	114
3.10 – SPECIES CO-OCCURRENCE MATRIX BASED ON IN-SITU SURVEYS	114
3.11 – PRESENCE RECORDS ASSOCIATED WITH MANGROVES OR CRABS	115
3.12 – SPECIES RICHNESS OF HYBRID CONSERVATION APPROACH.....	117

LIST OF ILLUSTRATIONS

1.1 - REFERENCE MAP FOR NORTHERN BRAZIL AND BAHIA LOMAS	27
1.2 – SURVEY PLOTS AND THE INTERTIDAL ZONE	27
1.3 – REFERENCE PICTURES OF MUD IN BAHIA LOMAS AND BRAZIL	28
1.4 – REFERENCE PICTURES OF SAND IN BAHIA LOMAS AND BRAZIL	29
1.5 – DIAGRAM OF CROSS-TIDAL TRANSECTS	30
1.6 – REFERENCE PICTURES OF MUD IN BAHIA LOMAS AND BRAZIL	31
1.7 – REFERENCE PICTURES OF MUD IN BAHIA LOMAS AND BRAZIL	32
1.8 – BOX-PLOTS OF NORMALIZED REMOTE SENSING OF MUD IN BOTH SITES	34
1.9 – BOX-PLOTS OF NORMALIZED REMOTE SENSING OF SAND IN BOTH SITES	35
1.10 – SPECTRAL RESPONSE OF CROSS-TIDAL TRANSECTS.....	37
1.11 – SPECTRAL FEATURE PLOTS FOR BRAZILIAN STUDY SITE	38
1.12 – SPECTRAL FEATURE PLOTS FOR BAHIA LOMAS STUDY SITE	40
2.1 – NORTHERN COAST OF BRAZIL STUDY AREA.....	61
2.2 – SURVEY DESIGN	67
2.3 – SAMPLE AREA SHOWING LANDSCAPE METRICS	68
2.4 – BOX-PLOTS COMPARING PRESENCE AND ABSENCE VALIDATION POINTS	73
2.5 – MODEL RESPONSE OF SELECT REMOTE SENSING VARIABLES	74
2.6 – MODEL RESPONSE OF SELECT LANDSCAPE VARIABLES.....	75
2.7 – MODEL RESPONSE OF SELECT CLIMATIC VARIABLES	76
2.8 – STUDY SITE WITH LATITUDE LINES DENOTED	77
3.1 – MAP OF 12 EXTRACTIVE RESERVES ACROSS BRAZILIAN STUDY SITE	96
3.2 – OVERLAPPING MANAGEMENT COVERAGE, LSRS MODELS	99
3.3 – OVERLAPPING MANAGEMENT COVERAGE, LSRSWC MODELS.....	100
3.4 – SPECIES RICHNESS ACROSS TOTAL STUDY AREA.....	101
3.5 – PERCENT OF RICHNESS PROTECTED – LSRS MODELS	104
3.6 – PERCENT OF RICHNESS PROTECTED – LSRSWC MODELS.....	105
3.7 – POTENTIAL CONSERVATION ZONE - BAÍA DO CUMÃ.....	110
3.8 – POTENTIAL CONSERVATION ZONE - BAÍA DE SÃO JOSÉ	111
3.9 – POTENTIAL CONSERVATION ZONE – RESEX CURURUPU	112
3.10 – EXTENT OF FLAGSHIP HABITAT PROTECTED BY CONSERVATION ZONES	116
3.11 – HYBRID CONSERVATION APPROACH WITHIN CONSERVATION ZONES	118

Introduction

Climate change, sea level rise (Galbraith et al. 2002, Iwamura et al. 2013, Galbraith et al. 2014), and coastal development (Murray et al. 2015) are dramatically changing coastal ecosystems worldwide. Migratory shorebirds travel annually from their summer breeding grounds in the high Arctic, stopping at coastal staging grounds along the way, to southern overwintering habitat, and returning northward the following year (Colwell 2010, Niles et al. 2010, Gratto-Trevor et al. 2012). Due to their reliance on numerous cross-continental breeding, stopover, and overwintering locations, shorebirds are particularly vulnerable to coastal ecosystem changes as disruptions at any migratory location can affect migratory and breeding success (Piersma and Lindstrom 2004, Mizrahi et al. 2012). This vulnerability means that shorebird populations can serve as an indicator species for coastal systems, with declining population numbers indicating serious damage or disruption to one or more of the stopover locations along the flyway (Piersma and Lindstrom 2004). Such was the case in the early 1990s with the rapid decline of the Red Knot (*Calidris canutus rufa*) across the Western Atlantic Flyway, whose decline pointed to the previously unrecognized overharvest of horseshoe crabs in Delaware Bay, USA (Baker et al. 2004). Unfortunately, red knots are not the only species indicating an issue; Semipalmated Sandpipers (*Calidris pusilla*) (Morrison et al. 2012), Black-bellied (Gray) Plovers (*Pluvialis squatarola*), and Ruddy Turnstones (*Arenaria interpres*) populations are all in decline (Andres et al. 2012a). Affected populations are found globally, across the Asian-Australasian flyway (Clemens et al. 2016), flyways in Europe (Stroud et al. 2004) and in North America (Bart et al. 2007, Morrison et al. 2012).

One major overwintering and stopover location in the Western Americas Flyway is the northern coast of Brazil, along the states of Pará and Maranhão (Niles and Cooper Ornithological Society 2008, Colwell 2010, Figure 1.1). This region encompasses two Ramsar sites: the Maraja archipelago at the mouth of the Amazon river; and, the Reentrancias Maranhenses. Both sites

consist of “complex estuarine system[s] of extensive islands, bays, coves, and rugged coastline covered mainly by mangrove forest.” The Reentrancias Maranhenses, located to the northwest of Sao Luis, is a complex series of bays and inlets, critically important for migratory shorebirds, fish, manatee, and the fishermen that subsist within the region (Ramsar Convention, <https://www.ramsar.org/wetland/brazil>). Across this region are a number of coastal protected areas, called Marine Extractive Reserves (MER), managed by the Brazilian federal conservation organization, the Chico Mendes Institute for Biological Diversity Conservation (ICMBio). MERs are structured in a bottom-up fashion, with regulations on use and extraction coming from local communities (De Moura et al. 2009). While these areas do encompass important shorebird foraging habitat, they are designed and managed for protecting the livelihoods of local artisanal fishermen, not migratory shorebirds (Santos and Schiavetti 2014). Accurately and logically predicting how migratory shorebirds are distributed across the Pará-Maranhão ecosystem is essential to understanding the effects of current management practices, identifying gaps in those practices, and making future shorebird conservation decisions in the region.

Migratory shorebirds, such as red knots, utilize the intertidal zone as key foraging habitat throughout the Western Americas Flyway, from stopover locations like Delaware Bay in the United States, to overwintering locations like the Gulf Coast, Bahia Lomas in Chile, and the states of Pará and Maranhão on the northern coast of Brazil (Niles and Cooper Ornithological Society 2008). The intertidal zone, or region exposed at low tide and inundated at high tide, is one of the habitats driving these processes due to the high productivity of macrophytobenthos (MacIntyre et al 1996) and benthic invertebrates (Herman et al. 1999) found within the sediments. Sediment size across intertidal flats significantly influences a variety of ecological processes. Primary productivity is typically found to be higher in mud (smaller grain sized) sediment than in sand (Nybakken and Bertness 2005, Dube 2012). Invertebrate species distributions are also influenced by sediment size, with sand and mud both hosting different, thriving communities (Sheaves et al 2016). The distribution of intertidal-feeding birds is

determined, in part, by the distribution of the benthic invertebrates they prey upon, and in turn, sediment grain size that these invertebrates occupy (Colwell and Landrum 1993, Erwin 1996). Characterizing, modeling, and managing the intertidal habitat in northern Brazil is critical for conserving this ecosystem crucial to the Western Americas Flyway.

Characterizing broad regions of the temporally specific intertidal zone, like the intertidal habitat across northern Brazil, is a daunting prospect. Remote sensing and geographic information systems (GIS) are used to analyze massive areas of land, making them ideal tools for such a task. There has been significant work using remote sensing to evaluate intertidal sediment across specific flats or bays of relatively small geographic area, identifying significant relationships between remote sensing metrics like multispectral reflectance or radar backscatter and intertidal sediment size (Yates et al. 1993, Rainey et al. 2003, Van der Wal et al 2005, Van der Wal and Herman 2007, Gade et al. 2014). Recently, there have also been advances in mapping the intertidal zone using multispectral reflectance, proving highly useful for understanding both the extent of the intertidal zone, and trends of gains and losses at continental (Murray et al. 2012, 2014, 2015) or even global scales (Murray et al. 2019). However, there has not been much work bridging both broad scale mapping and finer scale sediment size characterization.

This dissertation aims to understand the remote sensing of the intertidal zone in northern Brazil, leverage those remote sensing metrics to model intertidal shorebird habitat, and use that information to inform management and conservation decision making in northern Brazil. In Chapter 1, I start by characterizing intertidal habitat on a broad scale, by using remote sensing metrics, including Landsat 8 multispectral reflectance and Sentinel 1 radar backscatter. Two locations are compared, northern Brazil, and Bahia Lomas, Chile, another important shorebird location in the Western Americas Flyway. Understanding the patterns of remote sensing data and sediment types at these sites is a critical step for informing shorebird conservation, local management (such as the Marine Extractive Reserves found in northern Brazil), understanding habitat use of other intertidal species, and understanding how these regions can change over time.

In this chapter, two research questions were posed: (1) multispectral reflectance and SAR backscatter can be used to discriminate between mud and sand intertidal sediment types; and, (2) the relationship between multispectral reflectance, SAR backscatter, and sediment type is applicable across a span of geographic locations. Then, I applied our findings about these questions to classifying the intertidal land cover in northern Brazil using conventional unsupervised classification techniques and evaluated the accuracy and efficacy of using discrete classifications to characterize the intertidal zone.

All intertidal habitat is not made equal, certainly in the eyes of migratory shorebirds (Colwell and Landrum 1993, Burger et al. 1997, Bocher et al. 2014, Burger et al. 2018). Understanding not only the extent and composition of intertidal habitat, but also where in that habitat shorebirds are more likely to occur is a crucial step towards the ecological understanding of shorebirds in northern Brazil, and their management. One of the major drivers of shorebird distributions is intertidal sediment size (Bocher et al. 2014), which, as demonstrated in Chapter 1, strongly influences the response of remote sensing platforms. Also demonstrated in Chapter 1 is the difficulty in discretely classifying the mud-sand continuum. With those results in mind, one goal of Chapter 2 is to evaluate the effectiveness of remote sensing values as proxies for intertidal sediment composition in intertidal shorebird habitat modeling. The major objective of Chapter 2 is to develop species distribution models for the intertidal foraging habitat of eight migratory shorebird species that occupy the Pará-Maranhão coastline as either a migratory stopover location, or for the duration of the winter. Using the Maxent modeling package (Phillips et al. 2004), the relationship between remote sensing metrics and sediment established in Chapter 1, as well as relevant landscape and climate metrics, species distribution models are parameterized using shorebird presence data collected during two field seasons in northern Brazil (Winter 2016 and 2017). The efficacy of species distribution models based on remote sensing values, as well as the statistical and biological significance of the different classes of model variables (landscape,

remote sensing, and climatic) were evaluated, with the goal of informing future foraging habitat models and subsequent management.

In the third and final chapter, shorebird species models vetted in Chapter 2 are used in evaluating three different approaches to conservation decision making, to answer the question “how does changing your conservation lens change your conservation decision making?” I considered three different lenses: the single species “umbrella” and “flagship” approaches, and a “biodiversity” centric approach. Single species approaches focus on management planning around a single species whose range encompasses other species of conservation concern. These “umbrella species” are typically wide ranging, occupying broad and diverse habitats such that their protective “shadow” encompasses a variety of tangentially protected species (Shrader-Frechette and McCoy 1993, Wilcove 1993, Simberloff 1998). A “flagship species” approach utilizes a particularly charismatic species to cast this protective “shadow”. The species, often one of great conservation concern on its own, is used for its capacity to muster both stakeholder and regulatory support to protect both the flagship species, and those that fall under its shadow (Caro and O’Doherty 1999). Finally, prioritizing areas with the highest biodiversity has been proposed as the most resource efficient way of protecting biologically rich and important regions (Myers et al. 2000, Meir et al. 2004). I utilized the wide-ranging and numerous semipalmated sandpiper as an umbrella species, a species of international conservation concern such as the red knot as a flagship species, and distributions of eight shorebirds as a metric of shorebird biodiversity. Using the distribution models from Chapter 2, I evaluated the extent and composition of current protections in northern Brazil based on these three management scenarios. Finally, I identified three regions currently not under those protections that may be of conservation concern.

CHAPTER 1: REMOTE SENSING OF INTERTIDAL SEDIMENT

1.1 - Introduction

Nearshore intertidal regions are dynamic ecosystems that support an exceptional abundance and diversity of life (MEA 2005). These areas also play a significant role in a variety of economic and ecological processes from coastal protection (Bouma et al 2014), to nurseries for pelagic fish (MEA 2005), to foraging habitat for migratory wading birds (Colwell 2010). The intertidal zone, or region exposed at low tide and inundated at high tide, is one of the habitats driving these processes due to the high productivity of macrophytobenthos (MacIntyre et al 1996) and benthic invertebrates (Herman et al 1999) found within the sediments. Sediment size across intertidal flats significantly influences a variety of ecological processes. Primary productivity is typically found to be higher in mud (smaller grain sized) sediment than in sand (Nybakken and Bertness 2005). Invertebrate species distributions are also influenced by sediment size, with sand and mud both hosting different, thriving communities (Sheaves et al 2016). The distribution of intertidal-feeding birds is determined by the distribution of the benthic invertebrates they prey upon, and in turn, sediment grain size that these invertebrates occupy (Colwell and Landrum 1993, Erwin 1996). The intertidal zone is key foraging habitat for migratory shorebirds, such as Red Knots (*Calidris canutus*) throughout the Atlantic Americas Flyway, from stopover locations like Delaware Bay in the United States, to overwintering locations like the Gulf Coast, Bahia Lomas in Chile, and the states of Pará and Maranhão on the northern coast of Brazil (Niles and Cooper Ornithological Society 2008). Modeling and mapping the intertidal zone and different classes of sediment grain size at these locations is critical to understanding and managing this important ecosystem.

Remote sensing has been demonstrated as a highly effective tool for assessing habitat and protected regions across broad, landscape scales (Nagendra et al. 2013). Understanding how remote sensing can be used to discriminate between intertidal habitat, and if that discrimination is universal between geographic locations, is an important step towards mapping and managing

shorebird habitat across flyways. Several approaches have been used to map the intertidal zone and to characterize sediment type using a variety of remote sensing platforms and analytical methods. Murray et al (2012, 2014, 2015) developed an effective method of isolating the intertidal zone across continental scale regions using Landsat multispectral remote sensing data, Normalized Difference Water Index, and differencing between high-tide and low-tide images. While extremely successful at designating the binary extent of intertidal regions, these methods do not classify the intertidal zone into different sediment grain size classes. Research elsewhere has demonstrated the feasibility of remotely sensed discrimination of general sediment size classes. In western England, optical and shortwave infrared reflectance data collected using airborne sensing platforms were classified by establishing spectral-end members of mud and sand, using linear mixture modelling to distinguish along the mud-sand gradient (Rainey et al 2003). Landsat 5 satellite imagery was analyzed using both regression-based and spectral mixture methods to determine sediment size in east England (Yates et al 1993). Both of these studies, and multispectral remote sensing of the intertidal zone in general (van der Wal and Herman 2007), relied on the low spectral reflectance of mud in the green and near infrared spectrum relative to sand, typically due to higher moisture and organic matter retention that increases absorption of these wavelengths.

Microwave synthetic aperture radar (SAR) backscattering can be affected by both surface roughness and the dielectric properties of the soil due to the soil moisture retention (Jensen 2007). Typically, rough surface textures will have higher returns than smooth surfaces and very moist surfaces will have higher returns than dry surfaces (Jensen 2007). As such, microwave backscatter has been successfully used to classify mud and sand composition. Van der Wal et al (2005) correlated low backscatter from the ERS-1 and ERS-2 C-Band SAR satellite sensors with smoother surface textures and higher proportions of mud, while higher backscatter was associated with larger sediment sizes and rougher surface texture. Gade et al. (2014) had similar conclusions using a combination of satellite platforms operating with a number of different radar

bands (L, C, and X bands from ALOS PALSAR, ERS SAR, Radarsat-2 and ENVISAT ASAR, and TerraSAR-X, respectively). In both of these studies, the authors suggested that soil moisture content was consistently high across the study sites, making surface roughness the primary predictor of sediment size. Finally, a fusion of image data from multiple platforms has also been used, combining the strengths of both optical/shortwave infrared's response to moisture content and SAR's response to surface roughness to successfully model sediment size using regression analysis (van der Wal and Herman 2007). In all of the studies, using multispectral, radar data, or both, locations were focused on specific flats, estuaries, or coastlines, limiting the patterns observed to the specific regions examined.

Recent field work in two distinct intertidal regions (Figure 1.1), the northern coast of Brazil between Pará and Maranhão, and Bahia Lomas, Chile, in the Strait of Magellan, provides a unique opportunity for insights into the nuances of modeling intertidal habitat via remote sensing. These two locations are important wintering sites for migratory shorebirds along the Atlantic-Americas Flyway (Colwell 2010). As part of an effort to better understand the flyway and its migrants, several shorebird and shorebird habitat surveys have been conducted recently; two in Brazil (2016 and 2017) and one Bahia Lomas (2018). Northern Brazil currently has twelve Marine Extractive Reserves (MERs) distributed along its coastline that encompass intertidal habitat. MERs are not created with shorebirds in mind, rather, they are designed and managed for protecting local artisanal fisheries by excluding highly disruptive extractive practices like dredging, mining, and industrial fishing (Santos and Schiavetti 2014). Understanding the patterns of remote sensing data and sediment types at these sites is a critical step for informing shorebird conservation, local management, understanding habitat use of other intertidal species, and understanding how these regions can change over time. In this chapter, two research predictions were evaluated:

- (1) multispectral reflectance and SAR backscatter can be used to discriminate between mud and sand intertidal types; and,

(2) the relationship between multispectral reflectance, SAR backscatter, and sediment type is applicable across a span of geographic locations.

Then, I applied the findings about these predictions to classifying the intertidal land cover in northern Brazil using conventional unsupervised classification techniques and evaluated the accuracy and efficacy of using discrete classifications to characterize the intertidal zone.

1.2 - Methods

1.2a - Field Data Collection

Qualitative habitat observations were collected during point counts of wading shorebirds in the winter of 2016 and 2017 in northern Brazil, and a similar survey was conducted in January 2018 in Bahia Lomas (Figure 1.1). The surveys consisted of 250 meter fixed radius plots spaced along walking transects. Teams of surveyors would walk 500 meters, pause, record all birds across the intertidal area within a 250 meter radius of themselves, then walk another 500 meters and repeat the process. 700 survey points in Brazil and 200 points in Bahia Lomas were collected along walking transects with center points recorded using GPS units. Qualitative habitat observations were recorded for each point, focusing on the predominant sediment composition within the 250-meter radius plot including the approximate sediment size class, color, and firmness. Sediment type was distinguished into three classes from fine to coarse texture (i.e., mud/clay/silt, mixed/loam, sand) based on tactile observations using the “texture by feel” approach (Thien 1979). A more rigorous determination of sediment composition using laboratory analytical techniques was not feasible due to the remote field setting and the lack of access to laboratory facilities or the ability to transport sediment samples. In some situations where physical access to the sediment was not possible, visual observations were taken (i.e., from a small boat < 10 m from shore). We complemented our sediment classification with observations on the surface from: 1) presence of fiddler crab colonies, which roughen surface textures while making their burrows; and 2) ripples in the sediment surface. Finally, pictures were taken at most

sites and surrounding landscape from the central point of each survey plot (Figures 1.3 and 1.4). These pictures were used, in conjunction with field notes, in classifying the dominant sediment type of each survey point. Transect length and duration was determined largely by accessibility and tidal conditions during survey periods. From these notes, 632 points in Brazil, and 180 points in Bahia Lomas had sufficient qualitative habitat data to be classified into the one of three habitat types: mud, mixed, and sand. Circular vectors with 250-meter radii were generated for each survey point and used to extract the mean of the remote sensing data within the survey region.

1.2b - Reflectance data acquisition/preparation

Landsat 8 Surface Reflectance Code (LaSRC) imagery products were acquired from the USGS archive (<http://earthexplorer.usgs.gov/>) for the entirety of the study areas. LaSRC imagery, produced by the USGS are processed to account for atmospheric interference due to scattering or absorption, resulting in normalized surface reflectance values for each image. Due to the equatorial location of the Brazilian study site a large number of available images had significant cloud cover (> 40%), severely limiting image choice. As such, no preference was given to date or time of year for each image, only for cloud percentage and tidal stage. To compensate, multiple high tide and low tide images for each scene were acquired, totaling in 20 high tide and 27 low tide images from 2013 to 2018 for Brazil. Clouds and cloud shadows were removed using the Landsat 8 surface reflectance values and top-of-atmosphere thermal data via the methods outlined by Martinuzzi et al (2007). In short, thresholds were used to create cloud cover masks, which were shifted and expanded to cover corresponding shadows. The clouds and shadows were masked by the combined cloud and shifted-expanded shadow rasters. For each scene, the cloud/shadow masked images were composited by filling in cloud/shadow gaps of one image, with the cloud/shadow free regions of the other images. Pixels that were cloud or cloud shadows in all available imagery were coded as NA. Composite images were created for each

scene in the Brazilian study region, then mosaicked together, to create a site-wide image for both high tide and low tide imagery for subsequent analysis.

The Bahia Lomas study area proved much less troublesome being both smaller in size, encompassed by one Landsat Scene, and cloud cover was much less problematic, with one cloud free high tide (2017) and one cloud free low tide (2016) image acquired for the study region.

For all images, tidal stage was determined by the methods outlined by Murray et al. (2012), using Oregon State University's Tidal Model (Egbert and Erofeeva 2002), the date and time of each image's acquisition, and a user established reference point for each scene. The Oregon State University Tidal Model is a generalized inverse model of barotropic ocean tides, with versions designed at both global and select regional scales (<http://volkov.oce.orst.edu/tides/>). One of the regions with specifically calibrated tidal model was the Amazonian drainage basin, where the Brazil study is located. A second tidal model had been calibrated by OSU for the Patagonian Shelf where the Bahia Lomas study is located.

1.2c - Surface roughness data acquisition/preparation

Low tide vertical-vertical (VV) and vertical-horizontal (VH) images from the SENTINEL-1 C-SAR Level-1 Ground Range Detected products (<https://sentinels.copernicus.eu/web/sentinel/home>) by the European Space agency, accessed via Copernicus Open Access Hub (<https://scihub.copernicus.eu/dhus/#/home>) were acquired for the two study sites. SENTINEL-1 captures the "C band" portion of the electromagnetic spectrum in the microwave range of frequencies, ranging from 4.0 to 8.0 gigahertz and wavelengths of 3.9 to 7.5 cm (Jensen 2007). Tidal stage was determined using the same methods outlined above, with three images acquired per scene, totaling in 15 images for Brazil and 3 for Bahia Lomas. A 3x3 mean filter was used for noise reduction and then images were coarsened to 30-meter pixels to match the resolution of the Landsat data. For each scene, the mean pixel value of the three processed images was used to account for minor variations in tidal stage, georegistered to the

Landsat 8 data, then mosaicked together resulting in a low tide vertical-vertical image and vertical-horizontal image for the study region.

1.2d - Intertidal Mask

While surveys were conducted to a maximum of 250-meters, significant portions of the survey region were often not intertidal habitat, e.g. water, sand dunes, or mangroves. To solve this issue an intertidal zone-only mask was developed for both locations using methods outlined by Murray et al. (2012). A Normalized Difference Water Index ($NDWI = (Green - Near\ Infrared) / (Green + Near\ Infrared)$) was calculated using the mosaicked imagery, enhancing the presence of surface water. Water tends to have higher reflectance in the Green Wavelengths than in the Near Infrared; on land this is often reversed. Where water is present, the difference between Green and Near Infrared will be positive. A threshold was determined by visual inspection to designate all NDWI values above the threshold as water, all values below the threshold as land, for both high tide and low tide images. The high tide classified land image was then differenced from low tide land image, isolating the intertidal zone (Figure 1.2). This binary intertidal zone was used to mask the stacked images comprised of the cloud free Landsat 8 surface reflectance and smoothed Sentinel 1 backscatter data for subsequent analysis at both locations. To assess the accuracy of the intertidal isolation process, 174 random points were generated across the Brazilian study region and assigned to either “intertidal” or “other” land cover classes based on visual interpretation of all low tide Landsat and Sentinel 1 imagery.

1.2e - Pixel Analysis

The mean pixel value for each band within the intertidal zone was calculated for each plot using the intertidal-masked remote sensing data, the 250 meter radii vectors, and ArcGIS's Spatial Analyst, Zonal Statistics to Table tool. These means were compared via Tukey HSD tests to evaluate whether the habitat classes (mud, mixed, and sand) were significantly different at both

study sites. To compare the classes between locations, (e.g. Sand in Brazil vs Bahia Lomas), the mean pixel values were normalized as a percentage of the mean of the band values of that study site (e.g. (Mean Near IR pixel for plot [i] in Brazil/(Mean of all Brazil's Near IR plots)), resulting in values that essentially represent the relative reflectance values rather than absolute reflectance. Absolute reflectance values can be different based on sensor characteristics (i.e. sensor azimuth) between dramatically different latitudes (Jensen 2007), so relative reflectance more accurately captures the different patterns between locations. Statistics and relevant figures were produced with (R Core Team 2013), Rstudio software, and the ggplot2 package (Wickham 2016).

1.2f - Cross-Tidal Transects

Sediment moisture and surface structure are the dominant physical characteristics that drive spectral and radar responses (Jensen 2007). However, understanding which is playing a greater role can be challenging. To understand the relationship between moisture content and remote sensing response, spectral profiles of transects across the intertidal area and adjacent dunes were digitized across the Brazilian study site. Eight randomly selected sand plots and eight randomly selected mud plots had transects digitized going from high tide to low tide lines within the intertidal area. Eight random dunes directly adjacent to sand plots had transects digitized extending from the high tide line back inland, ending where the land cover clearly changed from sand dunes to something else, typically some kind of vegetation, as determined by visual interpretation. Theoretically, with surface texture remaining relatively consistent by staying within a single land cover class (sand vs mud), changes in spectral response would only be due to changes in moisture content: more moisture when moving from high tide, seaward to low tide lines; less moisture moving from high tide inland over dunes. Transects consisted of points 30 meters apart where remote sensing data was extracted, starting at the high tide line and ending at either the low tide line, or upland vegetation (Figure 1.5). These transects were done only at the Brazilian study site, because there were clear stretches of intertidal zone that could be classified

as entirely sand or mud, unlike Bahia Lomas, which is a single vast flat of heterogeneous patches of mud, mixed, and sand sediments.

1.2g - Classification

The Landsat 8 and Sentinel intertidal imagery for the Brazilian study site was classified using Erdas Imagine's unsupervised classification and cluster busting via isodata clustering across feature space. Ten initial classes were identified and calibrated by using 60% of the qualitative survey data and spectral feature plots, with the remaining 40% ($n = 245$) of survey data reserved for validation. The classification process was also effective at removing the remaining cloud shadow artifacts missed by the cloud removal process. Five classes were initially designated, Mud, Sandy Mud, Muddy Sand, Wet Sand, and Dry Sand, corresponding to the sediment size continuum outlined by Folk (1954) and reflected in the spectral feature plots of both optical and radar data (Figure 1.12). End members, mud and sand, were respectively found at the low and high end of the spectral feature spaces. These five classes were eventually collapsed into Mud, Mixed, and Sand due to the limited nature of the qualitative field data. To validate the accuracy of the classification results, the reserved 40% of survey points ($n = 245$) were overlaid on top of the classified raster. Within each survey points' 250 meter radius, the dominant classified land cover class was determined using zonal statistics (the "classified" class), and compared to the dominant land cover class determined by field notes and photographs (the "reference" class).

Inside vs Outside Marine Extractive Reserves

To evaluate extent and composition of intertidal habitat inside and outside the Marine Extractive Reserves in Brazil, a simple mask was used. A vector consisting of the boundaries of all Marine Extractive Reserves within the study area (provided by ICMBio) was used to mask the respective raster files, with pixel counts converted into area.

1.3 - Results

Field Observations

Mud in both locations (Figure 1.3) were typified by pocked surface textures, and dark gray to dark tan coloring. Unique to Bahia Lomas was the dried mud, with large plates or flakes and a brighter or lighter appearance (Figure 1.3). Sand sediment exhibited a wide range of colors across Brazil, ranging from a yellow-orange to light gray. Sand in Bahia Lomas was typically much darker and more consistent in appearance, though both locations often had a rippled or washboard-like surface (Figure 1.4).

Intertidal Delineation

Approximately 2005 square kilometers of intertidal zone was delineated across the Brazilian study region. The intertidal classification was found to a user's accuracy of 98.8%, producer's of 65.1%, overall of 73% (Table 1.1). Marine Extractive Reserves encompassed approximately 563 square kilometers, or 28% of the total Brazilian intertidal zone.

Pixel Analysis

Within Locations (Between classes)

Significant differences ($p < 0.05$) were found between Sand and Mud plots within the respective study sites, based on Tukey's HSD test of mean reflectance and backscatter values between sites (Table 1.2). In Brazil, all bands demonstrated significant differences between Mud and Sand classes (Figure 1.6 and Table 1.2). Similar patterns were observed in Bahia Lomas, with the exception of the Coastal/Aerosol Band from Landsat 8 (Figure 1.7 and Table 1.2). Depending on the location, some bands did not have significant differences between mixed and one of the two extremes (Brazil: Short-wave Infrared 2 and Vertical-Vertical for Mud-Mixed, Vertical-Horizontal for Sand-Mixed; Bahia Lomas: Coastal/Aerosol for Mud-Mixed, Coastal/Aerosol, Green, Vertical-Horizontal, and Vertical-Vertical for Sand-Mixed). Overall, as sediment size

increased in Brazil (mud to sand habitat), reflectance increased (Figure 1.5 and Table 1.2); as sediment size increased in Bahia Lomas (mud to sand habitat), reflectance decreased (Figure 1.6 and Table 1.2). Backscatter responds to sediment size more consistently, decreasing as sediment size increases in both study locations.

Between Locations (Within Classes)

Based on normalized remote sensing data, the reflectance of mud (Figure 1.8) and sand (Figure 1.9) classes for all Landsat 8 bands were significantly different between Brazil and Bahia Lomas ($p < 0.05$, Table 1.3). This was not the case with Sentinel 1 backscatter data, with sand's Vertical-Vertical not being significantly different between locations ($p > 0.05$), and mud not being significantly different for both Vertical-Vertical and Vertical-Horizontal (Table, 1.3).

Cross-Tidal Transects

Spectral profiles of tidal transects showed significant relationships between distance from high tide line and spectral response for most bands across Mud and Sand intertidal transects (Figure 1.10). In most bands and for dunes, sand, and mud, remote sensing values decreased the farther away from the high tide line and into the intertidal zone the transect went.

Coastal/Aerosol, Blue, and both radar bands, though not statistically significant, followed the same trend for Sand. Dune transects also had the same significant relationships for most bands, excluding Coastal/Aerosol and both radar bands, but typically weaker responses than Sand and Mud transects. The exceptions to this pattern were with the vertical-horizontal backscatter (no trend) and vertical-vertical backscatter (increasing) responses in Sand.

Discrete Classification

Unsupervised cluster-busting of the Brazilian intertidal zone, guided by spectral feature plots (Figure 1.11), resulted in 5 initial classes, which were recoded into mud, mixed, and sand to

reflect available ground data (i.e. mud to mud; wet and dry sand to sand; muddy sand and sandy mud to mixed). Of the area delineated by the intertidal mask, 26% was classified as mud, 64% as mixed, and 10% as sand. Marine Extractive Reserves did not have significantly preferential coverage of any of the three land cover types, with coverage reflecting relative proportions similar to the whole intertidal area (Table 1.8). Accuracy of the three classes was less than ideal, with sand and mud having reasonably high user's accuracy (100% and 65.38% respectively), mixed having moderate producer's accuracy (67.57%), and an overall accuracy of 36.73% (Table 1.4). However, when evaluating end-members (mud and sand) alone, accuracy ratings were high (>83%) (Table 1.5).

A similar approach, in part informed by the spectral feature plots (Figure 1.12) was used in classifying the Bahia Lomas study region. While the accuracy of the discrete classes was even more suspect (e.g overall accuracy: 37.93%, Table 6), the relationships between approximate sediment size and remote sensing values (reflectance and backscatter) were clear in the spectral feature plots. Similar to the Brazilian classification, end-members were more clearly differentiated from each other compared to the "mixed" class, but accuracy in Bahia Lomas was still poor (Table 1.7).

1.4 - Discussion

Before tackling the first research question (evaluating the efficacy of characterizing the intertidal zone using multispectral reflectance and SAR backscatter), it was necessary to isolate the intertidal zone from adjacent land cover to prevent misclassification. Isolating the intertidal zone using the methods developed by Murray et al. (2012) proved effective (overall accuracy of 73.6%) though errors of omission did occur (~34.9%) (Table 1.1). Errors of omission may be the product of not finding ideal pairings of high-tide and low-tide imagery. If images were not at highest high tide, or lowest low tide, it is possible that portions of the intertidal zone would be omitted from the classification, with intertidal area either still covered by water (not lowest low),

or not covered by water (not highest high). The process of cloud removal and imagery substitution to create cloud free images may also have contributed to less-than-ideal imagery or designating ideal tidal conditions. This means that our designated intertidal zone may be considered a relatively conservative estimate of total intertidal area within the study regions. Murray et al. (2019) have since developed a new, and possibly more robust approach using machine learning and the entire Landsat data series that may be used for delineating the intertidal zone in future research.

Remote sensing of the intertidal zone addressed the first research question on the efficacy of employing multispectral reflectance and SAR backscatter to discriminate between mud and sand intertidal habitat types in both northern Brazil, and Bahia Lomas. Sand and mud end-members were readily distinguished at both sites based on the mean of survey plot remote sensing responses, though the middle “mixed” class was difficult to separate (Figures 1.6 and 1.7). The patterns of distinct end-members (Tables 1.5 and 1.7) and muddled middle classes (Tables 1.4 and 1.6) continued with the unsupervised, discrete classification approach. Previous research, conducted with more thorough quantitative sediment size data, also struggled with classifying the mud-sand continuum into discrete classes (Yates et al 1993). Based on these two approaches, remote sensing using multispectral reflectance and SAR backscatter can effectively discriminate between mud and sand extremes of the intertidal habitat types but disentangling the middle of the continuum remains challenging. This may be due to the temporally dynamic nature of tidal inundation with shifts in sediment characteristics, including mud-sand mixture, moisture, or surface texture happening each tidal cycle (Widdows et al. 2000), making the capture of specific states of sediment especially challenging. Inconsistencies between the timing of in-situ survey data and remote sensing data may also play a role, where remote sensing images and respective values are acquired at different times and states of intertidal structure and composition. This would be particularly challenging in areas where appropriate, cloud-free images are sparse. With

these challenges in mind, more investigation is needed regarding the effects on the spectral reflectance response due to temporal changes of wave-washed beaches and sand flats.

The second research question examined the universality of the relationship between multispectral reflectance, SAR backscatter, and sediment size between the locations. The differences found in radar response between the two sites (Table 1.3) are likely due to the nature of reflectance and backscatter, and how they interact with the physical properties of the intertidal substrate. General observations made while conducting the field surveys at the two locations hint at similarities and differences of the physical properties of the sediment. Mud substrates appear relatively similar in both visible color (i.e., the spectral reflectance in the visible wavelength regions) and surface texture between the two sites, both with pocked, complex surface structure, and dark gray to brown in color. Bahia Lomas does distinguish itself with the occasional cracked, dry, and plated mud surfaces (Figure 1.3). The surface texture of sand for both locations appears consistently similar, with rippled or washboard surfaces. However, visible color of sand differs noticeably between both sites, with Bahia Lomas consistently being darker and Brazil having some regions with a more orange or red tone (Figure 1.4). Two general patterns emerge: differences in substrate color, primarily due to differences in sand, and similarities in surface texture between both locations, with some exceptions in Bahia Lomas' platy, cracked mud. The patterns of differences in color and surface texture continue to play out in the responses of the respective Landsat reflectance, and Sentinel backscatter data.

Typically, reflectance is influenced by soil moisture, with smaller grained soils (higher proportions of silt and clay, i.e. mud) retaining a higher concentration of water than larger sized soils (i.e., sand). Increased water retention results in lowered reflection across all visual and infrared bands. Brazil followed the same patterns as previous studies (Yates et al 1993, Rainey et al 2003, van der Wal and Herman 2007), with reflectance increasing as sediment size increased (Figure 1.6). However, Bahia Lomas exhibited the inverse relationship, with reflectance decreasing as sediment size increased (Figure 1.7). This trend is even more apparent when

comparing normalized reflectance data, with Bahia Lomas consistently having higher relative mud reflectance (Figure 1.8), and lower relative sand reflectance (Figure 1.9). This may be due to differences in local surface soil properties, conflating the reflective properties of the mineral composition of the sediment with the moisture retention. According to the UN-FAO's Harmonized World Soil Dataset, the majority of topsoil found across the study site in Brazil is classified as Ferralsols, typified by high iron content that results in a distinctive red to yellow color, or Plinthosols, also with high iron content. The upland areas adjacent to Bahia Lomas, and much of the Strait of Magellan is dominated by Phaeozem top-soils, classified as dark and rich in organic matter (FAO 2014). These dramatically different inland soil types, which are subsequently deposited onto the intertidal flats, may explain the different multispectral relationships observed.

The two physical characteristics driving radar backscatter values in sediment are surface roughness, and dielectric properties due to surface moisture content. Van der Wal et al. (2005) found that smooth surfaces were associated with mud and lower backscatter, and rough surfaces associated with sand and higher backscatter. Surface moisture can significantly influence how much electromagnetic energy penetrates, with high levels of moisture preventing penetration and increasing backscatter, while low levels of moisture facilitate penetration and reduce backscatter (Mikhail et al. 2001, Jensen 2007). The similar patterns in backscatter between Bahia Lomas and Brazil (Figures 8 and 9, Table 3) suggest that the locations have similar responses to the combined effects of surface roughness and moisture content. Van der Wal et al (2005) also found that surface roughness was the strongest correlate with sediment size compared to other variables, including surface moisture. Our results differed from Van der Wal's, in that intertidal mud locations had higher backscatter values than intertidal sand in both study sites (Figures 1.6 and 1.7). Cross-tidal transects conducted in muddy areas demonstrate visible, near-infrared and short-wave infrared reflectance marginally decreasing, and moisture content presumably increasing while moving from the high tide towards the low tide line (Figure 1.10). There is a similar trend of

decreasing mud radar backscatter as one moves from the high tide towards the low tide line. Figure 1.10 shows great variability in the mud backscatter response in proximity to the high tide line. This pattern could be a product of increased surface roughness due to features close to the high tide line such as mangroves, debris, or fiddler crab colonies and smoother surfaces in the more regularly inundated areas lower in the tidal prism. Distance from the high tide line had no significant effect on the radar backscatter of intertidal sand substrate. Dunes consist of persistently dry sand mostly above the high-tide line and exhibited similar spectral patterns to intertidal sand, but with higher reflectance values and a much broader variance. One explanation of the broad variance could be due to the changes in aspect across the dune faces, influencing how much signal is returned to the sensor. Taken together, our results for the main sampling protocol and the transects conducted in Brazil suggest that mud features have a higher backscatter response than sand due to both moisture retention. Visible, near-infrared, and short-wave infrared reflectance follow the trends of decreasing response as presumed moisture increases. Backscatter response is less clear, as high variability in mud plots close to the high tide line may be the product of variability in surface roughness due to features not directly related to sediment size like mangroves, debris, and fiddler crab colonies.

While significant relations were found between survey plots characterized by our methods using qualitative field data and remote sensing metrics, there are several known issues that could be addressed in future research. Foremost amongst areas for improvement is the qualitative nature of the in-situ calibration/validation data. Limited access to in-country soil labs and the difficulties around exporting soil samples back to the United States was the primary reason for utilizing a qualitative approach, rather than laboratory-based measurement of proportions of soil sample sediment sizes. Some of the issues with accurately classifying the mixed sediment types may be due to the challenges of surveyors accurately perceiving and qualifying sediment size. Mud and Sand endmembers are easily distinguished in both look (Figures 1.3 and 1.4) and texture (Thien 1979) but having approximately 12 different surveyors

accurately and consistently distinguishing between “muddy-sand” and “sandy-mud”, for example, is extremely difficult without rigorous prior training. Another potential problem is the reductive nature of utilizing a single dominant class to describe up to 0.2 km² of intertidal area. Significant variation could exist within the survey region that is not being captured, resulting in potentially heterogeneous sediment composition being categorized as homogeneous. Addressing the issues of limited qualitative data and oversimplification of plot heterogeneity would require a systematic sediment sampling approach for each plot, similar other study sampling regimes (Rainey et al 2003, van der Wal and Herman 2007). Our approach of qualitative habitat notes, while not as robust as systematic soil sampling, had the benefits of low costs and rapid data collection, while still successfully classifying end members and identifying sediment-size/remote sensing trends.

Remote sensing of the intertidal zone has its own challenges. Common to many remote sensing applications, mismatch between when the remote sensing image was taken and when the in-situ data was collected could lead to conclusions that do not accurately reflect ground conditions (Jensen 2007). Remote sensing of the intertidal zone has this difficulty two-fold: seasonal variation and tidal variation of the images. Landsat 8 image selection was further limited by significant cloud cover over the northern Brazil study site, with cloud free imagery taken during the survey period and at the appropriate tidal stage neigh impossible to find. Our approach of compositing several cloud-removed images for each scene, may have mismatches between tidal (e.g. spring vs neap low tides) or seasonal variations in multispectral values. Clouds were not problematic at all for the Sentinel 1 radar imagery acquisition because microwave radar penetrates atmospheric disturbance and cloud cover (Jensen 2007). Mismatch between tidal stage in the imagery vs exact tidal stage on the survey day still could occur. Our approach of acquiring multiple low tide images for each scene and calculating the average pixel value should produce a reasonable approximation of tidal conditions during survey dates, but discrepancies are still possible.

Future work characterizing the intertidal zone via remote sensing is viable, as clear relationships between remote sensing data and sediment size consistently emerge (Figures 1.6 and 1.7). However, the properties of local substrate must be taken into consideration as these patterns can differ between sites. Radar has great utility, as it has a more consistent response to physical properties of the soil (Figures 1.8 and 1.9) but, the dual response to surface moisture and surface roughness can be difficult to disentangle (Figure 1.10). Different radar frequencies respond very differently to soil moisture content, penetrating moist soils rather than being deflected (Williams and Greeley 2004). These differences can be leveraged to distinguish between the surface moisture, and aid in sediment classification (Gade et al 2014). Current space-based radar platforms (namely Sentinel 1 and Envisat) are operating in the C-Band, and few have the temporal and spatial resolution of Sentinel 1, making a study using multiple radar bands in such a temporally specific topic like the intertidal zone challenging. However, the NASA-ISRO SAR Mission (NISAR), set to launch in 2021, presents a likely option for such a study, with sampling intervals of 12 days or shorter, spatial resolution of 100 meters, and both L-Band and S-Band radar instruments (<https://nisar.jpl.nasa.gov/nisarmission/>). L-Band has demonstrated different capacities for penetrating surface sand, and even wet surface sand, unlike C-Band radar which is reflected (Williams and Greeley 2004). Regardless of the platform and radar frequency, ground truthing and calibration is critical to understanding the relationships between remote sensing and intertidal sediment in dramatically different geographic locations, and utilizing that information to inform management and conservation.

Delineating the intertidal zone is an important first step towards identifying important shorebird foraging habitat and informing conservation practices of migratory shorebirds. The methods developed by Murray et al. (2012) were effective at accomplishing this at both study locations, including the Marine Extractive Reserves (MERs) within northern Brazil. MERs are a series of management regions designed for the protection of artisanal fishing and sustainable extractive practices, while excluding large-scale disruptive processes like dredging, drilling, or

industrial fishing (Santos and Schiavetti 2014). These protected zones cover a significant portion (28%) of the Maranhao-Para intertidal zone (Table 1.8), an extent of intertidal protection similar to other studied regions; for example, 39% of Australia's intertidal zone is protected in some way (Dhanjal-Adams et al. 2016). While our results suggest that the highly accurate discrimination of discrete classes of sediment type using medium resolution remotely sensed imagery is problematic, a broad scale mapping of the spatial distribution of intertidal habitat types is feasible. I found that the approximate composition of intertidal area found within the MERs is proportional to the area that is protected; in other words, no intertidal land cover is preferentially protected by the MERs (Table 1.8). While this is reassuring, it is also clearly only the first step in understanding how MERs protect the intertidal zone, and the species that rely upon it. Unfortunately, this region is also similar to other regions, like Australia and the Yellow Sea (Murray et al. 2014, Murray et al. 2015), that share the same major threats to intertidal habitat; urbanization and development (Andrade et al 2016). Future management decisions should reflect the importance of the intertidal zone, the scope of that region that is affected by the Marine Extractive Reserves, and the potential risks of urbanization and development.

Moving beyond simply delineating the intertidal zone, to characterizing habitat within the intertidal zone is the critical next step for managing the suite of shorebird species that utilize the different intertidal habitats. Our two research predictions (1 - that multispectral reflectance and SAR backscatter can be used to discriminate between mud and sand intertidal types; 2 - that the relationship between multispectral reflectance, SAR backscatter, and sediment type is applicable across a span of geographic locations) aimed to better understand this next step. By evaluating within-site plots, I confirmed that characterizing end-member classes of the mud-sand continuum is viable (Table 1.5), and that differentiating between mixed classes remains challenging (Table 1.4). However, I also demonstrated consistent relationships between reflectance, radar backscatter, and sediment size within each location. Mud showed consistently lower visible, near infrared, and shortwave infrared reflectance and higher radar backscatter than sand in Brazil,

while mud in Bahia Lomas had consistently higher visible, near-infrared, and shortwave infrared reflectance and radar backscatter than sand (Figures 1.6, 1.7, and Table 1.2). Related to my second research prediction, I demonstrated the necessity for in situ calibration and validation data, as these relationships can differ between study locations (Figures 1.8, 1.9, and Table 1.3). This information could be leveraged for monitoring management and planning. For example, many management practices can alter intertidal sediment composition, such as dredging and dredge dumping, which in turn affect the biological processes of the intertidal zone (Essink 1998, Jaffe et al. 2007, van Maren et al. 2015). Shorebirds have demonstrated clear resource partitioning across different intertidal sediment types (Colwell and Landrum 1993, Bocher et al. 2014), and can have their distributions shifted by changes in sediment composition due to beach restoration management practices, like sand placement (Peterson et al. 2006). Based on our results, changes in remote sensing values of the intertidal substrate would reflect changes in intertidal sediment composition in these situations, though in situ data would be necessary for calibration and validation of the remote sensing-sediment size relationship at each site. Using remote sensing, in conjunction with in-situ data, to understand the extent and approximate composition of intertidal sediment could be effective for evaluating intertidal habitat in a variety of applications; from shorebird habitat to the effects of human activities on intertidal sediments including beach restoration (Niles et al. 2013) and dredging. It is clear from this work that discrete classification of intertidal sediment is implausible, but that trends in remote sensing values reflect trends in sediment composition. As such, you would expect changes in remote sensing response to the intertidal zone to reflect changes in intertidal habitat due to sediment size differences between the original sediment, and sand used for beach-fill

1.5 - Conclusion

Similar to previous research, I confirmed significant relationships between sediment size and visual, infrared, and radar remote sensing. I also confirmed that the mud-sand sediment

continuum is reflected along a continuous gradient in spectral feature space, with mud and sand endmembers readily distinguished, but middle, mixed classes less so. However, unlike previous research, I demonstrated that these relationships are not universal and require in-situ data for the calibration and validation of site-specific relationships. Discretely classifying the mud-sand continuum is neither impossible, but leveraging the clear relationship between remote sensing and sediment size could potentially be effective for characterizing the intertidal habitat using alternative techniques that incorporate the non-discrete nature of the sediment gradient. These approaches, such as spectral mixture analysis, maximum entropy modeling, or simple change detection could be used for a variety of applications, including beach restoration, the effects of dredging, understanding shorebirds intertidal habitat, and informing management and conservation decisions regarding the intertidal zone.

1.6 - Tables and Figures

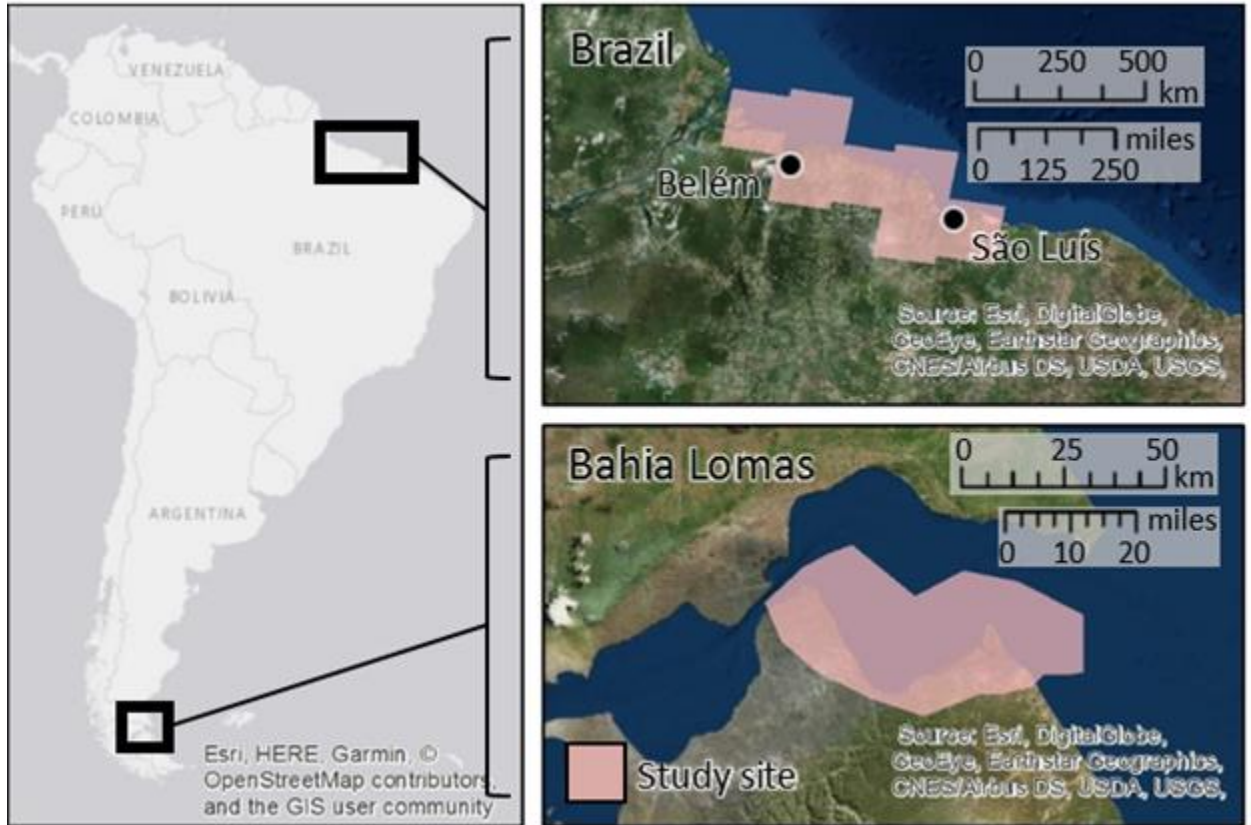


Figure 1.1: The two regions, northern Brazil and Bahia Lomas, with study sites roughly outlined in pink.

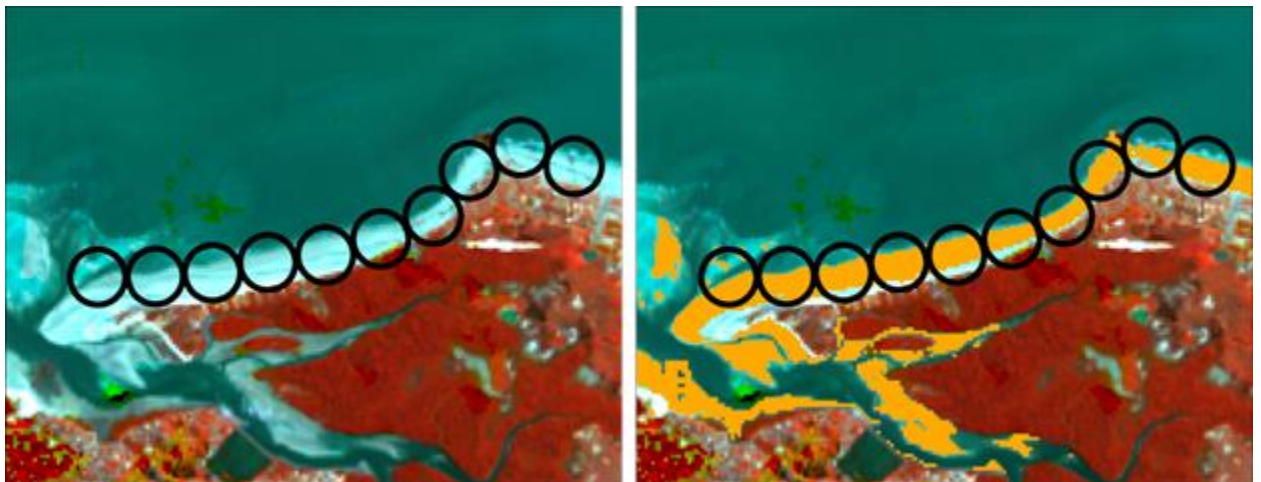


Figure 1.2: Circumferences of 250 meter radii survey plots on the left, showing that using only the plot vectors would erroneously include pixels that were not intertidal habitat. The right shows the region categorized as “intertidal”, in orange, using the methods outlined by Murray et al. Masking the remote sensing data with this mask prevents any data not surveyed within the intertidal surveys from being erroneously included in the analysis.



Figure 1.3: Pictures of typical mud sediment class found in Bahia Lomas (left) and Brazil (right). Both are typified by what appears to be rough surface texture, though the cracked, dry, plated surface (middle left) was unique to Bahia Lomas.

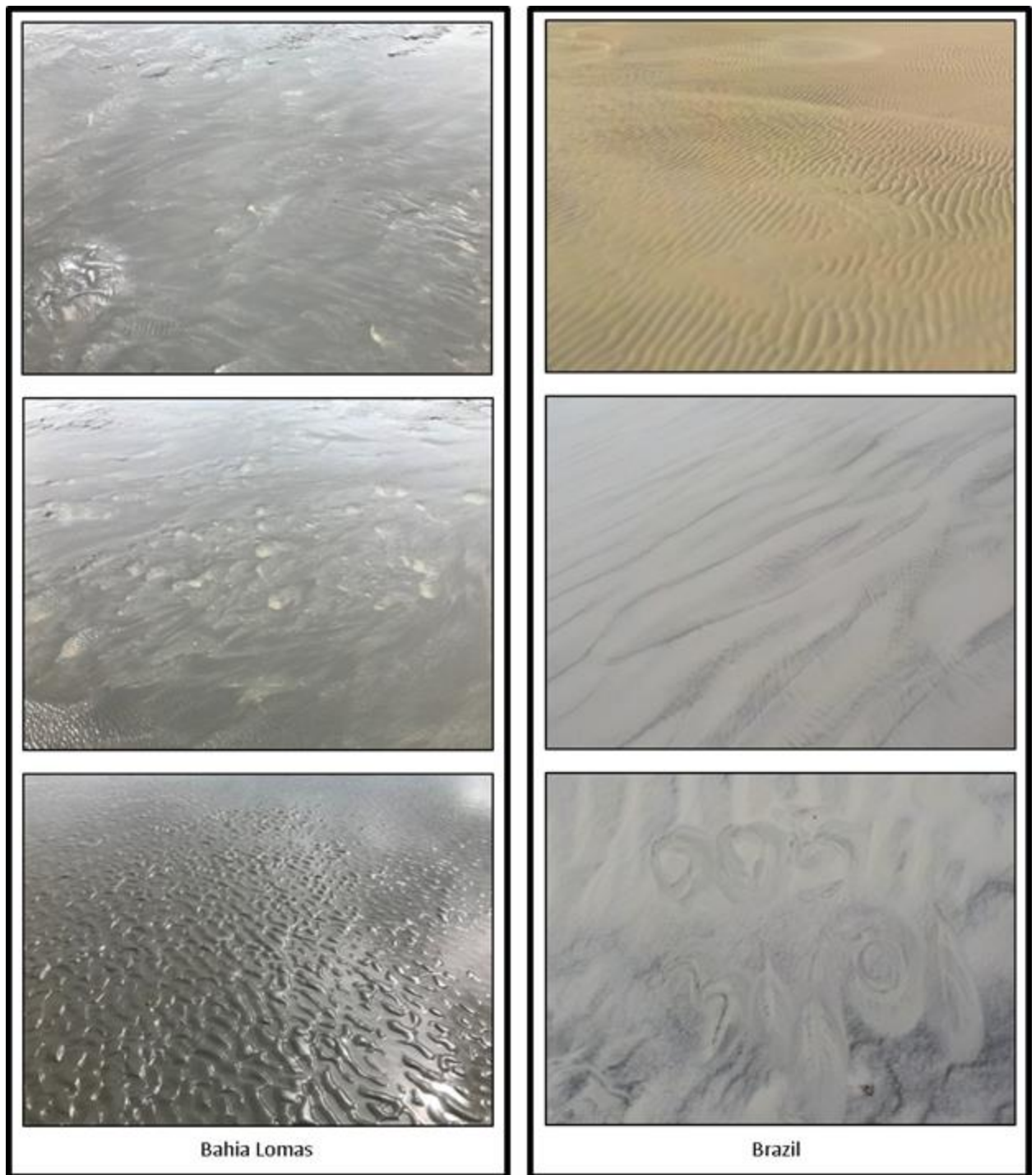


Figure 1.4: Pictures of typical sand sediment class found in Bahia Lomas (left) and Brazil (right). Sand in Brazil appeared to have a wider range of color, from pale gray to yellow-orange hue, relative to Bahia Lomas. Both are typified by rippled or washboard surface textures.

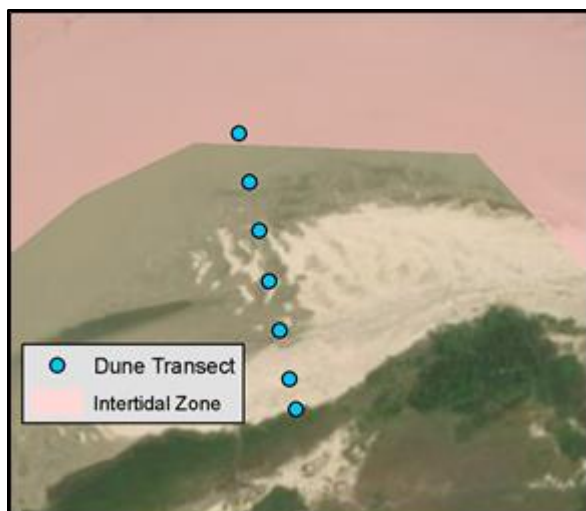


Figure 1.5: Example of cross-tidal transect, going from above tide vegetation, cross the dune, and to the edge of the intertidal zone.

Table 1.1: Error matrix for the Brazilian study site's intertidal mask accuracy assessment based on 174 randomly distributed points across the Brazilian study site. Land cover of each validation point was determined as either "intertidal" or "other" by studying numerous Landsat images. Cells filled with gray are where both the classified and reference land covers agree. Overall accuracy and Cohen's Kappa coefficient are listed in the bottom right.

		Reference			Users
		Intertidal	Other	Sum	
Classified	Intertidal	84	1	85	98.8%
	Other	45	44	89	49.4%
	Sum	129	45	Kappa:	47.9%
Producers		65.1%	97.8%	Overall:	73.6%

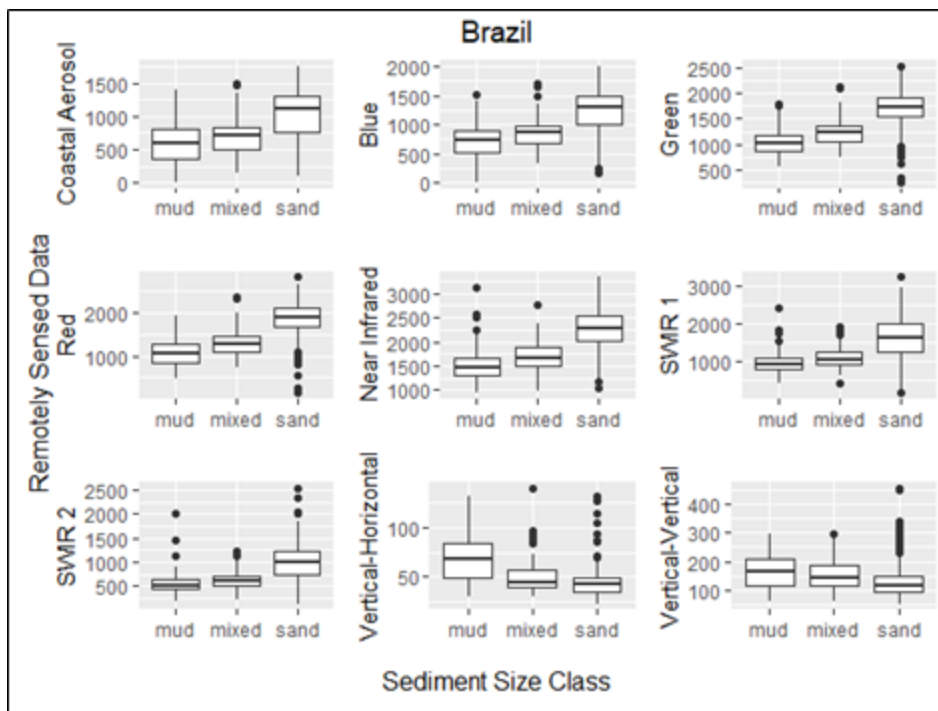


Figure 1.6: Box-plots of mean reflectance and backscatter plots for each plot in Brazil. Box ends are the upper and lower quartiles with the central line representing the median. Whiskers represent values outside of the upper and lower quartile, while dots represent outliers. Coastal/Aerosol, Blue, Green, Red, NIR, SWIR 1, and SWIR 2 reflectance values are from the Landsat 8 platform, while Vertical-Horizontal and Vertical-Vertical are the respective polarized backscatter from Sentinel 1.

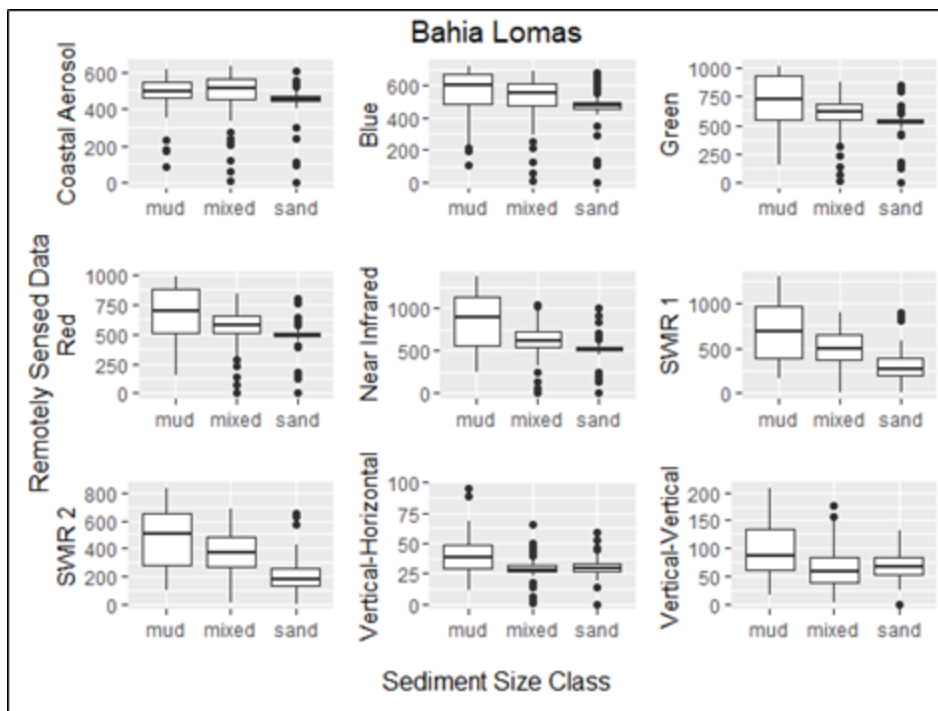


Figure 1.7: Box-plots of mean reflectance and backscatter plots for each plot in Bahia Lomas. Box ends are the upper and lower quartiles with the central line representing the median. Whiskers represent values outside of the upper and lower quartile, while dots represent outliers. Coastal/Aerosol, Blue, Green, Red, NIR, SWIR 1, and SWIR 2 reflectance values are from the Landsat 8 platform, while Vertical-Horizontal and Vertical-Vertical are the respective polarized backscatter from Sentinel 1.

Table 1.2: Tukey HSD P-values comparing Landsat 8 surface reflectance and Sentinel 1 backscatter of Mud vs Mixed, Sand vs Mixed, and Sand vs Mud classes in Brazil and Bahia Lomas. Each P-value represents a Tukey HSD pair-wise comparison of remote sensing data between sites designated as Mud, Mixed, or Sand based on in-situ field notes.

Sensor	Band	Bahia Lomas			Brazil		
		Mud-Mixed	Sand-Mixed	Sand-Mud	Mud-Mixed	Sand-Mixed	Sand-Mud
Landsat 8	Coastal Aerosol	0.803	0.381	0.074	0.003	<0.001	<0.001
	Blue	0.46	0.031	0.002	<0.001	<0.001	<0.001
	Green	0.004	0.051	<0.001	<0.001	<0.001	<0.001
	Red	0.002	0.031	<0.001	<0.001	<0.001	<0.001
	Near IR	<0.001	0.012	<0.001	<0.001	<0.001	<0.001
	SWIR 1	<0.001	<0.001	<0.001	0.04	<0.001	<0.001
	SWIR 2	0.006	<0.001	<0.001	0.09	<0.001	<0.001
	Sentinel 1	Vertical-Horizontal	<0.001	0.905	<0.001	<0.001	0.09
Vertical-Vertical		<0.001	0.018	<0.001	0.14	0.018	<0.001

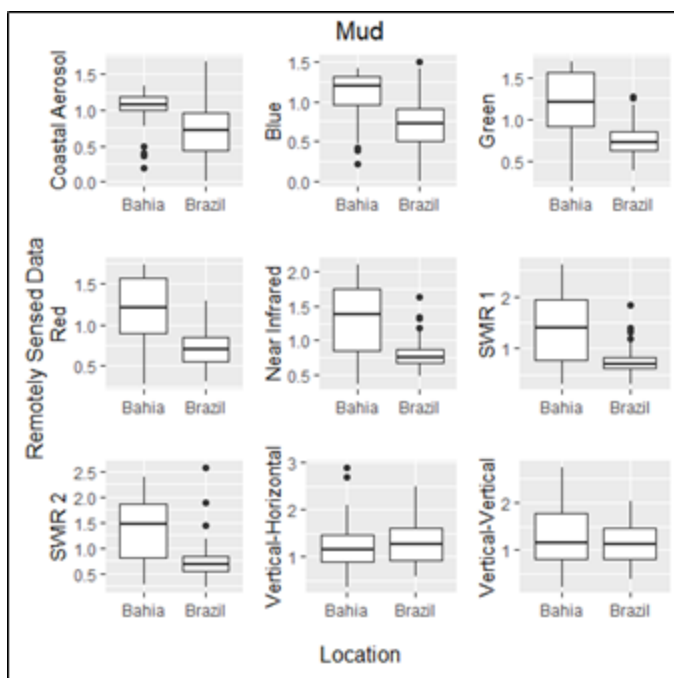


Figure 1.8: Comparison of normalized Landsat 8 surface reflectance and Sentinel 1 backscatter (e.g. (Blue reflectance for plot [i]) / (mean of blue reflectance for all plots in Brazil)) for Mud in Bahia Lomas and Brazil. Box ends are the upper and lower quartiles with the central line representing the median. Whiskers represent values outside of the upper and lower quartile, while dots represent outliers.

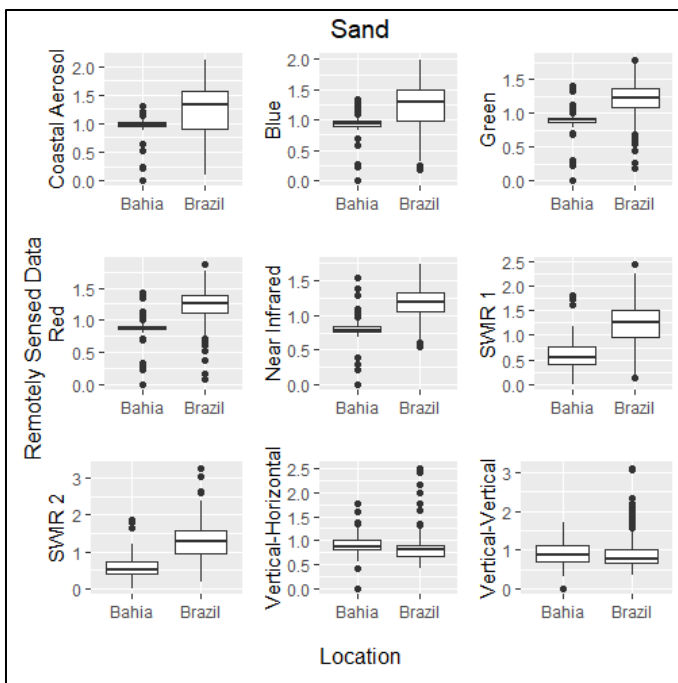


Figure 1.9: Comparison of normalized Landsat 8 surface reflectance and Sentinel 1 backscatter (e.g. (Blue reflectance for plot [i]) / (mean of blue reflectance for all plots in Brazil)) for Sand in Bahia Lomas and Brazil. Box ends are the upper and lower quartiles with the central line representing the median. Whiskers represent values outside of the upper and lower quartile, while dots represent outliers.

Table 1.3: P-values from Welch's t-test comparing normalized Sand values between Brazil and Bahia Lomas, and normalized Mud values between Brazil and Bahia Lomas, with P-values < 0.05 highlighted in gray.

Brazil vs Bahia Lomas			
Sensor	Band	Normalized Sand	Normalized Mud
Landsat 8	Coastal Aerosol	<0.001	<0.001
	Blue	<0.001	<0.001
	Green	<0.001	<0.001
	Red	<0.001	<0.001
	Near IR	<0.001	<0.001
	SWIR 1	<0.001	<0.001
	SWIR 2	<0.001	<0.001
Sentinel 1	Vertical-Horizontal	0.011	0.6368
	Vertical-Vertical	0.553	0.082

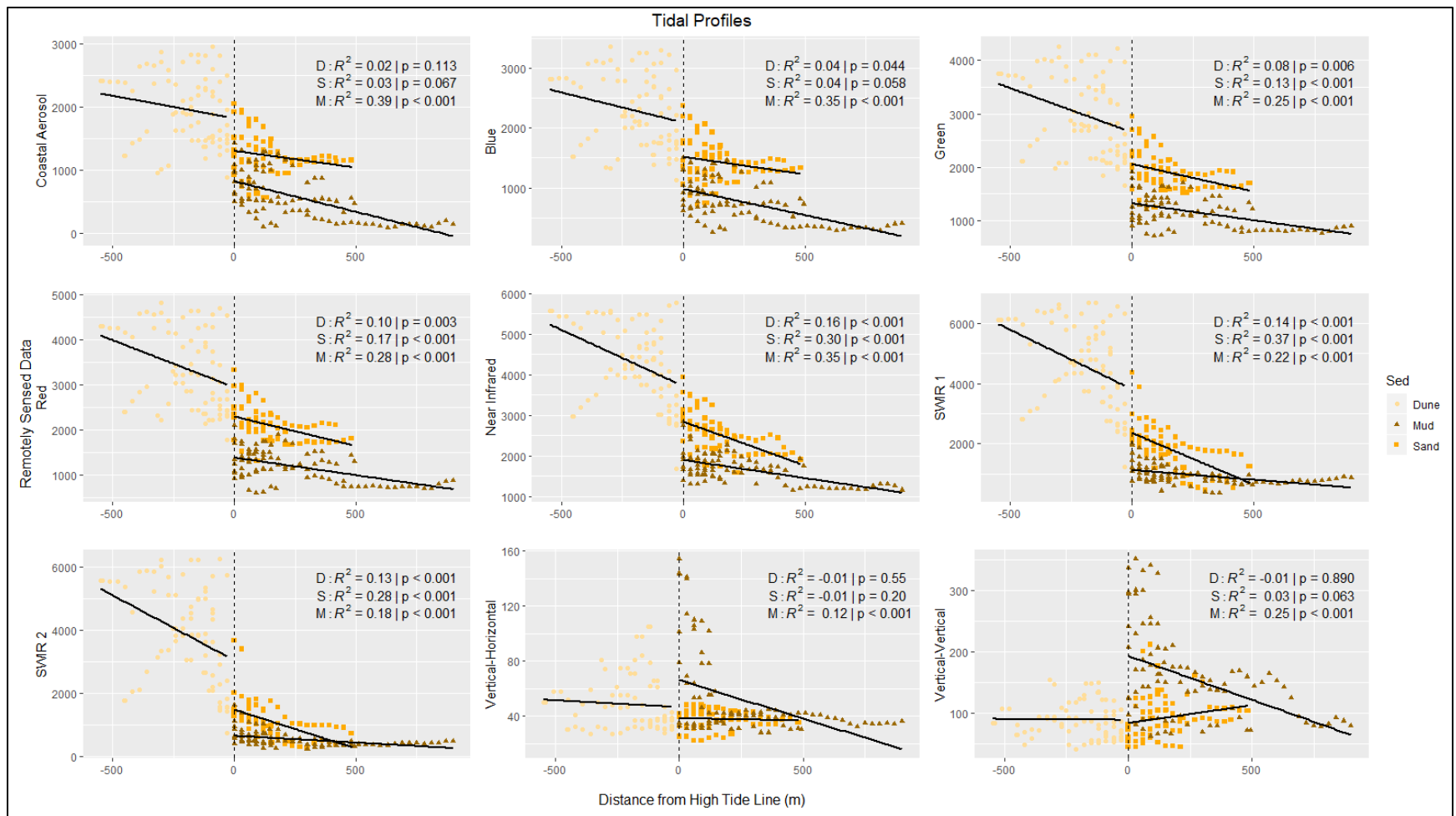


Figure 1.10: Points from transects of spectral response relative to the high tide line from 8 randomly selected dunes (yellow circles), sand flats (orange squares), and mud flats (brown triangles) across the Brazilian study area (sediment class determined based on point data). Number of points per transects vary depending on the size of the area exposed at low tide, or the size of the contiguous dune feature between the high tide line and next clear land cover feature.

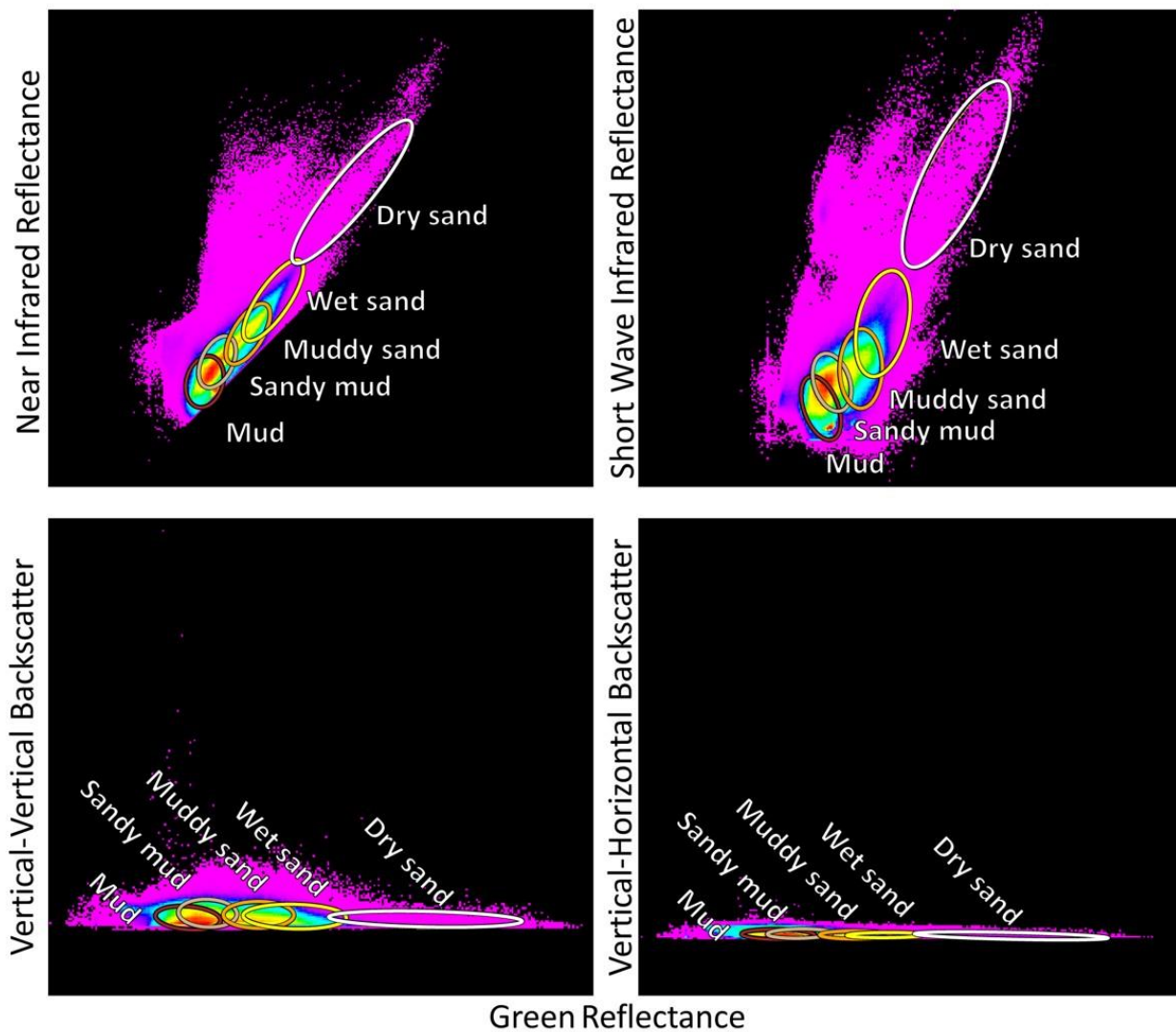


Figure 1.11: Spectral feature plots for the Brazilian study site intertidal zone with ellipses representing two standard deviations from the mean of each class. The top two show the relationship between near-infrared and green surface reflectance (left), and short-wave infrared and green surface reflectance derived from Landsat 8 (right). The bottom plots show the relationship between the vertical-vertical backscatter (left) and vertical-horizontal backscatter (right) via the Sentinel 1 SAR platform, and the green Landsat 8 surface reflectance values.

Table 1.4: Error matrix for the Brazilian study site's accuracy assessment. Using the ground data (n = 245) reserved as validation data, each plot had both a "reference" land cover class, derived from qualitative field notes, and a "classified" class, derived from the mode of classified land cover pixels within the 250 meter radius survey plot. Cells filled with gray are where both the classified and reference land covers agree. Overall accuracy and Cohen's Kappa coefficient are listed in the bottom right.

		Reference				
		Sand	Mixed	Mud	Sum	User's
Classified	Sand	31	0	0	31	100.00%
	Mixed	84	25	53	162	15.43%
	Mud	6	12	34	52	65.38%
	Sum	121	37	87	Kappa:	17.01%
Producer's		25.62%	67.57%	39.08%	Overall:	36.73%

Table 1.5: Error matrix for the Brazilian study site's endmember accuracy assessment of the reserved ground data, excluding the Mixed classification (n = 71). Each plot had both a "reference" land cover class, derived from qualitative field notes, and a "classified" class, derived from the mode of classified land cover pixels within the 250 meter radius survey plot. Cells filled with gray are where both the classified and reference land covers agree. Overall accuracy and Cohen's Kappa coefficient are listed in the bottom right.

		Reference			
		Sand	Mud	Sum	Users
Classified	Sand	31	0	31	100%
	Mud	6	34	40	85%
	Sum	37	34	Kappa:	83.19%
Producers		83.8%	100%	Overall:	91.5%

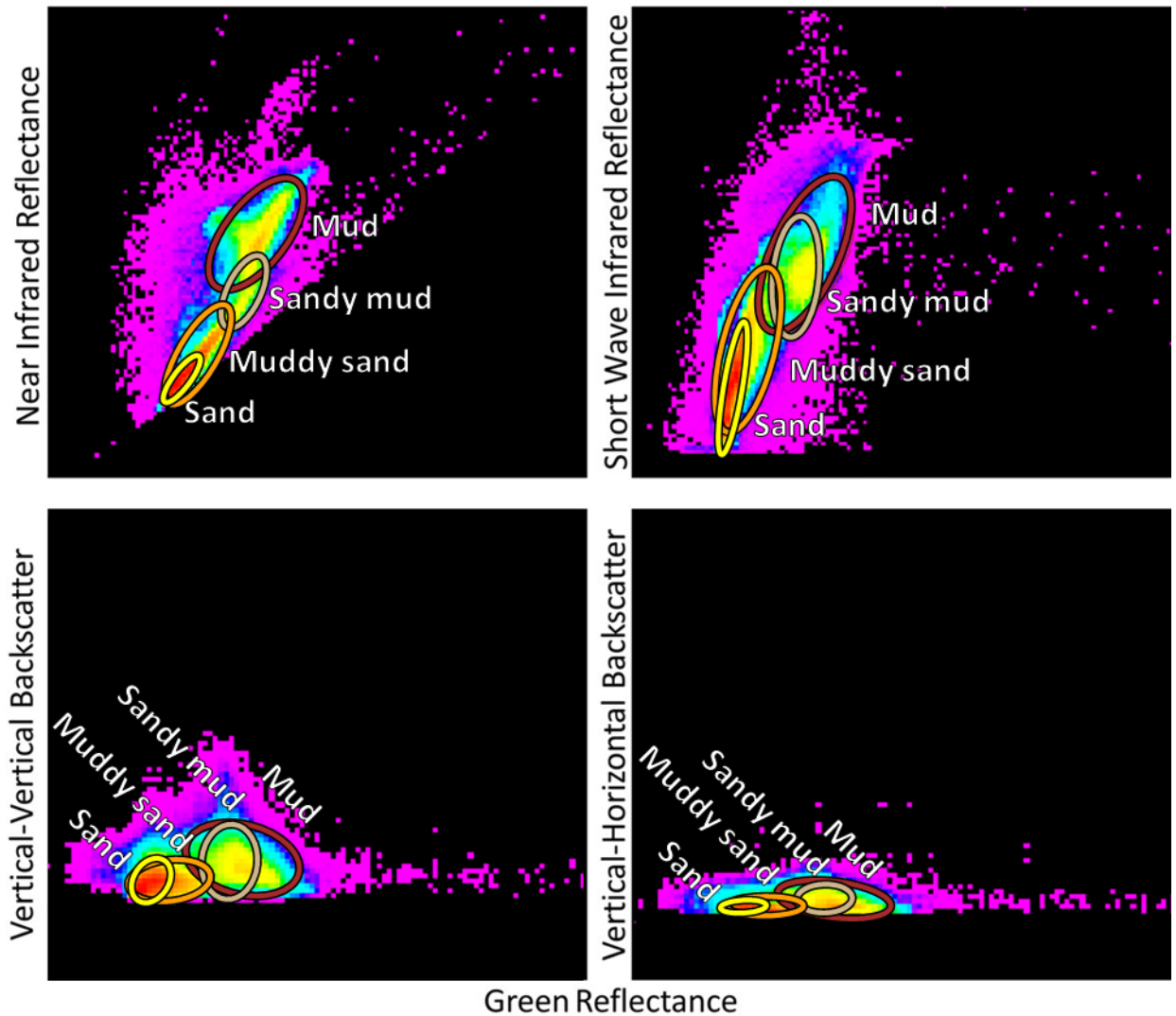


Figure 1.12: Spectral feature plots for the Bahia Lomas study site intertidal zone with ellipses representing two standard deviations from the mean of each class (Mud = maroon, Sandy mud = beige, Muddy sand = orange, Sand = yellow). The top two show the relationship between near-infrared and green surface reflectance (left), and short-wave infrared and green surface reflectance derived from Landsat 8 (right). The bottom plots show the relationship between the vertical-vertical backscatter (left) and vertical-horizontal backscatter (right) via the Sentinel 1 SAR platform, and the green Landsat 8 surface reflectance values.

Table 1.6: Error matrix for the Bahia Lomas site's accuracy assessment. Using the ground data (n = 180) reserved as validation data, each plot had both a "reference" land cover class, derived from qualitative field notes, and a "classified" class, derived from the mode of classified land cover pixels within the 250 meter radius survey plot. Cells filled with gray are where both the classified and reference land covers agree. Overall accuracy and Cohen's Kappa coefficient are listed in the bottom right.

		Reference				
		Sand	Mixed	Mud	Sum	User's
Classified	Sand	23	25	11	59	38.98%
	Mixed	29	35	20	84	41.67%
	Mud	12	11	8	31	25.81%
	Sum	64	71	39	Kappa:	2.77%
Producer's		35.94%	49.30%	20.51%	Overall:	37.93%

Table 1.7: Error matrix for the Bahia Lomas study site's endmember accuracy assessment of the reserved ground data, excluding the Mixed classification (n = 54). Each plot had both a "reference" land cover class, derived from qualitative field notes, and a "classified" class, derived from the mode of classified land cover pixels within the 250 meter radius survey plot. Cells filled with gray are where both the classified and reference land covers agree. Overall accuracy and Cohen's Kappa coefficient are listed in the bottom right.

		Reference			
		Sand	Mud	Sum	Users
Classified	Sand	23	11	34	68%
	Mud	12	8	20	40%
	Sum	35	19	Kappa:	7.73%
Producers		65.71%	42%	Overall:	57.41%

Table 1.8: Intertidal land cover across the Brazilian study site (Total), broken down into the area (Km²) and relative composition (% of MER) within the Marine Extractive Reserves, and the area (Km²) and relative composition (% of Out) outside the Marine Extractive Reserves.

	Inside MER			Outside MER			Total	
	Km ²	% of MER	% of total	Km ²	% of Out	% of total	Km ²	% of total
Mud	149	26.47%	28.33%	377	26.14%	71.67%	526	26.23%
Mixed	348	61.81%	27.27%	928	64.36%	72.73%	1276	63.64%
Sand	66	11.72%	32.51%	137	9.50%	67.49%	203	10.12%
Total	563		28.08%	1442		71.92%	2005	

Chapter 2: Distribution Modeling of Intertidal Shorebird Habitat

2.1 - Introduction

Many species of shorebirds migrate long distances from their overwintering feeding grounds in the southern hemisphere, to breeding grounds in the northern hemisphere (Colwell 2010, Niles et al. 2010, Burger et al. 2012, Gratto-Trevor et al. 2012, Lathrop et al. 2018). During these migrations, species will utilize numerous stops along the migration route as staging grounds or launch points for the next step of the migration (Warnock 2010, Brown et al. 2017, Anderson et al. 2019). Due to their reliance on numerous, cross-continental locations, migratory shorebirds are particularly vulnerable, as disruptions at any migratory location can affect migratory and breeding success (Piersma and Lindstrom 2004, Mizrahi et al. 2012, Anderson et al. 2019). This risk is reflected in declining populations of many migratory species including Red Knots (*Calidris canutus rufa*, Niles and Cooper Ornithological Society 2008), Semipalmated Sandpipers (*Calidris pusilla*, Andres et al. 2012a, Morrison et al. 2012), Black-bellied (Gray) Plovers (*Pluvialis squatarola*), and Ruddy Turnstones (*Arenaria interpres*, von Numers et al. 2020). Affected populations are found globally, across flyways in North America (Bart et al. 2007, Morrison et al. 2012), to Europe (Stroud et al. 2004), and the Asian-Australasian flyway (Clemens et al. 2016). These declines are partly a product of a number of human-driven factors, including the overharvest of key food resources such as horseshoe crab eggs in Delaware Bay, U.S.A (Baker et al. 2004, Niles and Cooper Ornithological Society 2008), sea level rise (Galbraith et al. 2002, Iwamura et al. 2013, Galbraith et al. 2014), and massive intertidal habitat loss, like what is occurring across East Asia (Murray and Fuller 2015) and the Yellow Sea (Studds et al. 2017).

One major overwintering and stopover locations in the Western Americas Flyway is the northern coast of Brazil, along the states of Pará and Maranhão (Niles and Cooper Ornithological Society 2008, Colwell 2010) (Figure 2.1). This region encompasses two Ramsar sites: the Maraja archipelago at the mouth of the Amazon River; and, the Reentrancias Maranhenses. Both sites

consist of “complex estuarine system[s] of extensive islands, bays, coves, and rugged coastline covered mainly by mangrove forest.” The Marajo archipelago, in particular, contains one of the largest contiguous mangrove formations in the world, consisting of 8,900 km² of mangrove forest, or approximately 70% of all mangroves in Brazil. The Reentrancias Maranhenses, located to the northwest of Sao Luis, is a complex series of bays and inlets, critically important for migratory shorebirds, fish, manatee, and the fishermen that subsist within the region (Ramsar Convention, <https://www.ramsar.org/wetland/brazil>). Accurately and logically predicting how migratory shorebirds are distributed across the Pará-Maranhão ecosystem is essential to making informed shorebird management and conservation decisions in the region.

Species distribution models (SDM) can be effective tools for determining where a species is likely to occur by using records of a species’ presence and a suite of environmental variables to characterize the habitat most likely to contain said species (Franklin and Miller 2009). One of the most widely adopted approaches is through the Maximum Entropy framework. Maximum entropy modeling, including the MaxEnt modeling package (Phillips et al 2006), utilizes machine learning to evaluate presence records and environmental variables associated with those presence records. Variables are considered both in isolation and in combination with the other environmental variables input into the model based on maximum likelihood and maximum entropy to determine what the most effective model is for estimating the predicted probability of presence for any given combination of environmental variables (Phillips et al 2006, Phillips et al 2008, Elith et al. 2009, Elith et al 2011). MaxEnt has been utilized to model countless species and their distributions (Stabach et al. 2009, Illera et al 2010, Howell and Veloz 2011, Latif et al. 2013) including the breeding habitat of the Atlantic Americas Flyway migratory shorebird, the Red Knot (*Calidris canutus rufa*) (Lathrop et al. 2018). Essential in these models are the environmental variables that characterize a species habitat. The most common variables include metrics of climate, landscape structure, and land cover (Bradie and Leung 2017). Understanding

which variables are effective at characterizing intertidal foraging habitat of migratory shorebirds is key to developing distribution models for informing management and conservation.

The intertidal zone, consisting of sand and mud flats exposed at low tide and covered at high tide, is used extensively by migratory shorebirds, with a majority of their time spent foraging for food (Burger et al. 1997, Jourdan et al. 2021). The intertidal zone is the primary foraging habitat of a majority of migratory shorebirds across the globe (Colwell 2010, Mu and Wilcove 2020). Within this region, different species utilize different microhabitats, with species preferentially foraging on different substrates or at different times (Colwell and Landrum 1993, Bocher et al. 2014, Philippe et al. 2016, Faria et al. 2018, Burger et al. 2018). A primary driver of these distributions is the size of the intertidal mud-sand sediment, which, in turn, determines the distribution of the intertidal invertebrate microfauna that the shorebirds feed upon (Thrush et al. 2003, van der Wal et al. 2008). Different sediments, such as larger-grained sand and smaller-grained mud, host different, yet equally thriving invertebrate communities (Sheaves et al. 2016). Changing sediment size, through beach replenishment, for example, changes benthic invertebrate distributions and, subsequently, shorebird distributions (Peterson et al. 2006, Folmer et al. 2010). Other human activities, namely disturbance, has been shown to influence shorebird intertidal foraging behavior and distribution (Burger 1986, Pfister et al. 1992, Burger and Niles 2013, Martin et al. 2015), including pedestrians (Burger et al. 2007), use of all-terrain-vehicles (Tarr et al. 2010), and the presence of dogs (Navedo et al. 2019). Understanding the intertidal habitat composition, particularly sediment size distribution, across a migratory stopover is clearly a critical component for characterizing intertidal foraging habitat and the subsequent distributions of shorebirds.

Remote sensing has been utilized to map the intertidal zone and to characterize sediment type using a variety of platforms and analytical methods. Murray et al. (2012) developed an effective method of isolating the intertidal zone across continental scale regions using optical remote sensing data, Normalized Difference Water Index, and differencing between high-tide and

low-tide images. Optical and shortwave infrared reflectance data collected using airborne (Rainey et al 2003) and satellite platforms (Yates et al 1993) have been analyzed using both regression based and spectral mixture methods that have relied on the low spectral reflectance of mud in the green and near infrared spectrum relative to sand. Microwave synthetic aperture radar (SAR) backscattering has been used to measure surface roughness and successfully correlated with mud and sand composition (van der Wal et al 2005, Gade et al 2014). Mud was associated with smoother surface textures and lower backscatter, while sand had higher backscatter due to its rippled surface. Multiplatform methods have also been used, combining the strengths of both optical/shortwave infrared and SAR remote sensing to successfully model sediment size using regression analysis (van der Wal and Herman 2007). Finally, in Chapter 1, I compared remote sensing in northern Brazil and Bahia Lomas, Chile, demonstrating that the relationship between remote sensing metrics and sediment size can vary between locations but is consistent within each location. Utilizing this established relationship between remote sensing and sediment size, I aim to bridge the final gap, linking remote sensing and shorebird distributions across northern Brazil.

The objective of this chapter is to develop species distribution models for the intertidal foraging habitat of eight migratory shorebird species (black bellied plovers, red knot, ruddy turnstones, sanderlings, semipalmated plovers, semipalmated sandpipers, whimbrels, willets, Table 2.1) that occupy the Pará-Maranhão coastline in northern Brazil as either a migratory stopover location, or for the duration of the winter. Based on the established relationship between remote sensing metrics and sediment, as well as relevant landscape and climate metrics, these models will be parameterized using shorebird presence data collected during two field seasons in northern Brazil (Winter 2016 and 2017). The efficacy of species distribution models based on remote sensing values, as well as the statistical and biological significance of the different classes of model variables (landscape, remote sensing, and climatic) will be evaluated, with the goal of informing future foraging habitat models and subsequent management. With those goals in mind, I predict that:

1.) Remote sensing metrics will play a significant role models that discriminate between predicted habitat and non-habitat in northern Brazil

2.) Remote sensing metric response will follow previously established relationships between remote sensing and intertidal sediment size, reflecting known patterns in shorebird habitat preference

2.2 - Methods

2.2a - Survey methods

Wading shorebird presence and abundance surveys were conducted during the winter migratory stopover period of 2016 and 2017 in northern Brazil (Figure 2.2). Survey methods consisted of point counts conducted by pairs of observers and recorders, using fixed radius plots positioned along transects, with all wading birds counted within a 250 meter radius of the observers. To maximize detection probability, survey size was set by consulting the surveyors, who determined, in situ, 250 meters as the maximum range for consistently and accurately detecting and identifying shorebirds under the present survey conditions. Transects were conducted by either walking or while in a boat when the shoreline was inaccessible or untraversable. Transect length and duration was determined largely by accessibility and tidal conditions during survey periods. Efforts were made to distribute transects across tidal stages and a variety of habitat types including mangrove creeks, sand flats, mudflats and beaches. A total of 700 survey points were recorded across the study region between the two survey periods, with 60% used for model calibration, and the remaining 40% for model validation.

2.2b - Climatic Variables

Climate variables were derived from the WorldClim data set (Harris et al. 2014, Fick and Hijmans 2017) which provides historical climatic data in raster grid cell form (monthly averages from 2010 to 2018) at a scale of 30 seconds. Rasters were first masked to the study area to limit

processing time. Each variable was calculated based on averaging the pixels from the monthly data of the months between October and April, the approximate time that migratory species occupy northern Brazil. These “averages during migration stay” rasters were then resampled to match the 30 meter² resolution of the Landsat data.

2.2c - Remote sensing methods

Landsat 8

Landsat 8 Surface Reflectance Code (LaSRC) imagery products

(<https://www.usgs.gov/media/files/landsat-8-surface-reflectance-code-lasrc-product-guide>) were acquired for the entirety of the study area. LaSRC imagery, produced by the USGS are processed to account for atmospheric scattering or absorption, resulting in normalized surface reflectance values for each image. Due to the equatorial location of the Brazilian study site, cloud cover was a major issue, severely limiting image choice with a large number of available images having significant cloud cover (> 40%). As such, no preference was given to date or time of year for each image, only for cloud percentage and tidal stage. To compensate, multiple high tide and low tide images for each scene were acquired, totaling in 20 high tide and 27 low tide images from 2013 to 2018. Clouds and cloud shadows were removed using the Landsat 8 surface reflectance values and top-of-atmosphere thermal data via the methods outlined by Martinuzzi et al (2007). In short, thresholds were used to determine cloud cover, which was shifted and expanded to cover corresponding shadows. The clouds and shadows were masked by the combined cloud and shifted-expanded shadow rasters. For each scene, the cloud-masked images were composited by filling in cloud/shadow gaps of one image, with the cloud/shadow free regions of the other images. Composite images were created for both high tide and low tide imagery for each scene in the Brazilian study region, then mosaicked together, to create a site-wide image for analysis that encompassed seven Landsat reference tiles, or approximately 207000 square kilometers.

For all images, tidal stage was determined by the methods outlined by Murray et al. (2012), using Oregon State University's Tidal Model (Egbert and Erofeeva 2002), the date and time of each image's acquisition, and a user established reference point for each scene. The Oregon State University Tidal Model is a generalized inverse model of barotropic ocean tides, with versions designed at both global and select regional scales (<http://volkov.oce.orst.edu/tides/>). One of the regions with a specifically calibrated tidal model was the Amazonian drainage basin, where the Brazil study is located.

Sentinel 1

Vertical-vertical (VV) and vertical-horizontal (VH) polarized C-band images from the Sentinel 1 C-SAR Level-1 Ground Range Detected products (<https://sentinels.copernicus.eu/web/sentinel/home>) were acquired via Copernicus Open Access Hub (<https://scihub.copernicus.eu/dhus/#/home>). Tidal stage was determined using the same methods outlined above, with three images acquired per scene, totaling 15 low tide images for the Brazil study area. A 3x3 mean filter was used for noise reduction and then images were coarsened to 30 meter pixels to match the resolution of the Landsat data. For each scene, the mean pixel value of the three processed images was used to account for minor variations in tidal stage, orthorectified to the Landsat 8 data, then mosaicked together resulting in a low tide vertical-vertical image and vertical-horizontal image for the study region.

2.2d - Landscape Metrics (Figure 2.3)

Distance to rivers

Rivers can influence both the nutrient content (Riera et al. 2000) and sediment composition (Yamada et al. 2012) of coastal ecosystems. The nutrient and sediment changes can influence invertebrate distributions, subsequently, shorebird distributions. To account for this possibility, a point was digitized for every river that empties into the study region, determined using

hydrological data and visual interpretation of satellite data, resulting in 228 points representing different river mouths. Using these points, a Euclidean distance raster was generated with a 30 meter pixel resolution, estimating the distance of each 30 meter pixel from a river mouth.

Distance to developed areas

Disturbance from human activities could influence shorebird foraging behavior and subsequent distributions across intertidal flats (Burger 1986, Burger et al. 2007, Burger and Niles 2013). As a proxy for disturbance potential, a raster of Euclidean distance to developed areas was generated. Developed areas were determined through satellite image interpretation, aided by Brazilian census data. Regions with significant populations and noticeable footprints, typically villages with a number of buildings and permanent infrastructure like docks and powerlines, were represented by digitized points where developed areas intersected with coastal habitat. Mean distance of each plot was used in the model.

Distance to Mangroves

Mangroves are often utilized by a variety of shorebird species as refuge or roosting habitat. Proximity to mangroves has been demonstrated in previous research as an important component in habitat choice for some shorebirds species in some migratory locations (Lunardi et al 2012, Zwarts 1988). Mangroves are a dominant component of the landscape in northern Brazil and earlier work in the region indicates that they may play an important role there as well (Kober and Bairlein 2009). Mean distance was calculated for each plot and utilized in the Maxent model.

Tidal exposure

How often different segments of a tidal flat are exposed throughout a tidal period may also influence shorebird foraging patterns (Burger et al. 1977). To estimate what portions of flats are exposed at low and mid tides, additional imagery taken at mid-tide was acquired and processed in

the same fashion as described above to isolate the intertidal zone. This, combined with the low tide intertidal area already isolated, resulted in a raster where the intertidal zone was differentiated into two categories: areas exposed at low tide and areas exposed at mid tide. The most common value of each plot was then used as the habitat metric.

Permanence

Site fidelity, or individuals using the same location from one year to the next, is highly prevalent in some overwintering locations for some species of migratory shorebirds (Leyerer et al. 2006, Warnock and Takekawa 2008). Permanence, or the approximately likelihood of any given patch of intertidal zone existing from one year to the next, may be an important characteristic that species use to determine habitat value. A crude metric of permanence was developed based on the intertidal imagery accrued for this project. For each pixel, the intertidal zone was delineated in two images, one from an earlier date and one from a later date. Because of the challenges associated with cloud-free, tide-specific image acquisition at the site, replicating consistent dates or even date ranges was impossible. As such, “old” and “new” imagery ranged between 1 and 3 years apart in age. Each pixel was then categorized as: present *only* in the earlier image (1), present *only* in the later image (2), or present in both earlier and later images (3). The mode, or most common value was then calculated for each plot.

2.2e - Isolating intertidal region

While surveys were conducted to a maximum of 250 meters from the tidal edge, significant portions of that survey region were often not intertidal foraging habitat, e.g. water, sand dunes, or mangroves. These features, while often noted, were not considered when counting foraging wading birds. Only regions clearly within the intertidal zone were examined and recorded for the purposes of identifying foraging habitat during the survey. Because of this, looking at all remote sensing and landscape data within the 250 meter plots could include features

not part of the intertidal region, leading inaccurate assessments of the spectral characteristics of the intertidal foraging area surveyed (Figure 2.2). To compensate for this issue an intertidal zone-only mask was developed for both locations using methods outlined by Murray et al. (2012). A Normalized Difference Water Index ($NDWI = (Green - Near\ Infrared)/(Green + Near\ Infrared)$) was calculated using the mosaicked imagery, enhancing the presence of surface water. Water tends to have higher reflectance in the Green Wavelengths than in the Near Infrared; on land this is often reversed. Where water is present, the difference between Green and Near Infrared will be positive. A threshold was determined by visual inspection to designate all NDWI values above the threshold as water, all values below the threshold as land, for both high tide and low tide images. The high tide classified land image was then differenced from low tide land image, isolating the intertidal zone. This binary intertidal zone was used to mask the cloud free Landsat 8 surface reflectance, smoothed Sentinel 1 backscatter data, landscape metrics, and climate variables averaged over the migration stay.

2.2f - Species Distribution Modeling

Data Preparation

A single value was estimated for each environmental parameter for each survey point based on summary statistics of the intertidal pixels that fell within the 250 meter radius region of each survey point: mean and standard deviation of pixel values for each remote sensing band, mean distance to rivers, mean distance to developed areas, mode of tidal exposure and permanence values, mean average temperature, lowest minimum temperature, highest maximum temperature, mean average solar radiation, mean average precipitation, and mean average wind speed. For each species, points were either designated as presence points, where a sighting was recorded, or absence, when no sighting of that species was recorded. Sixty percent of the data was then randomly assigned to “calibration data”, while the other forty percent was reserved as “validation data” (Table 2.1). Input data for MaxEnt were the records of presence for each species with the

summary of pixel values for each environmental variables within the intertidal masked 250 meter survey plots. To match the scale of survey plots and input data to projected data, environmental layers were generated using 250 meter radius moving window filters and the original layers. For example, each remote sensing band had two layers, one where each 30 meter pixel represented the mean of all 30 meter pixels within a 250 meter radius in the original raster; another where each 30 meter pixel represented the standard deviation of all 30 meter pixels within a 250 meter radius.

MaxEnt Modeling Package

Maxent estimates the probability of presence conditioned on the environment using presence-only data. Presence-absence models, with data sets of presence and absence records, determine the probability of presence as a function of environmental variables, utilizing the proportion of occupied sites in the landscape (prevalence). Presence-only models like Maxent, lack absence data and inherently cannot calculate prevalence. Maxent estimates the probability of presence starting with the ratio of the conditional density of the covariants at the presence sites, and the unconditional density of covariates across the whole landscape using an exponential model. The output is transformed to a logistic model, with the transformed prevalence value (transformed to “Tau”) arbitrarily set to a constant 0.5 (Elith et al. 2011). I used MaxEnt version 3.4.1 (https://biodiversityinformatics.amnh.org/open_source/maxent/) with the leave-one-out cross-validation approach where the calibration occurrence data (60% of all data) is randomly split into 10 equal-sized “folds”, the model is run 10 times with a different fold left out each time for evaluation, and then the average of all runs is used in the final evaluation. To account for overfitting of the model, a ‘bias’ file was generated using the 250-meter buffered survey points. Bias layers act as exclusionary regions by Maxent when generating the background samples so that the background data is sampled from where surveys occurred, so that the pseudo-absence background data has the same sample biases as the survey data itself. For each of the eight

species, seven models were run: one for each set of landscape, remote sensing, and Worldclim variables on their own; one for each pair of variable sets (landscape-remote sensing, landscape-Worldclim, remote sensing-Worldclim); one using all three sets of variables (landscape-remote sensing-Worldclim). This resulted in a total of 56 models (eight species * seven models per species).

Maxent evaluates each variable within the model based on the metrics of “percent contribution” and “permutation importance”. Percent contribution is derived during the iterative model training process, where variables contribute either negatively or positively to model response each iteration, with these contributions summarized by the percent contribution value. Permutation importance is derived when training presence and background variable data are randomly permuted, with subsequent models evaluated based on drop in training AUC scores, normalized as percentages. In other words, each variable is evaluated by assigning a random value to it, and seeing how poorly the models function with the randomly assigned value compared to the actual data. The two metrics, percent contribution and permutation importance, can then be used to interpret the importance of different variables for model function (Phillips et al. 2006, Elith et al. 2009, Elith et al. 2011).

A common approach to overall model evaluation uses measures of predictive success, specifically the area under the curve (AUC) scores generated by Maxent. Receiver operator curves (ROC) are generated by plotting model sensitivity (proportion of correctly classified presence) as a function of commission error using, not true absences, but pseudo-absences generated from background data. AUC scores serve as summaries of these plots, indicating the probability that true presence will have a higher model output than a true absence or, in the case of Maxent, a pseudo-absence (Phillips et al. 2006). AUC scores can be useful tools for discriminating between models, though some criticism points out that, unlike other metrics of model performance (e.g. AIC, BIC), AUC does not penalize models for the numbers of variables

it uses. In other words, AUC scores do not prioritize parsimony, and can result in exceptionally complex models whose biological significance is difficult to determine (Golicher et al. 2012).

Amarel Computer Cluster

Because of the volume of models (56 total models), Rutgers' Amarel Computer Cluster (<https://oarc.rutgers.edu/amarel/>) was utilized to dramatically increase the speed of model run-times. Environmental variable rasters and presence records were imported into the Amarel system, and Maxent was run utilizing the Amarel Computing Cluster's drastically increased processing power, reducing model run times from approximately 24 hours per model, to approximately 2 hours per model. A detailed explanation of this process is available in the Appendices.

Validation

Outputs of Maxent models were summarized for the area within each of the reserved validation points. For each species, validation data was split into presence points, where the respective species was observed, and absence points, where the species was not observed (Table 2.2). Welch's T-Test was used to determine if the mean predicted probability of presence (the Maxent output) values for the presence points were significantly different than the mean Maxent values for the absence point. Welch's T-Test is designed for populations with unequal variances, but does assume a normal distribution of values within the population. This approach to validation was repeated for each species model, with their respective presence and absence points.

2.3 - Results

Model AUC and Validation results

Half of the models (Table 2.2) had higher AUC scores than the suggested minimum for useful discrimination of 0.75 (Elith et al. 2006), two had AUC scores near the minimum (semipalmated plovers 0.726, semipalmated sandpipers 0.718) and two were well below the minimum threshold

(ruddy turnstones and red knots). The mean model outputs of the validation points were significantly different (Welch's T-Test, $p < 0.05$) between presence and absence points for most models, with the exceptions of sanderling and black bellied plover models (Table 2.2).

Variable significance

Of the top reporting model for each of the eight species (highest AUC values with T-Test $p < 0.05$), all but one (BBPL) used the landscape variables, and five (ruddy turnstones, sanderlings, semipalmated plovers, whimbrels, willets) utilized all landscape, remote sensing, and Worldclim variables (Table 2.2).

Of the thirty-two models across all species that included remote sensing values, 23 of the 32 (72%) included the mean of vertical-horizontal backscatter for the plot ("b8mean"), and 21 of the 32 models included the standard deviation of vertical-horizontal backscatter ("b8std") in the top 5 contributing variables. Of the landscape variables, permanence was the most common with 27 of the 32 models (84%) including it in the top 4 variables based on either percent contribution or permutation importance. Distance to mangroves was also prevalent in 24 of the 32 models (75%) that included landscape variables. For several species (black bellied plovers, ruddy turnstones, semipalmated sandpipers, whimbrels), mangrove distance played a significant role in every model it was included in. Distance to developed regions was in the top 4 for 18 of the 32 models (56%).

2.4 Discussion

The models I developed successfully estimated the predicted probability of presence. Using the criterion of $AUC \geq 0.75$ as a threshold metric for model suitability (Elith et al., 2006), the MaxEnt models for ruddy turnstone, whimbrel, and willet qualify as valid predicted probability of presence estimates (Table 2.2). The remaining species' models (black bellied plovers, red knot, sanderlings, semipalmated plovers, semipalmated sandpipers), while having

AUC scores that suggest unreliability in terms of differentiating between likely and unlikely habitat ($AUC < 0.75$), all reported at least one model with significant differences of predicted probability of presence between presence and absence validation points (Table 2.2). Furthermore, presence validation points consistently reported higher predicted probability of presence compared to absence points for models of each species (Figure 2.4), indicating that models successfully discriminated between presence and absence points. Several models were considered viable in terms of both AUC and presence-absence validation, but model choice based on these two metrics presented its own questions.

The two metrics of model efficacy, AUC and T-test comparing presence-absence validation points, did not always corroborate each other. For example, the only black bellied plover model to have significant differences between presence and absence validation points also had the second lowest AUC score for the species, which was below the suggested threshold (model $AUC = 0.703$ vs threshold AUC of 0.75 , Table 2.2). With the goal of presence-only models accurately predicting presence of a species, it would be expected that model evaluation metrics reflect the effectiveness of models in discriminating between presence and absence points. With our models, this does not appear to be the case. Across all species, models with higher AUC scores were not more likely to pass the validation test, with no significant difference in AUC scores for models that passed the validation versus those that did not (T-Test p -value = 0.2284). It is possible that further independent validation may be needed to confirm the effectiveness of these models, which could be possible in future work utilizing either independent, on-the-ground surveys, or aerial surveys like those conducted by Morrison et al. (2012). The model evaluation metric itself may contribute to this discrepancy. There has been criticism of using AUC scores for model evaluation, particularly in comparison to more conventional metrics like Akaike or Bayesian information criteria. Criticism is largely centered around AUC lacking penalization for the number of variables used in a model. This can result in prioritizing highly complex models with large numbers of variables whose biological significance

cannot be interpreted (Golicher et al. 2012). With AUC score held up as the standard metric for evaluating Maxent model efficacy, understanding the relationship between AUC scores and independent validation data needs further investigation.

One possible explanation for the discrepancy in the two metrics of model efficacy is the bias layer that was utilized to prevent overfitting. A bias mask layer can be used in the Maxent package to compensate for areas that were oversampled by the survey effort, typically a mask of the survey area itself or occurrence data of taxonomically related species. In this case, surveys were typically conducted in areas that were easier to access via boat or walking. Areas outside the mask are then excluded from the background sampling, ensuring that the background pseudoabsences have the same sample biases as the occurrence data (Phillips et al. 2009). It is possible that our bias file may be overcompensating, as models run without the bias file had much higher AUC scores that more closely aligned with the T-Test of the validation points. For example, a red knot model with a bias layer included had an AUC score of 0.552, while the same model run without a bias layer reported an AUC score of 0.698, with both models reporting statistically significant differences between presence and absence validation data. It may be that our study design was still sufficiently random given the nature of how transects of survey plots were selected.

Remote sensing metrics proved to be important variables for determining predicted probability of presence in 5 out of the 8 top performing models when defining “top performing” as the models with highest AUC score with significantly different presence and absence validation points (Table 2.2). Models typically responded to the mean remote sensing values of plots in a manner consistent with previous findings on remote sensing and sediment size. Maxent generates two response curves for each variable: one where each other variable remains constant as the variable in question is varied, and one where the model was run *only* using the variable in question. I focused on the latter (Figures 2.4, 2.5, and 2.6), as they are easier to interpret if there are strong correlations between variables, which was likely for metrics like remote sensing

(Phillips et al. 2006). Black bellied plovers, ruddy turnstones, whimbrels, and willets all had model response negatively correlated with remote sensing reflectance values, with increased reflectance resulting in decreased model response. Radar backscatter had a positive correlation, with increasing model response as backscatter values increased (Figure 2.5). Based on previous research, northern Brazil exhibits decreasing reflectance and increasing backscatter in association with higher proportions of fine sediments, or mud (Chapter 1). Conversely, sanderlings had a positive correlation between model response and reflectance, with increasing responses as reflectance increased. Radar response was more ambiguous for sanderlings, though slightly stronger responses for lower radar backscatter values (Figure 2.5). In northern Brazil, high reflectance is typically associated with larger sediment size, e.g. sand substrate, as was lower backscatter values (Chapter 1). These results are reasonably consistent with previous research, which identified shorebird niches based on intertidal sediment microhabitats at other migratory locations (Bocher et al 2014, Burger et al 2018). For example, both willets and whimbrels prey extensively on fiddler crabs (Backwell et al. 1998), which typically make their burrows in finer, muddy substrate. Furthermore, Kober and Bairlein (2009) found on the Bragantian Peninsula in northern Brazil (which falls within this study region), that sanderlings preferred coarse substrate and black-bellied plovers preferred fine substrate, closely aligning with the model responses of both species. Remote sensing metrics responding consistently with shorebird ecology suggests potential future applications. MaxEnt models have regularly been used for projecting distributions of species by applying models calibrated on existing data to predicted future environmental variables (Araujo and New 2007, Phillips and Dudik 2008). The models developed here could be used to detect landscape-scale changes in habitat use by running the models on new, readily available remote sensing data acquired at future dates (Amici et al. 2017). Based on AUC scores, validation results, and prior understanding of the remote sensing-sediment relationship, MaxEnt models utilizing remote sensing metrics are viable estimates of predicted probability of presence,

grounded in ecological knowledge, and may be useful metrics for evaluating changes in habitat composition over time.

Of the landscape variables, distance to mangrove and permanence were both highly prevalent, with distance to developed areas also playing a role in some models. Black-bellied plovers, willets, and whimbrels again had similar responses, specifically to mangrove distance, with higher model response closer to mangroves (Figure 2.6). Mangroves can provide important refuge to some species of shorebirds (Lunardi et al 2012, Kober and Bairlein 2009, Zwarts 1988) and a major prey species, fiddler crabs (Backwell et al. 1998), possibly explaining the variable's impact on the models. When considering the two species most affected by the distance to developed regions variable, sanderlings and semipalmated sandpipers, the variable response was unclear. Sanderlings had a generally inverse relationship between distance to developed and model response, but semipalmated sandpipers responded most to middle distances. There is significant research supporting the effects of human disturbance on shorebird behavior and foraging (Navedo et al 2019, Tarr et al. 2010, Burger et al. 2007, Burger et al. 1986), which may explain the response of the sanderlings, but the biological significance of the semipalmated sandpiper response to distance to developed remains unclear. The metric of distance to developed area used here does not differentiate between the types of development or human use within the region. It has been demonstrated that shorebird species have different responses to different types of human disturbance (Tarr et al. 2010, Burger and Niles 2013, Burger and Niles 2017), which our metric does not account for. This discrepancy may also influence the varying response of sanderlings and semipalmated sandpipers.

While the crude metric of permanence that was developed appeared to be significant from a modeling perspective, interpreting its biological significance is tricky at best. Permanence was defined as one of three categories: intertidal only in an earlier image, intertidal only in a later image, or intertidal in both images. Image acquisition was limited based on relevant timeframes, tidal stages, and cloud cover, resulting in few images for comparison for each scene, with widely

ranging gaps between image dates. While there are obvious methodological limitations to this piloted approach, the results had significant effects on modeling. Many species, including sanderlings, semipalmated plovers, whimbrels and willets all responded most to pixels that fell into the second category, where most pixels in a plot were found in the later date, but not the earlier date (Figure 2.6). It could be interpreted that site fidelity is not as important to these species, otherwise sites that are consistently intertidal (the third category of the permanence metric) would be more highly ranked. As it stands, its biological significance remains unclear, though these results suggest a more thorough investigation of the concept of permanence would be beneficial. Recent work developing a set of global intertidal maps across the whole Landsat time series and Google Earth Engine (Murray et al. 2019) may prove to be a useful tool for developing a more robust metric of permanence.

Climate variables were highly prevalent in many models but proved to be rather difficult to parse. For example, average wind-speed was significant for both whimbrels and willets which had wind-speed response graphs that were nearly identical. Models responded inversely to wind-speed, with low wind speed having a higher response than high wind-speed (Figure 2.7). However, wind-speed only ranged from 1 to 2 meters per second, meaning that a relatively small increase in wind speed had a significant impact on model function. The models are supposed to reflect observed shorebird distributions which, in this case, suggests that shorebirds preferentially use intertidal habitat with slightly lower windspeeds. Similarly, temperature values ranged only 1 degree across the study site and had equally significant differences in model response between the upper and lower bounds (Figure 2.7). While theoretically possible, it seems unlikely that such marginal changes in climate have real biological significance to habitat use of highly mobile, endothermic species like migratory shorebirds. Though climatic variables are significant in distribution modeling of many other species and locations (Bradie and Leung 2017), their biological significance towards intertidal foraging habitat in northern Brazil may be limited. The study site is both near the equator, covers a relatively narrow range of latitudes, and the specific

habitat in question, the intertidal zone, is relatively homogenous in elevation and topography (Figure 2.8) unlike other studies utilizing climatic variables that span continents and latitudes. Between these site qualities, the specific habitat, and the species being modeled, it seems unlikely that the climate variables have real biological significance in this context.

There are areas for improvement with both the data and modeling approach. Some species, namely the red knot, had a very small sample size for calibration data ($n=16$). This likely is a major contributor to the poor model performance for the red knot and increasing sample sizes may also improve performance in the other species that had more moderate sample sizes. Increasing the sample size through either new sampling efforts or pulling from older records would be immensely helpful. However, this may present new challenges with the already difficult task of matching surveys to available (and cloud free) satellite imagery. Because of the difficulty associated with acquiring cloud free, tide-specific imagery, imagery often was not from similar timeframes as survey efforts, with some mismatches as extreme as years apart. While obviously not ideal, models and remote sensing metrics still performed well. Another issue with that may be a factor with the surveys and model is detection probability. Detection probability is likely a minor issue in this particular study due to both the species of interest, survey design, and modeling approach. Migratory shorebirds foraging on open flats are not nearly as difficult to detect as, for example, grassland birds (Diefenbach et al. 2003). Furthermore, surveys design specifically incorporated conservative estimates of the maximum distance that the highly experienced surveyors could correctly and consistently identify shorebirds. Finally, like all MaxEnt presence-only modeling approaches, our models do not inherently account for issues of detection probability and assumes detection probability is constant across the study region (Yackulic et al. 2013). Detection errors may influence the distribution of habitat use predicted by the models. Commission errors incorrectly identifying presence locations where no birds were found, may result in a broader predicted habitat use, while omission errors could result in more restricted extents of predicted habitat. Other modeling approaches, namely abundance-based N -

mixture models (Kéry and Royle 2016), can explicitly incorporate estimates of detection probability, and have successfully done so for shorebird abundance modeling (Studds et al. 2017). However, detection probability is still a significant issue in these types of models, and a MaxEnt approach significantly reduces those errors by ignoring absence data entirely, and requiring only a single confirmed sighting of a species, not accurate count estimates (Elith et al. 2011).

There are alternative modeling tools to the presence-only Maxent approach I utilized. The survey data used to calibrate Maxent models is originally an abundance data set, with absences noted as well. I opted for the presence-only Maxent approach because of the simplicity in model execution, and robust literature that supports both the general approach of presence-only modeling, and the Maxent modeling package specifically. Alternative modeling approaches may be useful for further discriminating habitat use, including Bayesian hierarchical generalized linear models based on presence-absence or abundance (Franklin and Miller 2009). Presence-absence modeling has some advantages over presence-only modeling, namely how presence-absence models manage prevalence (proportion of occupied sites) and sample biasing issues. Prevalence can be directly estimated in presence-absence modeling, unlike in presence-only modeling where statistical work-arounds and estimations are used as a proxy (Phillips et al 2006, Elith et al 2011). Sampling bias remains a problem in presence-only models, but in presence-absence, the bias in the presence data generally cancels out with the bias in the absence data, making it a non-issue (Zadrozny 2004). Future work fully utilizing the abundance survey data may lead to new conclusions about alternative model approaches and their effects on management decision making.

2.5 Conclusions

Distribution modeling using remote sensing values was successful at accurately classifying predicted probability of presence for some species (ruddy turnstones, whimbrels, willets) Internal model metrics, like AUC values, do not always corroborate external validation

methods, which can be problematic from a model-choice perspective and needs further investigation. Based on the discrepancies between AUC and validation t-tests, even best performing models still will require significant validation and testing using independent survey data. Models performing poorly according to AUC scores (black bellied plovers, red knots, sanderlings, semipalmated plovers, semipalmated sandpipers) may still provide model results that effectively differentiate between presence and absence points. Remote sensing variables, particularly vertical-horizontal radar backscatter and near infrared reflectance, contributed significantly to model function and were logically consistent with known biology. Climate variables, while often statistically significant, were not logically consistent with known biology, which may be due to the climatically homogenous nature of the study site. Finally, some landscape variables, like permanence, demonstrated modeling significance but their relevance to biological processes was difficult to parse and requires further refinement. Future efforts of making parsimonious, statistically sound, and biologically relevant shorebird distribution models for use in conservation and management decision-making in northern Brazil should utilize remote sensing and landscape metrics, as climatic variables appear biologically inappropriate for this context.

2.6 – Tables and Figures

Table 2.1: Common name, four-letter alpha code, and Latin name of the eight modeled migratory shorebird species. Listed for each species is the number of presence points used in model calibration, validation, and in total, as well as the number of reserved absence points used in validation.

Species Common Name	Alpha Code	Latin Name	Presence points			Absence points
			Calibration	Validation	Total	Validation
Black-bellied plover	BBPL	<i>Pluvialis squatarola</i>	126	83	209	159
Red Knot	REKN	<i>Calidris canutus rufa</i>	16	10	26	232
Ruddy Turnstone	RUTU	<i>Arenaria interpres</i>	76	53	129	189
Sanderling	SAND	<i>Calidris alba</i>	120	30	150	212
Semipalmated Plover	SEPL	<i>Charadrius semipalmatus</i>	109	64	173	178
Semipalmated Sandpiper	SESA	<i>Calidris pusilla</i>	204	75	279	167
Whimbrel	WHIM	<i>Numenius phaeopus</i>	183	105	288	140
Willet	WILL	<i>Tringa semipalmata</i>	113	67	180	175

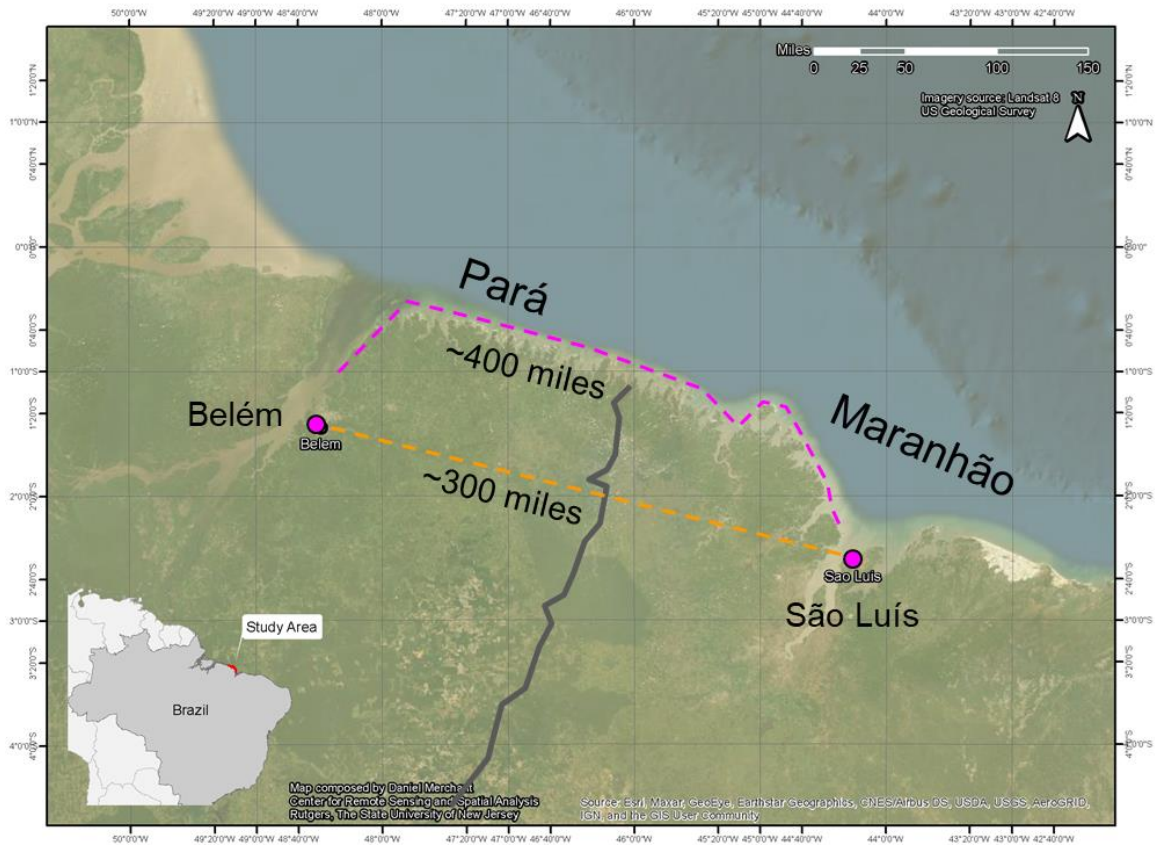


Figure 2.1: Study area located on the northern coast of Brazil (area in red on insert map, bottom left), straddling the states of Pará to the west, and Maranhão to the east. The coastline is roughly 400 miles long (purple), with 300 miles (orange) between the respective capitals of Belém and São Luís.



Figure 2.2: Surveys consisted of 250 meter radius plots (black) conducted along transects across beach and mud flats accessed either by boat or foot. To ensure that environmental variables sampled for plot characteristics only represented the intertidal zone, a mask (orange) was utilized to limit plot statistics to the intertidal zone.

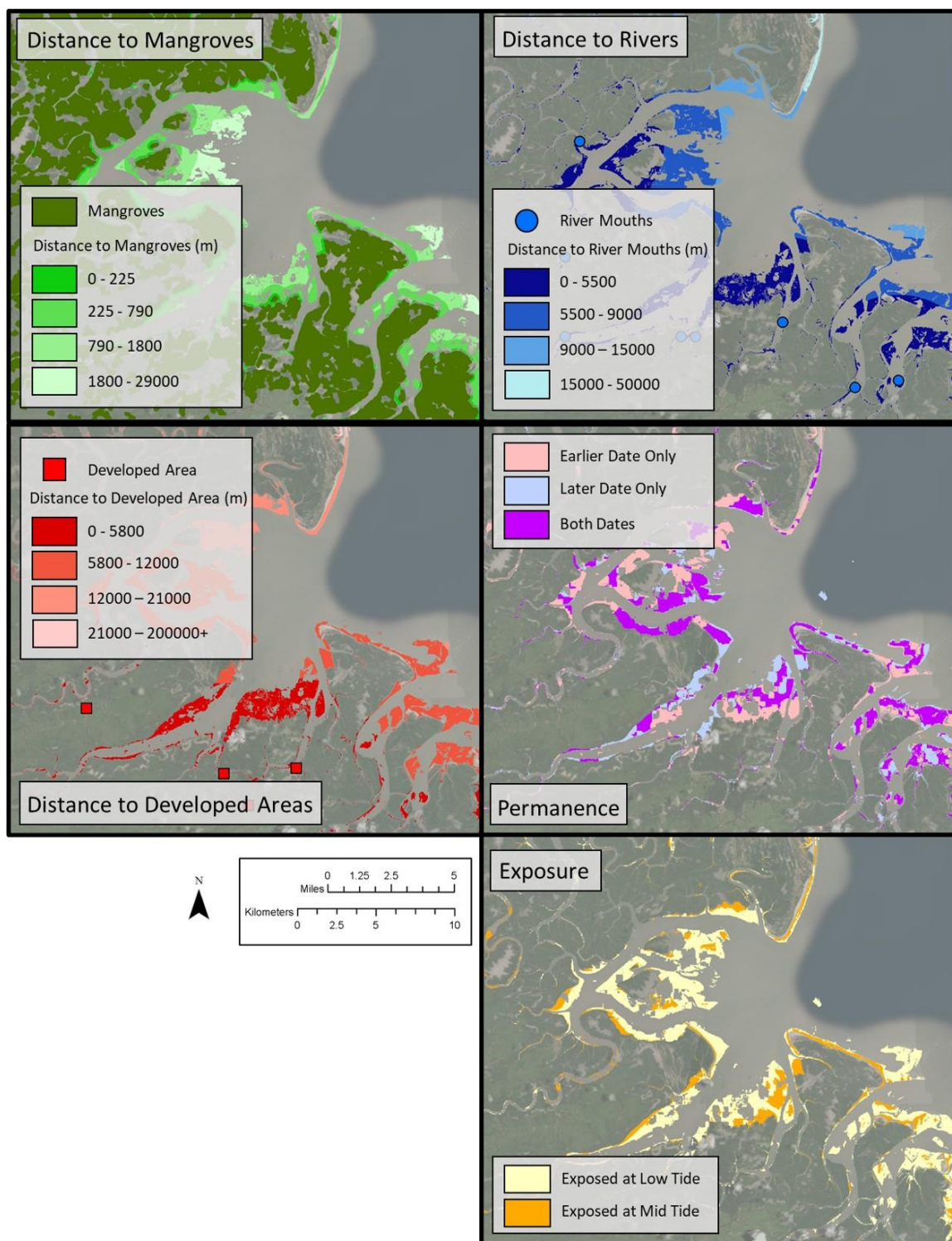


Figure 2.3: A sample of area of how the 6 landscape metrics are represented within the intertidal zone.

Table 2.2: AUC scores and T-Test comparing presence and absence points of reserved validation data for models that used the variable sets (landscape, remote sensing, and Worldclim) in isolation, pairs, and all together. Boxes in pink indicate models with AUC scores greater than the 0.75 threshold suggested for useful discrimination of presence (Elith et al. 2006), while boxes in blue indicate a model that passed the validation test with mean predicted probability of presence higher in presence points compared to absence points of the reserved validation data.

	Landscape Only		Remote Sensing Only		Worldclim Only		Landscape and Remote Sensing		Landscape and Worldclim		Remote Sensing and Worldclim		Landscape, Remote Sensing, and Worldclim	
	AUC	T-Test	AUC	T-Test	AUC	T-Test	AUC	T-Test	AUC	T-Test	AUC	T-Test	AUC	T-Test
BBPL	0.775	0.4392	0.629	0.5562	0.703	0.001166	0.783	0.5562	0.806	0.2746	0.746	0.0892	0.781	0.3675
REKN	0.572	0.0073	0.493	0.003	0.642	0.1747	0.504	0.003	0.561	0.05429	0.55	0.0395	0.552	0.046
RUTU	0.696	0.0545	0.671	<0.001	0.644	0.00389	0.709	<0.001	0.727	0.03675	0.734	<0.001	0.761	0.0011
SAND	0.584	0.8685	0.618	0.1941	0.709	<0.001	0.707	0.1941	0.73	0.00575	0.681	<0.001	0.744	0.0237
SEPL	0.654	0.6228	0.646	0.03546	0.712	0.4591	0.695	0.0354	0.724	0.0109	0.709	<0.001	0.726	0.029
SESA	0.652	0.1872	0.578	0.2321	0.67	<0.001	0.69	0.2321	0.721	<0.001	0.655	<0.001	0.718	0.0034
WHIM	0.752	0.0013	0.644	0.1543	0.672	<0.001	0.776	<0.001	0.789	<0.001	0.75	<0.001	0.791	<0.001
WILL	0.767	0.0023	0.712	<0.001	0.788	<0.001	0.841	<0.001	0.841	<0.001	0.827	<0.001	0.85	<0.001

Table 2.3.a: Top four contributing variables, either due to percent contribution or permutation importance, for each model based on species (left) and variable category (top). Boxes with pink highlight indicate models with AUC scores above the threshold for use based on previous literature (> 0.75). Boxes in blue represent models that pass the validation test, with presence validation points having significantly different ($p < 0.05$) predicted probability of presence from absence validation points based on a T-Test of plot means. Boxes in purple have both AUC scores above the threshold (> 0.75), and passed the validation test ($p < 0.05$). Red boxes indicate the best performing model for a given species, defined by the highest AUC score that passed the validation T-Test.

Species	Top Variables	Landscape Only		Remote Sensing Only	
		Percent Contribution	Permutation Importance	Percent Contribution	Permutation Importance
BBPL	1	mangdist, 67.1	mangdist, 50.3	b8std, 36	b3mean, 24.4
	2	exposure, 12.2	devdist, 28.5	b8mean, 11.1	b4std, 11.6
	3	devdist, 10.1	riverdist, 12.8	b9std, 7.8	b8mean, 11.6
	4	permanence, 6.5	exposure, 7.8	b1mean, 7.5	b1mean, 11.2
REKN	1	permanence, 75.2	exposure, 57.1	b8mean, 66.4	b8mean, 41.9
	2	riverdist, 11.6	permanence, 42.3	b1mean, 9.5	b8std, 16.9
	3	exposure, 11.4	devdist, 0.4	b6std, 5.1	b6std, 10.7
	4	devdist, 1.3	riverdist, 0.1	b8std, 4.4	b5mean, 9.7
RUTU	1	mangdist, 48.5	mangdist, 48.9	b8std, 38.5	b5mean, 34.8
	2	permanence, 21.8	riverdist, 24.5	b9std, 20.8	b8std, 12.6
	3	riverdist, 13.8	devdist, 14.5	b1std, 9.5	b1std, 10.6
	4	devdist, 10.5	permanence, 8.6	b5mean, 8.3	b4std, 8.6
SAND	1	permanence, 53	permanence, 49.3	b7mean, 20.1	b3mean, 21.2
	2	devdist, 20	devdist, 23	b4mean, 18.3	b4mean, 16.2
	3	riverdist, 17.2	riverdist, 18.4	b8mean, 18	b4std, 15.2
	4	mangdist, 9.6	mangdist, 9.3	b4std, 10.7	b1mean, 10.5
SEPL	1	mangdist, 47.8	mangdist, 50.4	b9std, 24.3	b2mean, 18.6
	2	permanence, 26.9	permanence, 17.2	b8mean, 17.8	b6mean, 10.9
	3	devdist, 13.6	devdist, 16.6	b8std, 13.7	b4std, 10.6
	4	riverdist, 8.4	riverdist, 8.4	b2mean, 10.3	b5mean, 10.5
SESA	1	mangdist, 36.8	mangdist, 44.8	b1mean, 19.4	b5mean, 18.4
	2	permanence, 35.4	devdist, 24	b8std, 15.8	b2mean, 13.1
	3	devdist, 20	permanence, 19.9	b5mean, 12.2	b8mean, 9.9
	4	riverdist, 6.1	riverdist, 9.6	b8mean, 10.1	b4std, 9.5
WHIM	1	mangdist, 62.7	mangdist, 51.5	b4mean, 43.5	b4mean, 16.5
	2	permanence, 19.4	devdist, 25.8	b8std, 10.6	b9std, 12.2
	3	devdist, 7.9	permanence, 11.9	b9std, 8.3	b6std, 11.7
	4	exposure, 5.9	riverdist, 6.9	b1mean, 7.8	b4std, 9.8
WILL	1	mangdist, 61.6	mangdist, 73.7	b3mean, 38	b3mean, 29.1
	2	permanence, 18.8	riverdist, 8.1	b8std, 13.2	b2mean, 10.7
	3	devdist, 8.8	devdist, 7.8	b8mean, 8.8	b8mean, 8.3
	4	riverdist, 8.3	permanence, 7.3	b4mean, 7.7	b4std, 7.6

Table 2.3.b: Top four contributing variables, either due to percent contribution or permutation importance, for each model based on species (left) and variable category (top). Boxes with pink highlight indicate models with AUC scores above the threshold for use based on previous literature (> 0.75). Boxes in blue represent models that pass the validation test, with presence validation points having significantly different ($p < 0.05$) predicted probability of presence from absence validation points based on a T-Test of plot means. Boxes in purple have both AUC scores above the threshold (> 0.75), and passed the validation test ($p < 0.05$). Red boxes indicate the best performing model for a given species, defined by the highest AUC score that passed the validation T-Test.

Species	Top Variables	Worldclim Only		Landscape and Remote Sensing	
		Percent Contribution	Permutation Importance	Percent Contribution	Permutation Importance
BBPL	1	tminmin, 38.4	precavg, 67.9	mangdist, 36.6	mangdist, 20.9
	2	precavg, 26	tmaxmax, 15.1	b8mean, 8.8	b6mean, 9.5
	3	tmaxmax, 15.2	tminmin, 9.1	b8std, 7.4	b5mean, 9.2
	4	windavg, 15.1	windavg, 5.8	exposure, 7.2	b8mean, 8.6
REKN	1	tmaxmax, 58	tmaxmax, 57.8	permanence, 44.2	permanence, 28.3
	2	windavg, 23.1	windavg, 29.4	b8std, 11.1	b8std, 23.5
	3	tavgavg, 16.5	precavg, 7.8	exposure, 8.5	exposure, 11.6
	4	precavg, 2.3	sradavg, 4.8	b2std, 6.8	riverdist, 7.3
RUTU	1	precavg, 45.7	precavg, 44.3	b8std, 35.2	b5mean, 26.6
	2	sradavg, 35.1	sradavg, 29.1	permanence, 14.5	b1std, 9.7
	3	tavgavg, 12.9	tavgavg, 12.6	mangdist, 11.2	b6mean, 8.5
	4	windavg, 3.7	tminmin, 12.9	riverdist, 7.1	b8std, 7.4
SAND	1	sradavg, 46.2	sradavg, 23.6	permanence, 21	permanence, 26
	2	tminmin, 18.3	tmaxmax, 22.7	b8mean, 13.6	b1std, 13.3
	3	precavg, 17.9	tminmin, 21.5	b6mean, 13.4	b7mean, 12.4
	4	tmaxmax, 7.5	windavg, 20.1	b1mean, 9.8	b8mean, 10
SEPL	1	tmaxmax, 42.2	tminmin, 37.7	b8mean, 18.6	b8mean, 20.7
	2	tminmin, 32.2	tmaxmax, 33.1	b8std, 17.7	b9mean, 11.3
	3	windavg, 12.8	precavg, 20.6	permanence, 12.6	b4std, 9.1
	4	precavg, 6.2	sradavg, 6.7	mangdist, 10.3	mangdist, 8.1
SESA	1	windavg, 44	windavg, 40	permanence, 18.3	b7mean, 9.3
	2	tmaxmax, 36	precavg, 34	mangdist, 16.6	mangdist, 7.5
	3	precavg, 9.1	tmaxmax, 19.9	devdist, 11.4	b3mean, 6.7
	4	tminmin, 5	tminmin, 2.5	b8mean, 9.6	b8mean, 6.3
WHIM	1	windavg, 35.6	precavg, 81.6	mangdist, 40.4	mangdist, 17.7
	2	tavgavg, 20.7	tmaxmax, 9.2	permanence, 13.1	b4mean, 13.9
	3	precavg, 20.6	tavgavg, 5.1	b4mean, 11.4	devdist, 10.5
	4	tmaxmax, 13.9	tminmin, 3.6	b9std, 5	b8mean, 9.9
WILL	1	windavg, 43.8	windavg, 29.4	mangdist, 24.1	b5mean, 21
	2	tmaxmax, 22.4	tmaxmax, 25.5	b3mean, 18.4	mangdist, 14.8
	3	tavgavg, 19.8	precavg, 16.8	permanence, 10	b8mean, 9.9
	4	tminmin, 8.9	tminmin, 13.3	b8mean, 7.3	riverdist, 5.4

Table 2.3.c: Top four contributing variables, either due to percent contribution or permutation importance, for each model based on species (left) and variable category (top). Boxes with pink highlight indicate models with AUC scores above the threshold for use based on previous literature (> 0.75). Boxes in blue represent models that pass the validation test, with presence validation points having significantly different ($p < 0.05$) predicted probability of presence from absence validation points based on a T-Test of plot means. Boxes in purple have both AUC scores above the threshold (> 0.75), and passed the validation test ($p < 0.05$). Red boxes indicate the best performing model for a given species, defined by the highest AUC score that passed the validation T-Test.

Species	Top Variables	Landscape and Worldclim		Remote Sensing and Worldclim		Landscape, Remote Sensing, and Worldclim	
		Percent Contribution	Permutation Importance	Percent Contribution	Permutation Importance	Percent Contribution	Permutation Importance
BBPL	1	mangdist, 49	mangdist, 36.4	b8std, 19.2	b8mean, 21.2	mangdist, 32.8	mangdist, 19.9
	2	devdist, 10.1	devdist, 24.7	tminmin, 17.5	b3mean, 16.7	windavg, 7	b8mean, 16.2
	3	windavg, 8.8	precavg, 19.7	windavg, 11.2	b2mean, 10.1	devdist, 6.8	b5mean, 12.1
	4	precavg, 7.6	windavg, 6	b8mean, 9.8	b9mean, 6.7	b8std, 6.3	devdist, 7
REKN	1	tmaxmax, 40	permanence, 31.5	tmaxmax, 41.6	tmaxmax, 25.6	tmaxmax, 26.9	b8std, 22.3
	2	permanence, 36.2	exposure, 26.1	windavg, 16.8	b8std, 15.5	permanence, 25.9	tmaxmax, 14.3
	3	tavgavg, 8.6	tmaxmax, 17.5	tavgavg, 12	b9std, 12.9	b8std, 11.3	exposure, 14.1
	4	windavg, 6	riverdist, 13.5	b1std, 5.6	b6std, 10.7	b1std, 5.9	permanence, 9.1
RUTU	1	mangdist, 45.3	mangdist, 51	b8std, 36.3	b5mean, 33.5	precavg, 17.2	precavg, 12.8
	2	permanence, 21.4	precavg, 15.3	precavg, 9.3	b8mean, 11.1	b8mean, 11.9	b8std, 11.1
	3	devdist, 9.2	riverdist, 9.8	b5mean, 8.8	b6mean, 9.6	permanence, 11.1	mangdist, 10.7
	4	riverdist, 7.3	devdist, 7.7	sradavg, 8.5	b1std, 9.4	b9mean, 10.4	riverdist, 9.5
SAND	1	permanence, 28.7	sradavg, 25.5	b7mean, 21.4	sradavg, 22	permanence, 19.2	sradavg, 11.9
	2	sradavg, 21.3	permanence, 16.6	sradavg, 19.8	b1std, 12.5	b6mean, 11.1	devdist, 11.4
	3	precavg, 10.8	precavg, 15.2	tminmin, 13.8	b4mean, 9	b1mean, 9.8	permanence, 11.1
	4	riverdist, 9.7	tmaxmax, 12.3	b1mean, 8.6	tminmin, 6.6	sradavg, 9.6	b4mean, 8.3
SEPL	1	tmaxmax, 38.5	mangdist, 21.1	tmaxmax, 29.6	b1mean, 13.8	tmaxmax, 25.7	b8mean, 13.6
	2	permanence, 11.7	riverdist, 16.6	tminmin, 21.7	b5mean, 10.1	b8std, 8.4	b1mean, 10.1
	3	tminmin, 11.4	precavg, 12.8	windavg, 8.5	b9mean, 9.9	permanence, 7.9	b9mean, 8
	4	windavg, 10.7	permanence, 11.6	b8mean, 7.4	b8mean, 8.9	tminmin, 7.7	b5mean, 7.5
SESA	1	tmaxmax, 24.4	precavg, 34.9	windavg, 26.7	b5mean, 23.6	tmaxmax, 15.4	b5mean, 19.2
	2	permanence, 18	devdist, 21.5	tmaxmax, 22.2	b1mean, 13.4	mangdist, 12.5	devdist, 8.3
	3	mangdist, 17.3	mangdist, 16.2	prprecavg, 6.8	windavg, 9.1	permanence, 11.9	mangdist, 8.2
	4	windavg, 14	windavg, 8.1	b5mean, 6.5	b7mean, 8.9	windavg, 10	b8mean, 7.6
WHIM	1	mangdist, 49.9	precavg, 33.5	b8std, 17.6	b8mean, 15.8	mangdist, 35.2	b8mean, 18
	2	permanence, 15.8	mangdist, 26.1	windavg, 13.8	windavg, 10.8	permanence, 11.4	b5mean, 13.2
	3	windavg, 6.8	devdist, 17.6	tavgavg, 7.9	b5mean, 9.6	windavg, 6.8	windavg, 8
	4	devdist, 5.2	permanence 4.4	b4mean, 7.8	b2mean, 8.8	b8std, 4.5	mangdist, 7.9
WILL	1	mangdist, 27.8	mangdist, 46.2	windavg, 30	b9mean, 14.6	mangdist, 21.8	windavg, 16.7
	2	windavg, 22.8	windavg, 15	tmaxmax, 13.2	b5mean, 12.8	windavg, 19.1	b8mean, 15.3
	3	tmaxmax, 13.9	precavg, 13.4	tavgavg, 12.8	windavg, 9.8	tavgavg, 11.1	mangdist, 14.8
	4	tavgavg, 13	devdist, 8.6	b8std, 7.8	b8mean, 9.6	tmaxmax, 10.8	b5mean, 13

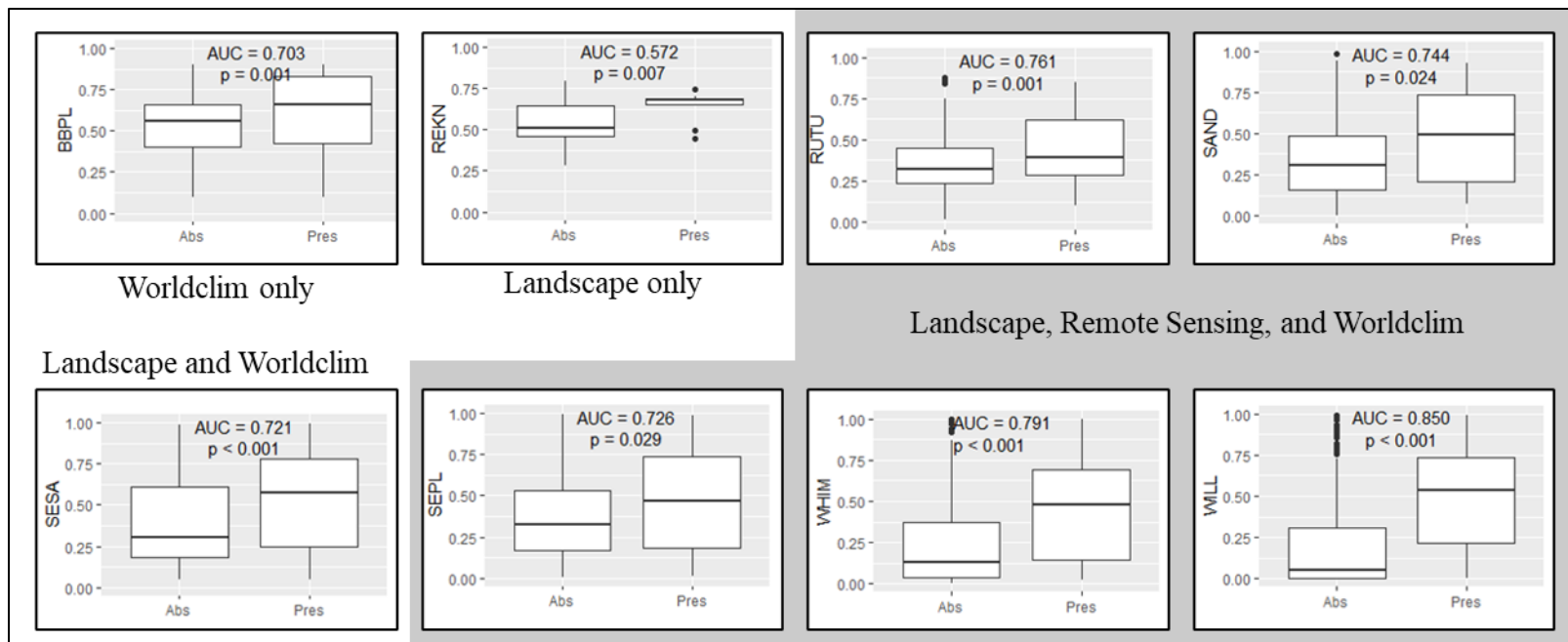


Figure 2.4: Box-and-whisker plots comparing the mean predicted probability of presence between presence and absence validation points of the top performing model for each species. Top models were the Worldclim only model for Black-bellied plovers (BBPL), Landscape only model for Red Knots (REKN), the Landscape and Worldclim model for Semipalmated Sandpipers, and the model using all three sets of variables was the top performing model for the remaining species (Ruddy Turnstones - RUTU, Sanderlings – Sand, Semipalmated Plovers – SEPL, Whimbrels – WHIM, and Willets – WILL). Mid-lines of the boxes represent the median, while the boxes above and below the midline represent the first upper and lower quartiles, vertical lines represent the upper and lower second quartiles, and dots represent outliers.

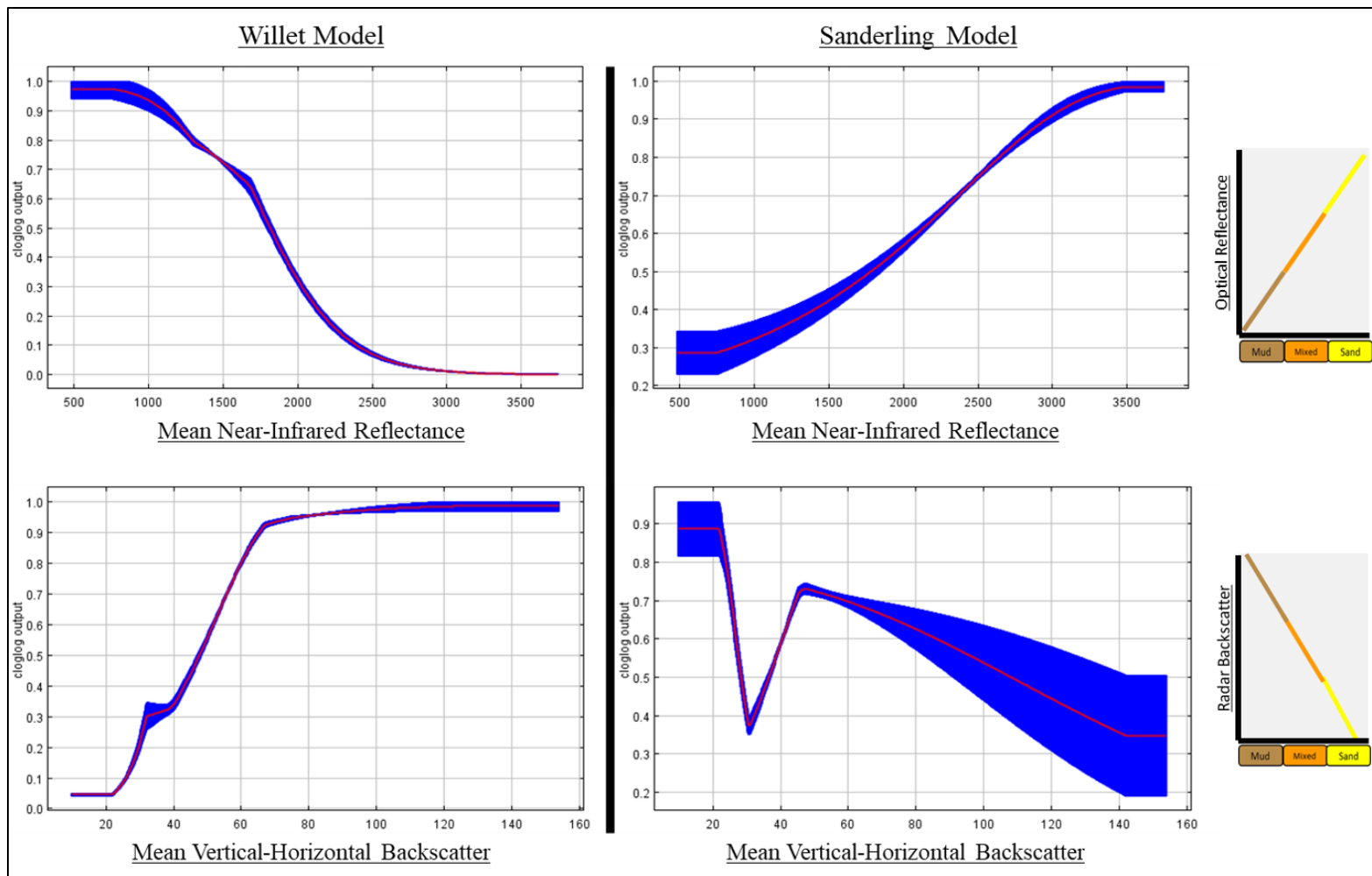


Figure 2.5: Model response for selected remote sensing variables of Willet and Sanderling models that used all variable classes (landscape, remote sensing, and climatic variables). Variable value is on the x-axis while model response is on the y axis. Red lines represent the average model response based on all 10 replicate runs, with the blue band represent the standard deviation based on those replicate runs. Also provided on the right are graphs representing the approximate relationship between optical reflectance (y-axis top), radar backscatter (y-axis bottom), and sediment size (x-axis both), as determined for Northern Brazil (Merchant et al. 2020).

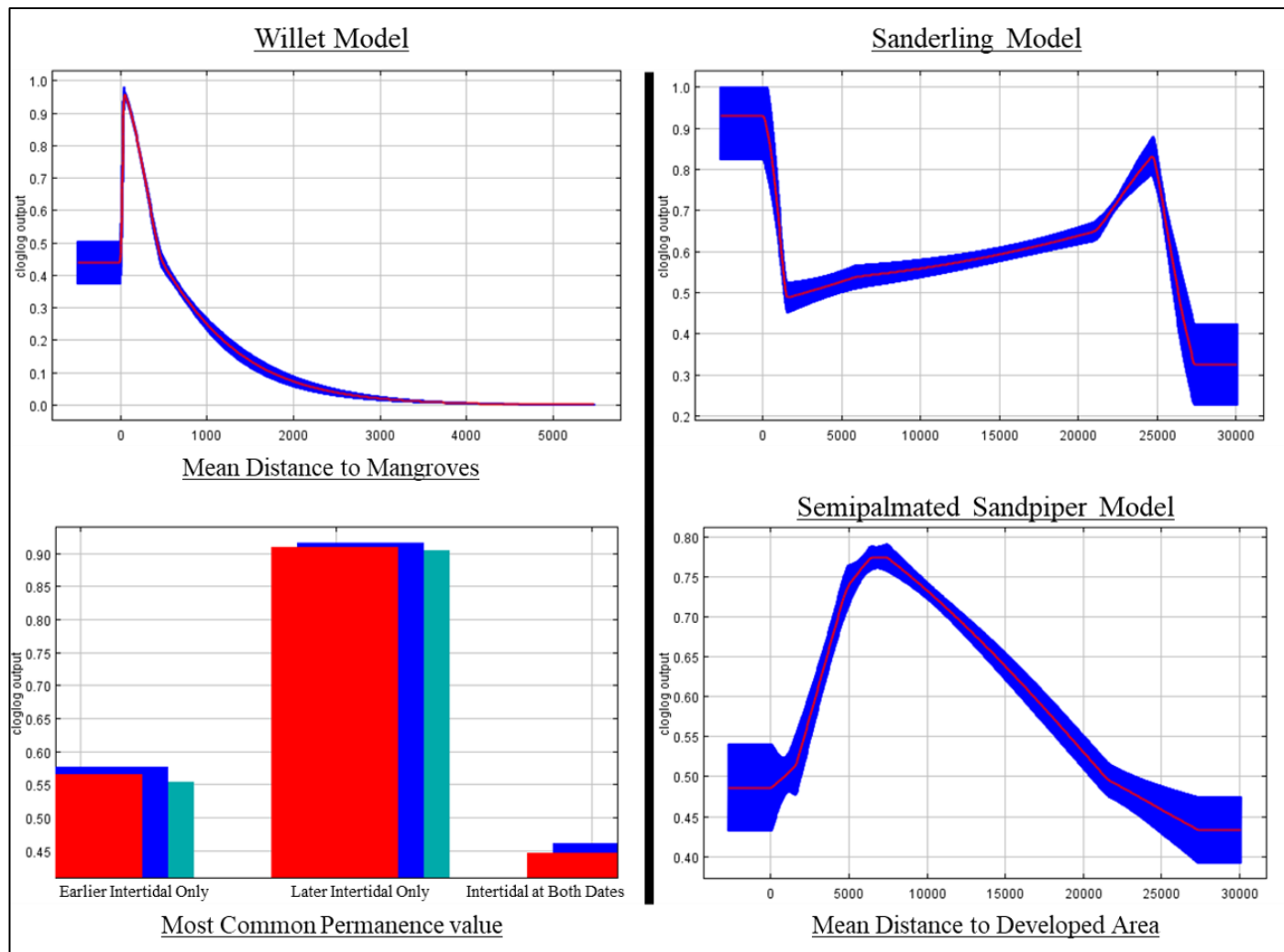


Figure 2.6: Model response for selected landscape variables of Willet and Sanderling models that used all variable classes (landscape, remote sensing, and climatic variables). Variable value is on the x-axis while model response is on the y axis. Red lines represent the average model response based on all 10 replicate runs, with the blue band represent the standard deviation based on those replicate runs.

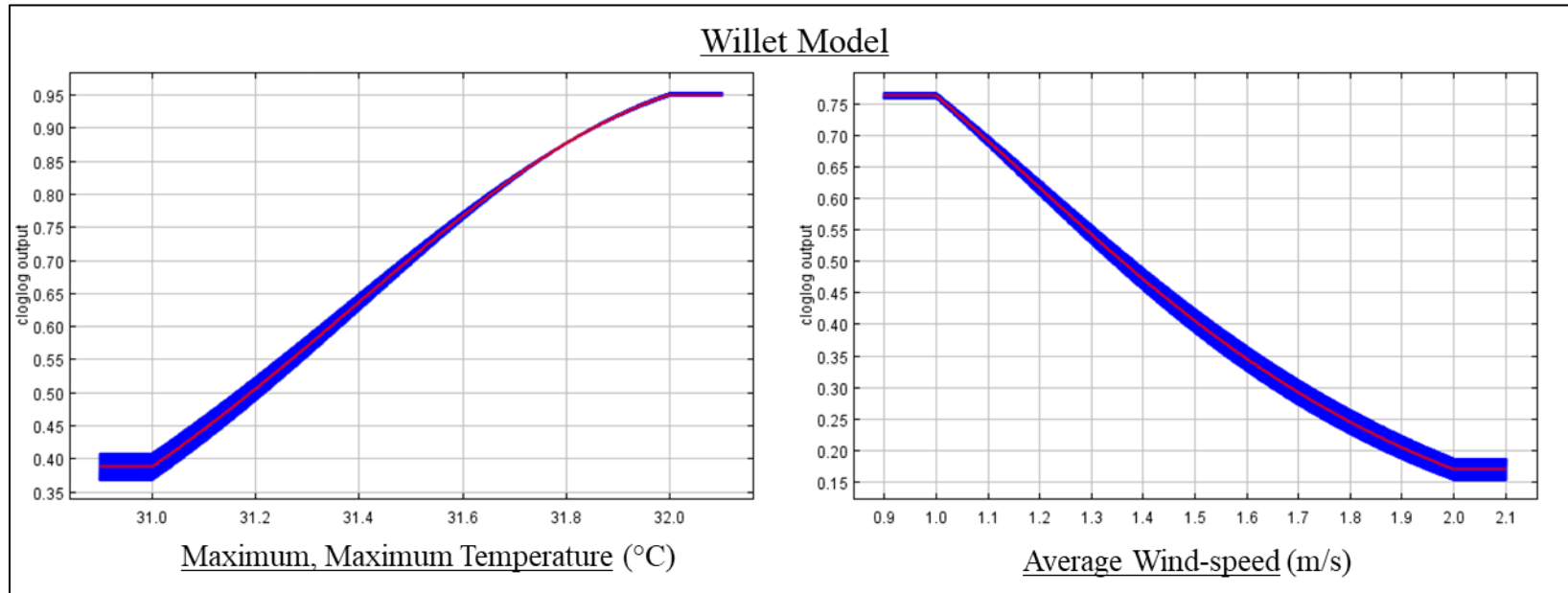


Figure 2.7: Model response for selected climatic variables of willet models that used all variable classes (landscape, remote sensing, and climatic variables). Variable value is on the x-axis while model response is on the y axis. Red lines represent the average model response based on all 10 replicate runs, with the blue band represent the standard deviation based on those replicate runs.

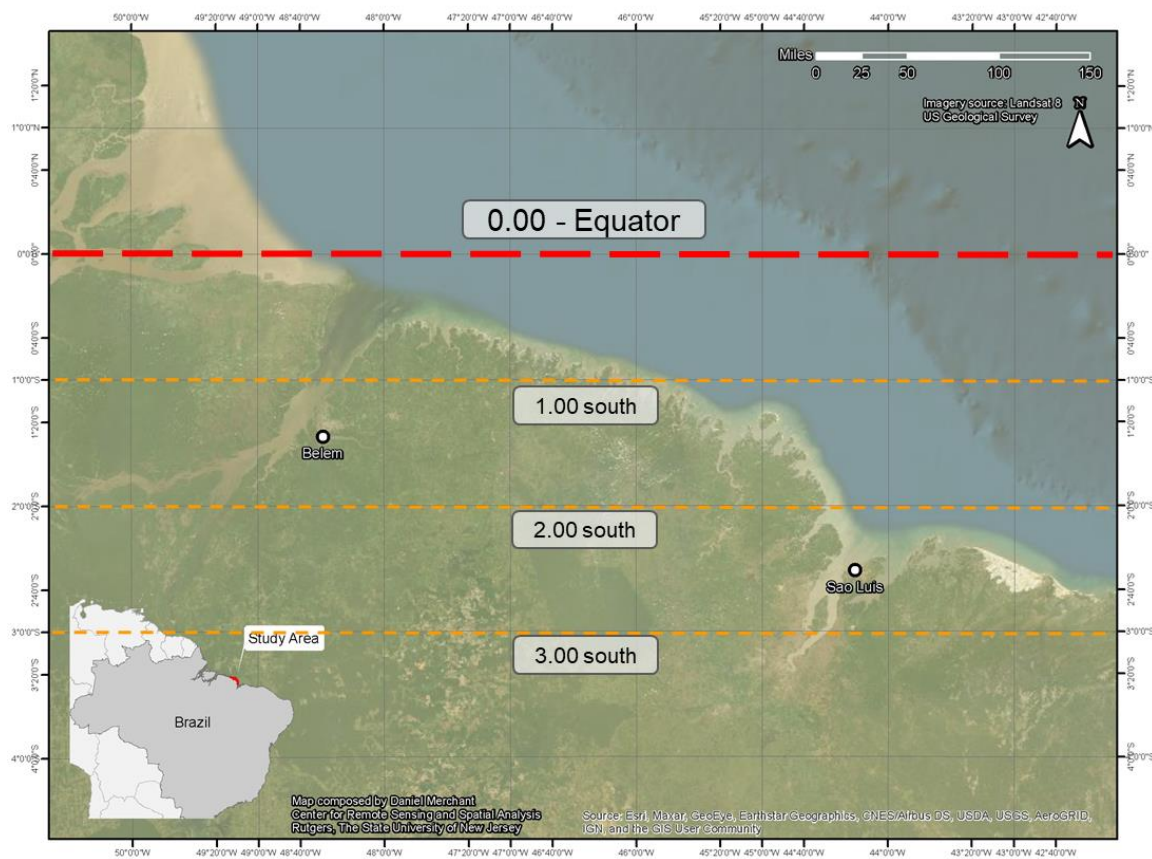


Figure 2.8: Map of study area with latitude lines denoted. Study area is limited to a narrow latitudinal range between the equator and about 3 degrees south of the equator, making it relatively homogenous from a climatic perspective.

Chapter 3: Multispecies Conservation Decision Making

3.1 - Introduction

Shorebird species along the Atlantic American coastline, like Red Knots (*Canutus rufa rufa*) and Semipalmated Sandpipers (*Calidris pusilla*), make annual migrations from breeding grounds in the Canadian high Arctic, to overwintering grounds across South America, including the northern coast of Brazil (Colwell 2010, Niles et al. 2010, Gratto-Trevor et al. 2012, Brown et al. 2017). Because of their reliance on numerous, widely dispersed geographic regions for migratory and breeding success (Warnock 2010, Mizrahi et al. 2012), disruption to any component of their migratory route could lead to dramatic population declines. This fragility means that shorebirds can function as an indicator species, where population declines at any stage of their migration may indicate problems or disruption elsewhere (Piersma and Lindstrom 2004). Unfortunately, the current indication is that Neararctic migratory shorebirds are imperiled, with population numbers dropping globally (Clemens et al. 2016, Studds et al. 2017). The Atlantic Americas Flyway is no exception, with significant loss of populations during the 1980's and 90's, with more recent counts stable but well below conservation targets (Bart et al. 2007, Andres et al 2012b). Loss for many species has been closely linked to disruption at a key stopover location, Delaware Bay U.S.A (Baker et al. 2004), which has subsequently been intensely studied with management steps taken to address the problem (Burger et al. 2012, Niles et al. 2013, Burger et al. 2018). Other migratory stops are less thoroughly understood, including northern Brazil, which hosts one of the largest populations of overwintering shorebirds (Niles and Cooper Ornithological Society 2008). Understanding how migratory shorebird habitat is managed at this location is important for setting and meeting conservation planning goals.

Current protections of the key ecosystem in northern Brazil is largely structured around the Brazilian Extractive Reserve (ER) system. Managed by the Brazilian federal Chico Mendes Institute for Biological Diversity Conservation (ICMBio), Extractive Reserves are a type of protected area that differ from classic “fortress” conservation which aims to prevent any use or

disruption to the ecosystem. Instead they “explicitly aim to safeguard the livelihoods and cultures of traditional human populations” that subsist within the region (De Moura et al. 2009). They do this by allowing extraction of resources by local populations, with the regulation coming not from top-down, but bottom-up in the form of local community-based control systems. Originating in the Amazon in 1990, the ER strategy quickly expanded to the marine environment, with the first Marine Extractive Reserve (MER) established in 1992, and 22 Marine Extractive Reserves (MERs) currently along the Brazilian coast (De Moura et al. 2009, Santos and Schiavetti 2014). While the primary intention of the MERs was to protect the fisheries and livelihood of the resident fishermen through regulations on fishing practices, catch limits, or exclusion zones (De Moura et al. 2009), the intertidal foraging habitat that is critical to overwintering shorebirds also falls within the MERs’ boundaries (Kober and Bairlein 2009, Mu and Wilcove 2020). However, the effectiveness of MERs as protected areas is not necessarily clear, with only a small fraction of MERs meeting the management goals they set (Santos and Schiavetti 2014). There are approximately 12 Marine Extractive Reserves that cover the migratory stopover location in northern Brazil (Figure 3.1). Identifying and characterizing areas that serve as habitat for a variety of shorebirds is critical for understanding how these MERs currently protect shorebirds, and for making future conservation and management decisions that may benefit shorebirds while still fulfilling the MERs original mission.

There are several common frameworks for multi-species conservation planning: umbrella species, flagship species, and an overall biodiversity approach. Umbrella species conservation focuses on a single species with a wide geographic range that encompasses the distributions of other valued and important species. Conservation efforts focus on protecting a single umbrella species, with the understanding that a variety of other species will tangentially be protected (Shrader-Frechette and McCoy 1993, Wilcove 1993, Simberloff 1998, Andelman and Fagan 2000). A similar approach, flagship species are species that generate significant public interest, useful when drumming up support for conservation and management efforts (Caro and O’Doherty

1999). Typically, they are large, showy, charismatic vertebrate species that have already garnered some level of public interest. Flagship species can serve as umbrella species if they have wide geographic ranges that encompass other, less charismatic species. However, this is not necessarily the case, as their primary merit is their public appeal (Caro and O'Doherty 1999). Finally, prioritizing maximum biological diversity in the form of diversity hot-spots has also been proposed as an approach to conservation (Myers et al. 2000, Meir et al. 2004). Areas with the highest diversity of species would be given priority, regardless of the community assemblage of the prioritized areas. These approaches may lead to vastly different, even conflicting conservation and management decisions.

Evaluating the migratory shorebird assemblages of northern Brazil presents an opportunity for better understanding the effects that umbrella, flagship, and biodiversity approaches might have on conservation decision making in northern Brazil. Semipalmated sandpipers are of the most ubiquitous shorebirds across the flyway, occupying the breadth of available habitat (Rodrigues 2000, Colwell 2010), making them an ideal umbrella species. Red knots have received significant attention from both the conservation community and the public with their dramatic life history (Baker et al. 2004), a PBS documentary made about their conservation issues (Argo 2008), and their addition to the Endangered Species Act (US Fish and Wildlife Service 2013), making them a viable flagship migratory shorebird species. However, red knots are significantly less abundant than semipalmated sandpipers in northern Brazil, potentially covering much less with their “umbrella” (Rodrigues 2000, Lunardi et al. 2012). This provides an opportunity to understand the effects of managing solely for a species of particular conservation interest (red knots) or for species that cast wider shadows (semipalmated sandpipers), and how those management approaches protect the biodiversity of the full shorebird assemblage.

I evaluated the three “shadows” cast by the three different approaches to conservation prioritization, flagship (red knot), umbrella (semipalmated sandpipers) and biodiversity (all eight species), identifying the both the extent of the “shadows” and the communities that fall under

each. Utilizing Maxent species distribution modeling, I estimated the potential habitat distributions of eight migratory shorebird species across northern Brazil, including the flagship red knots and umbrella semipalmated sandpipers. Based on these models, I identified areas of conservation interest under each management perspective (flagship, umbrella, and biodiversity), evaluated the composition of species protected by each method, and evaluated similarities and differences between each management scenario. Finally, I overlaid existing MER boundaries on top of the predicted conservation regions in order to identify gaps and inform future management decisions under the different management scenarios.

3.2 - Methods

Location and Survey methods

The study site is located in northern Brazil, across the coastline between the city of Belem in Pará state, and the city of São Luís in Maranhão state. Across this region are 12 Marine Extractive Reserves (Figure 1), ranging in size from Reserva Extractivista (Resex) de São João da Ponta (34 km²) to the west, and Resex de Cururupu (1852 km²) in the east. Point-counts of shorebirds were conducted in the winters of 2016 and 2017, with 250 meter fixed radius plots conducted along transects running parallel to the tide line (Figure 2.2). More detailed methodologies are available in Chapter 2.

3.2a - MaxEnt Modeling

Presence-only-based distribution models were derived for each of the eight species using a maximum entropy modeling approach via the Maxent modeling package for the intertidal foraging habitat of each of the eight species. Maxent, developed by Phillips et al. (2006), estimates the predicted probability as a function of environmental variables and presence-only survey data for pixels across a rasterized landscape. Environmental variables for the models

consisted of landscape metrics (distance to rivers, distance to developed areas, distance to mangroves, tidal exposure, and tidal permanence), remote sensing metrics that characterized the intertidal sediment (seven bands of optical, near infrared, and short wave infrared from the Landsat 8 platform, and two bands of vertical-horizontal and vertical-vertical polarized C-band synthetic aperture radar from the Sentinel 1 platform), as well as climatic variables from the WorldClim data set (Harris et al. 2014, Fick and Hijmans 2017). Two classes of models were used to delineate habitat in this study, one that utilized all of the landscape, remote sensing, and WorldClim variables (LsRsWc) and one that utilized only the landscape and remote sensing metrics (LsRs). While WorldClim proved to be statistically important for model function, its biological significance was suspect in this particular setting (Chapter 2). For more details on the approach to using Maxent, including the environmental variables used and model evaluation, refer to the methods detailed in Chapter 2.

Thresholding

Predicted probability of presence derived by Maxent is not an absolute value, but rather, relative to the model itself. The pixel with a value of 0.3 for “Species A” may not be as important as the same pixel value for a model of “Species B” (Phillips et al. 2006). In order to more directly compare the predicted distributions, the continuous model output can be converted into the binary categories of “predicted presence” (1) or “predicted absence” (0) using thresholds based on model performance metrics. There are a number of metrics used, but the most common is the equal training sensitivity and specificity metric derived by Maxent. Equal training sensitivity and specificity aims to balance errors of commission and omission with model outputs above the threshold considered presence pixels (1), while values below are considered absence pixels (0) (Cao et al. 2013). Species richness can then be predicted by overlaying the binary rasters and adding the rasters together, in this case, producing pixel values ranging between 0 (not predicted habitat for any species) to 8 (predicted habitat for eight different species) (Holmes et al. 2015).

Similarly, to estimate species assemblages, or which species were predicted to co-occur with others, a unique number was assigned to each species (1, 10, 100, etc.). The binary distribution rasters were then multiplied by their respective unique numbers, and added together, resulting in each pixel ranging in numbers of 1 (black bellied plovers only) to 11111111 (all species predicted in this pixel). Because of the sheer number of potential combinations (8!), only the top 10 most common by area were evaluated in depth.

3.2b - Comparing Conservation Strategies

To compare coverage of habitat based on the three approaches to conservation prioritization (flagship species, umbrella species, and biodiversity), the threshold-derived binary rasters of presence were used for the flagship species, red knot, and the umbrella species, semipalmated sandpiper. For the biodiversity approach, a binary layer was derived by designating all areas that had 5 or more species as high priority, and areas with 4 species or less as not prioritized. These binary layers were then used to assess how much habitat was protected underneath each scenario across the whole landscape and within the Marine Extractive Reserves. To evaluate how the approaches differentially protected species diversity, the protected regions under each scenario were used to mask the species richness raster, producing rasters that designated species richness of each pixel and protected by either the Flagship (red knot) or Umbrella (semipalmated sandpiper), or Biodiversity (richness ≥ 5) scenarios. To more directly compare species richness under each scenario, an area-weighted or area-normalized species richness value was calculated where species richness values (0 through 8) were multiplied by the area those values occupied, and divided by the total area under the specific scenario.

3.2c - Identifying New Conservation Zones

Overlaying coverages of each conservation approach resulted in rasters for each modeling method where each pixel represents whether or not one, two, or all three approaches

designated that pixel as important habitat, as well as the specific combination of conservation scenarios. Using these rasters and image interpretation, a gap analysis (Scott et al. 1993) was undertaken to identify areas outside of existing Marine Extractive Reserve protections that appeared to have a high proportion of protected area based on the flagship, umbrella, and biodiversity conservation strategies, and the respective models that utilized landscape and remote sensing (LsRs) and landscape, remote sensing, and WorldClim (LsRsWc).

3.2 - Results

Areas Protected by Strategies

Approximately 198 km² (LsRsWc) or 248 km² (LsRs) of habitat were designated by the flagship red knot species models, 488 km² or 461 km² designated by the umbrella semipalmated sandpiper models, and 259 km² or 246 km² by the biodiversity approach (Table 3.1). For the LsRsWc models, Marine Extractive Reserves protected approximately 44%, 17%, and 22% of the areas designated as important by the flagship, umbrella, and diversity approaches, respectively. LsRs models had approximately 33%, 19%, and 22% of the flagship, umbrella, and diversity priority areas protected by the Marine Extractive Reserves (Table 3.1). There was significant overlap of coverage between the two modeling approaches across all management regimes, ranging from 61% (flagship, LsRs) to 76% (umbrella, LsRs) (Table 3.2). The umbrella species approach protected approximately 36% of the red knot habitat designated by the red knot models, regardless of modeling approach. The biodiversity approach (species richness ≥ 5), protected slightly less red knot habitat, at about 27% (Table 3.3). The different management approaches resulted in different, often overlapping coverages. The categories with broadest spatial extent were solely designated as habitat by the umbrella approach (30.8% and 35.5% for LsRs and LsRsWc models respectively, Figures 3.2 and 3.3), followed by areas designated as important by both biodiversity and umbrella (28.8% and 31.3% for LsRs and LsRsWc models respectively, Figures 3.2 and 3.3) and finally flagship (24.6% and 19.4% for LsRs and LsRsWc models

respectively, Figures 3.2 and 3.3). Only 9.7% or 7.2% of habitat was considered important by all three approaches to management decision making (Figures 3.2 and 3.3).

Species Richness Protected

Using species richness as a metric of biodiversity, each pixel within the study area was assigned a species richness value based on the number of species whose distribution models designated that pixel as suitable habitat. The landscape followed a predictable pattern, with an inverse relationship between species richness and area across the landscape for both modeling approaches ($R^2 \sim 0.7$ for LsRs and 0.8 for LsRsWc, Figure 4). LsRs models designated 18.43% (246 km²) of the intertidal zone as habitat for 5 or more species, and 36.30% (487 km²) not designated as habitat for any species (Table 3.4). LsRsWc models designated 19.43% (260 km²) of the intertidal zone as habitat for 5 or more species, and only 19.53% (261 km²) not designated as habitat for any species (Table 3.5). In both modeling approaches, MERs protected an average of ~25% of each level of species richness (1 through 8). There was a slight bias towards protecting species rich habitats (8 species), though the bias is far more pronounced in the LsRsWc model (58%, Table 3.5 vs 36%, Table 3.6). To evaluate the percent of each richness class protected under each management scenario, percent of each richness class in the total landscape was plotted versus each species richness class. In other words, if a model covered 100% of species richness 8, 100% of the pixels with species richness 8 across the whole landscape would be protected. In both modeling regimes, flagship red knots protected a much lower percentage of each richness class than the umbrella semipalmated sandpipers, though, based on a simple linear regression between species richness and % of area protected, both species had at least a slight bias towards high species richness of 7 or 8 (Figures 3.5 and 3.6). Species richness, normalized by area based on each community, was significantly higher under the umbrella (semipalmated sandpipers) and biodiversity approach (~4.5 and 6 respectively) than both a flagship (red knot) scenario, or the study site as a whole (~2.4 for both) (Tables 3.4 and 3.5).

Community Assemblages Protected

Over 250 unique combinations of shorebird species were produced. The top 10 most frequent communities by area were focused on. The most prevalent “community” often consisted of either a single species (red knot or ruddy turnstones), or six species communities that exclude red knots and sanderlings (black bellied plovers, ruddy turnstones, semipalmated plovers, semipalmated sandpipers, willets, whimbrels). This was consistent across both modeling approaches, management scenarios, and the study site as a whole (Tables 3.6 and 3.7). The most prevalent assemblage that featured red knots were either red knots by themselves, or with a single additional species such as sanderlings (LsRs MER and Flagship, Table 3.6) and ruddy turnstones (LsRsWc MER and Flagship, Table 3.7). A majority of umbrella species assemblages included willets (nine and six of the ten communities considered) and whimbrels (eight and nine of the ten communities considered). Black bellied plovers coexisted nearly as regularly, appearing in six out of ten communities for both modeling approaches (Tables 3.6 and 3.7).

Comparison of Modeling Approaches

Models overlapped between 60% (Flagship, LsRs) and 76% of coverage (Umbrella, LsRs) with umbrella species models the most similar, and the biodiversity models the most different (Table 3.2). Comparing conservation strategies under each modeling approach, the umbrella approach consistently had the largest coverage across the intertidal zone (460 and 488 km², Table 3.1), similar area-normalized species richness (4.35 and 4.46, Tables 3 and 4), prioritization of more species rich areas ($R^2 = 0.893$ and 0.813 , Figures 3.3 and 3.4), and most-common community assemblages protected (Table 3.6 and Table 3.7). The biodiversity approach demonstrated similar consistencies between modeling approaches. The largest difference appears to be with the red knot “flagship” habitat models, with predicted the “shadow” 50 km² larger in

LsRs models than LsRsWc models, compared to the differences of 28 km² and 14 km² for the umbrella and biodiversity approaches, respectively (Table 3.2).

New Conservation Zones

Gap analysis identified three areas outside of existing Marine Extractive Reserves that contained significant shorebird habitat under the different management scenarios. Baía do Cumã is found between the municipalities of Guimaraes and Alcantara in Maranhão state (Figure 3.7), and has approximately 35.5 km² of intertidal habitat (Table 3.8). Though only a small portion is designated as important habitat by flagship red knot models, the area-weighted species richness for the region is high, relative to the landscape at large (3.84 and 4.71 for the LsRs and LsRsWc, respectively, Table 3.8). Baía de São José is found to the southeast of São Luís, the state capital of Maranhão (Figure 3.8), and has approximately 90 km² of total intertidal habitat. Similar to Baía do Cumã, only a small portion of the area (less than 10%, Table 3.9) is designated as flagship red knot habitat, though it also has a high relative area-weighted species richness (3.81 and 3.55 for the LsRs and LsRsWc models respectively, Table 3.8). Finally, directly adjacent to the largest existing marine extractive reserve, Resex Cururupu, is an area consisting of several islands that has a significant portion of its 98 km² of intertidal area designated as important habitat by the flagship red knot models (approximately 35 km², or 35%, from either or both models, Table 3.9) (Figure 3.9). This area does have a relatively high proportion of red knot habitat, but has a lower area-weighted species richness value (2.65 and 2.95 for the respective LsRs and LsRsWc models) compared to the first two conservation zones (Table 3.8).

3.4 - Discussion

The conclusions drawn from a modeling-based management approach, like the one presented here, are only as valid as the models that serve as the foundation. As was discussed in Chapter 2, the models are far from perfect, often with AUC scores below the suggested threshold for discerning between presence and absence (Table 2.2). The red knot models from Chapter 2 demonstrated that this may be due to small sample sizes of data used to calibrate the model ($n = 16$) or an overcompensation for sampling bias. I addressed these issues in this chapter by using all available red knot presence data for calibration ($n = 26$) and running the red knot model without a background sample bias mask. This resulted in an AUC score of 0.749, just shy of the recommended benchmark of 0.75, while still demonstrating significant differences between presence and absence points. Further external validation of these models would be advisable and possible with reference to previously conducted aerial surveys (Morrison et al. 2012) or even data from geolocators used in tracking migration patterns (Smith et al. 2020). However, there may be challenges matching the scale of models based on point-count surveys with that of aerial surveys or geolocators designed for tracking content-spanning movement. Confirmation of modeled distributions with independent, spatially explicit point count surveys may be advisable before significant resources are dedicated to conservation decisions based on this approach. Despite this caution, it can be said with confidence that the delineated extents of shorebird distributions demonstrate significant difference between presence and absence points, making a strong case for any inferences regarding shorebird distributions under different conservation scenarios across northern Brazil.

In terms of simple coverage, similar patterns emerge between conservation scenarios across both modeling regimes. The flagship approach is the most conservative ($\sim 225 \text{ km}^2$), umbrella the widest ($\sim 470 \text{ km}^2$), and the biodiversity approach similar to the flagship ($\sim 250 \text{ km}^2$) (Table 3.1). This generally follows the convention that the relatively smaller population of flagship red knots would have a more restrictive range than a high-population, generalist species like the umbrella semipalmated sandpipers (Rodrigues 2000, Colwell 2010). The extent of these

coverages differ significantly, particularly when considering the overlap between all three. A majority of flagship (61% in both models) and significant portion of umbrella coverage (~43% for both models) is found in isolation from the other management regimes. Less than 10% of the total area designated by any of the regimes is protected by all three (Figures 3.2 and 3.3). This is problematic when considering how the umbrella species and biodiversity approaches protect the numerically sensitive red knots. Umbrella species protect only ~36% of the delineated red knot habitat, with biodiversity even more restricted to ~26% (Table 3.5). Maxent variables of red knots had higher model responses to lower values of vertical-horizontal radar backscatter, and higher model response closer to river mouths. Semipalmated sanderlings had responded differently, with higher model response to high vertical-horizontal radar backscatter and no clear preference for distance to rivers. Based on the modeling discussion in Chapter 2, this would suggest that red knots prefer larger grain substrate (low vertical-horizontal backscatter) with relatively frequent inundation from freshwater, while semipalmated sandpipers prefer smaller sediment (high vertical-horizontal backscatter) with no preference to rivers. This discrepancy in apparent habitat preference may explain the widely differing shadows cast by each management perspective. Making management decisions solely on the spatial extent of either umbrella or biodiversity frameworks may leave more numerically and spatially restricted species, like the flagship red knot, at risk.

Very little of the total landscape was highly species rich with pixels of species richness 7 covering about 45 km² (less than 4% for both models, Tables 3.3 and 3.4), even less so for all 8 species (less than 1% for both models, Tables 3.3 and 3.4). All conservation strategies (flagship, umbrella, and biodiversity) disproportionately protected more species rich habitat (Figures 3.3 and 3.4). While not surprising for a biodiversity approach, it may be less obvious for the single species approaches. As richness increases, it would be more likely for the focal species (flagship red knot or umbrella semipalmated sandpipers) to be included in the richness count. However, the umbrella approach had an even higher preference for species richness than the biodiversity

approach that explicitly preferred species rich habitat (richness > 4). This may be a product of semipalmated sandpipers' broad niche and ability to utilize a wide range of habitats and resources (Baker and Baker 1973). Furthermore, previous research within the northern Brazil study site indicates that food scarcity may be a limiting factor (Kober and Bairlein 2009), resulting in greatly overlapping niches between shorebirds. Limited resources result in more overlapping niches as species utilize the same resources, while abundant resources can lead to more distinct niches or specialization (Emlen 1966, MacArthur and Pianka 1966, Zwarts and Wanink 1993). Semipalmated sandpipers' broad use of a diversity of otherwise limited resources may result in them cooccurring regularly with more specialist species.

The single most frequent assemblage delineated across the landscape and within marine extractive reserves, were actually single species 'assemblages', either red knots (LsRs, Table 3.6) or ruddy turnstones (LsRsWc, Table 3.7), depending on the model choice. Marine extractive reserves appear to protect similar species richness as the landscape (weighted richness of 1.99 versus 1.7 or 1.61 vs 1.68, Tables 3.4 and 3.5 respectively), as well as similar assemblages, with a slight preference for richer assemblages (Figures 3.5 and 3.6). While interpreting the species assemblages is challenging, one trend from the modeling is apparent: red knots and sanderlings do not regularly co-occur with multiple species simultaneously. This may be a function of them flocking in single species flocks or foraging individually. Research on Delaware Bay, U.S.A. suggests that red knots can regularly co-occur with ruddy turnstones at other flyway locations (Burger et al. 2018). However, the food resources between the two locations, horseshoe crab eggs in Delaware Bay (Baker et al. 2004) and benthic macroinvertebrates in northern Brazil (Kober and Bairlein 2006), may result in different flocking-foraging behaviors. The most prevalent species rich assemblage (e.g. richness >4) across the landscape, extractive reserves, and management scenarios is one that consists of all species *except* red knots and sanderlings. With the exception of the flagship regions based on red knots, assemblages with *both* red knots and sanderlings are apparently rare, according to the models. Aside from assemblages with all species

present, only the seven-species assemblages lacking whimbrels have both red knots and sanderlings (Flagship and Diversity, LsRs models, Table 3.6). These modeling results run somewhat contradictory to the survey data used to calibrate and validate them. Survey data suggests that red knots regularly occurred with other species (only 3.4% of presence points did *not* co-occur), though they co-occurred with sanderlings the least. Sanderlings were the least likely to occur with other species, but that was still a relatively small proportion of their occurrence (18.9%, Table 3.10). Previous research sheds some light on these patterns. A more direct approach at evaluating shorebird assemblages used cluster analysis and PCA to identify three distinct foraging guilds in the Bragancian Peninsula, located within the Maranhão-Pará coast (Kober and Bairlein 2009). The most separate of these guilds consisted of sanderlings and marbled godwits, and the most inclusive guild included ruddy turnstones, black bellied plovers (grey plovers in their manuscript), red knots, semipalmated sandpipers, and semipalmated plovers. These guilds align reasonably well with both the models and the survey records, with sanderlings designated as the most distinct. However, the discrepancy with models indicating that red knots are more regularly alone remains unexplained.

Species distribution models generally predict realized niches based on environmental characteristics (Guisan and Zimmermann 2000), though models that incorporate species interactions, known as joint species distribution models, are possible (Pollock et al. 2014). Our models did not account for species interactions which may result in the misrepresentation of community assemblages. This representation may not be entirely inaccurate, but rather a product of scale. Foraging niche partitioning in shorebirds has been widely documented to be exceptionally fine-scaled, with different species preferentially feeding on microhabitats mere meters apart (Backwell et al. 1998, Burger et al. 2007, Lunardi et al. 2012). With our surveys of 250 meter radius circles, and pixel sizes of 900 square meters, it is possible that significant microhabitat variation exists within each pixel, thus allowing for the diverse assemblages predicted by the models. Temporal niche partitioning may also play a role, as many species will

utilize the same habitat, but at different tidal stages (Burger et al. 1977). Species may be using the same patch of foraging habitat, as predicted by our model, but at different times or tidal stages. The models used in this analysis do not incorporate or consider tidal stage explicitly, which may also contribute to the discrepancy between our predicted species assemblages, and those seen in other literature. Some assemblage types may be inferred based on the qualitative habitat notes taken during surveys. For example, ruddy turnstones and sanderlings showed clear preference of areas associated with mangroves compared to areas associated with fiddler crabs (locally referred to as crab flats), which may be reflected in the relative prevalence of the ruddy turnstone/sanderling “assemblage” (Table 3.7). Willets and semipalmated sandpipers both slightly preferred crab flats over mangroves (19% vs 12% and 13.9% vs 10.2%, Table 11), which could likewise be reflected in the semipalmated sandpipers/willet assemblages (Table 3.7).

Marine extractive reserves covered a fairly representative sample of the landscape (~25% of most species richness categories, Tables 3 and 4) with a slight preference for highly rich areas, depending on the modeling methods ($R^2 = 0.011$ or $R^2 = 0.157$ respectively for LsRs and LsRsWc models, Figures 3.3 and 3.4). Coastal protected areas in northern Brazil encompass similar percentages of intertidal flats as important stopover locations found in other flyways. In the East Asian-Australasian Flyway, approximately 23% of tidal flats in China, and only 12% of flats in South Korea are protected by existing management (Murray and Fuller 2015). Australia has slightly better protections continent wide (39%), though areas most used by shorebirds may also be the least protected (Dhanjal-Adams et al. 2016). While northern Brazil is reasonably protected compared to other flyways, those protections likely do not have shorebird conservation as their *raison d’être*. Based on the distribution models and estimated species richness, MERs do not currently demonstrate prioritization of shorebird-important regions (Tables 3.3 and 3.4). More importantly, current management regulations are designed to protect the local artisanal fisheries (De Moura et al. 2009), so that even the areas currently under the MERs may not be adequately managed for shorebird-centric conservation. Shorebirds can be particularly susceptible to

interruptions to foraging due to human disturbance during migratory stops (Burger et al. 2007, Burger and Niles 2013). More directly, subsistence hunting is a serious pressure on shorebird populations in the Caribbean and neighboring regions of South America, with significant annual harvest (Ottema and Spaans 2008, Andres et al. 2011). Ensuring cooperation with diverse stakeholders, like local fishing communities that use beaches for vehicle transport or supplementally hunt shorebirds, is critical for the success of biodiversity conservation (Gavin et al. 2018). Incorporation of shorebird conservation management into existing MER regulations, such as seasonal limits to vehicle use or hunting, managed and enforced by the local communities, will be an important step to protecting shorebird habitat already under the wing of MERs.

Identifying important shorebird conservation zones outside of the MERs is critical for future shorebird management decisions. Using the three conservation strategies (flagship, umbrella, and biodiversity), three potential areas for shorebird conservation prioritization were identified, Baía do Cumã (Figure 3.7), Baía de São José (Figure 3.8), and a region directly adjacent to the largest existing MER, Resex Cururupu (Figure 3.9). Umbrella and biodiversity approaches highlighted Baía do Cumã and Baía de São José, which subsequently had much higher area-weighted species richness (~4.3 and ~3.7, Table 3.8) compared to existing marine extractive reserves and the landscape as a whole (~1.7, Tables 3.3 and 3.4). The high species richness may not be surprising, given the bias towards diversity that both umbrella and biodiversity demonstrated compared to the landscape (Figures 3.3 and 3.4). The area adjacent to Resex Cururupu is quite different, with more moderate coverage by both the umbrella and biodiversity regimes, possibly contributing to its area-weighted richness scores closer to the landscape (2.65 and 2.95, Table 3.8). However, the Cururupu area is distinct because of its relatively high proportion of habitat designated by the flagship red knot models (36%) compared to the other two conservation zones (16% and 10%, respectively, Table 3.9).

The two modeling approaches produced different absolute numbers of areas protected and did not precisely overlap in coverage (Table 3.2), but trends in conservation effects of the different modeling approaches were similar (Tables 3.3 and 3.4). The discrepancy in area-normalized species richness (2.96 vs 3.23, Tables 3.3 and 3.4) and biases towards more species rich areas ($R^2 = 0.294$ vs 0.294 , Figures 3.3 and 3.4) may be a product of the different extent of red knot habitat delineated by each method. LsRs models have approximately 25% more habitat identified as presence habitat compared to the LsRsWc model (248 km² vs 198 km², Table 3.2). Climatic data has been proven to be highly impactful on large-scale distribution models, which may explain its influence on distributions of flagship red knots (Hirzel and Le Lay 2008). However, in the case of equatorial northern Brazil, climate is relatively homogenous so the biological significance is difficult to determine at best (Chapter 2). Considering both the relative corroboration between modeling approaches, and the uncertainty around the importance of climatic variables in the context of northern Brazil, a simplified approach could utilize only the landscape-remote sensing based models with confidence.

These three locations could be archetypal examples of locations chosen under the different conservation strategies. Both Baía do Cumã and Baía de São José have high coverage by the umbrella semipalmated sandpipers, though Baía do Cumã has 67% of its extent delineated by the biodiversity approach (Table 3.9), and has a subsequently higher area-weighted species richness (Table 3.8). An umbrella-only approach may not differentiate between the locations, where a biodiversity approach clearly would. Finally, while the area adjacent to Resex Cururupu does not have the same coverage by the umbrella and biodiversity scenarios, nor does it have the subsequent elevated area-weighted richness, it *does* have a much higher proportion habitat for the flagship species, red knots (Figure 3.10). Efforts specific to protecting the red knot may prioritize similar areas, at the potential cost of protecting much more diverse communities. A hybrid approach utilizing both flagship and biodiversity approaches could compensate for these issues. Using only the LsRs models, total area covered by the hybrid approach (430 km², Table 3.12) is

more much more inclusive than either flagship (248 km²) or biodiversity (246 km²), but more conservative than the umbrella species perspective (460 km², Table 3.2). A hybrid flagship-biodiversity approach still results in considerably higher weighted richness than the landscape (4.1 vs 1.99), as well as 100% coverage of the species rich areas *and* the rarer flagship red knots (Table 3.12). Baía do Cumã, Baía de São José, and the area west of Resex Cururupu are still identified as important gaps in existing conservation (Figures 3.11).

3.5 - Conclusion

Existing coastal management in northern Brazil, the Marine Extractive Reserves, protects 26% of intertidal habitat, but without clear preference for areas utilized by shorebird species. Different modeling approaches, those that utilize WorldClim data and those that do not, may produce different spatial extents, but still identify similar trends in species richness and community composition protected under the different management scenarios. These similarities, in addition to the uncertainty around WorldClim variables in Brazil and an eye towards parsimonious modeling, mean that models based only on landscape and remote sensing variables appear sufficient for management decision making. Between the three management scenarios, with the expansive umbrella approach covered the most habitat and reasonably high diversity, the diversity approach effectively produced diverse, if more conservative ranges, and the flagship red knots generally protected less, both in terms of range and diversity. While umbrella and diversity approaches are successful at protecting diverse communities, community assemblages of rarer or specialist species, like the red knots, may fall outside their protective shadows. A hybrid approach that uses both diversity and the extent of rarer species produces results that meet the management goals identifying gaps in existing conservation to protect the most at-risk species, while conserving the diverse assemblages they coexist with.

3.6 – Tables and Figures

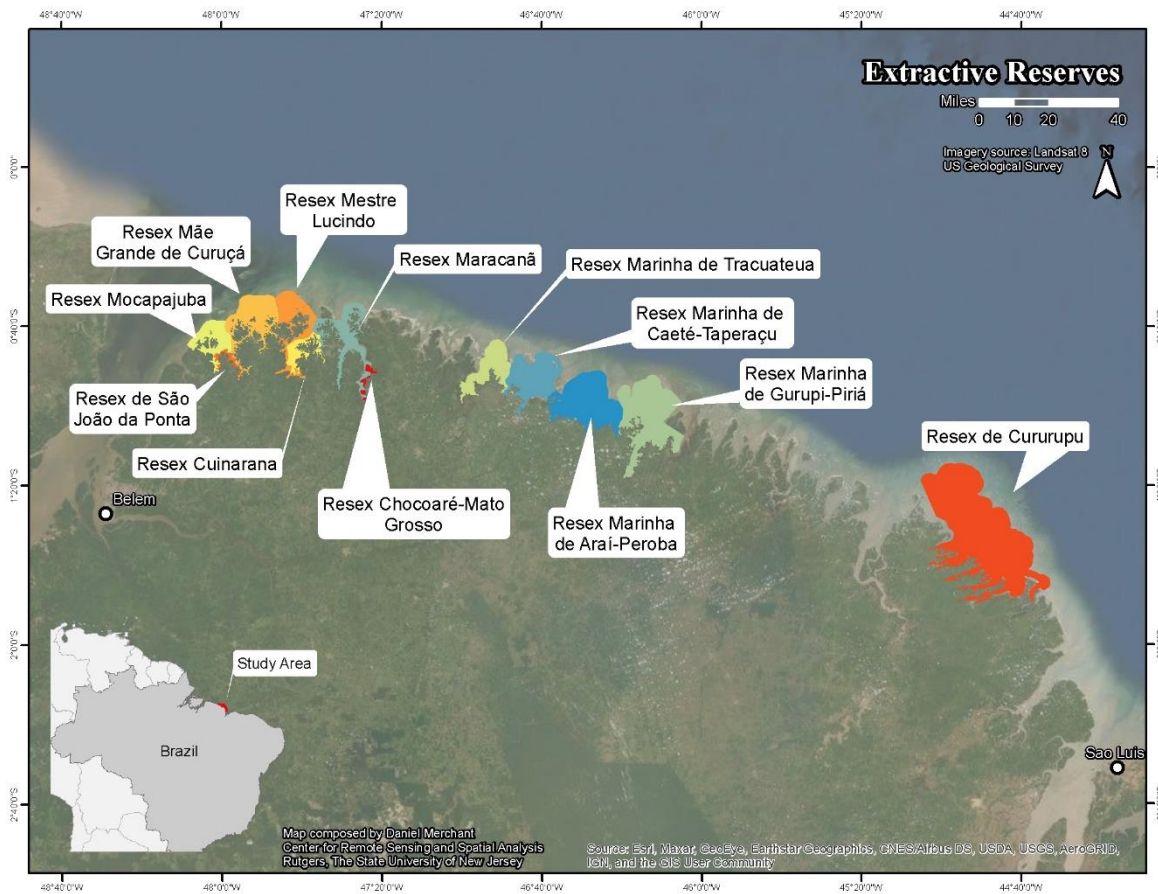


Figure 3.1. Borders of the 12 Extractive Reserves (MERs) or Reserva Extrativistas (Resex) located across the study site in northern Brazil. Extractive Reserves are conservation regions designed with both conservation and local subsistence use in mind.

Table 3.1. Area of habitat inside and outside the Marine Extractive Reserves (MERs) that would be designated as important based on either the flagship approach (red knots, REKN), the umbrella species approach (semipalmated sandpipers, SESA), or a biodiversity approach (species richness ≥ 5). Results include both modeling approaches, one utilizing all variables, and the other only using landscape and remote sensing variables

	Landscape, Remote Sensing, and Worldclim			Landscape and Remote Sensing		
	Flagship	Umbrella	Diversity	Flagship	Umbrella	Diversity
Total (km ²)	198.32	488.18	259.79	248.48	460.7	246.43
In MER (km ²)	87.91	82.19	57.75	83.10	86.47	54.34
Out MER (km ²)	110.41	405.99	202.04	165.08	374.23	192.05
In MER (%)	44.33%	16.84%	22.23%	33.48%	18.77%	22.07%

Table 3.2. How much each modeling approach, landscape and remote Sensing (LsRs) versus models run with all variables (LsRsWc), overlap in their predicted management priority areas. “Overlap” designates percentage of each model that both modeling approaches highlighted, while “Unique” are what percentage of coverage that only that modeling method (LsRs or LsRsWc) delineated. Total coverage area for each model at the bottom

	Flagship (REKN)		Umbrella (SESA)		Biodiversity	
	LsRs	LsRsWc	LsRs	LsRsWc	LsRs	LsRsWc
Overlap	60.69%	75.95%	76.04%	71.76%	66.15%	62.75%
Unique	39.31%	24.05%	23.96%	28.24%	33.85%	37.25%
Total (km ²)	248.18	198.32	460.7	488.17	246.43	259.79

Table 3.3. Total predicted red knot (REKN) intertidal foraging habitat based on Maxent models using either all model variables, or only landscape and remote sensing variables. Additionally shown is how much of the delineated REKN habitat is protected by either the umbrella species (semipalmated sandpipers) approach, or by the biodiversity approach, with pixels having species richness greater than or equal to 5 designated as priority conservation.

Predicted Red Knot Intertidal Foraging Habitat	Total REKN Habitat (km ²)	Under Umbrella (SESA)		Under Biodiversity	
		km ²	%	km ²	%
Landscape, Remote Sensing, and WorldClim Models	198.32	68.60	34.59%	53.50	26.98%
Landscape and Remote Sensing models	248.18	90.54	38.92%	64.84	26.13%

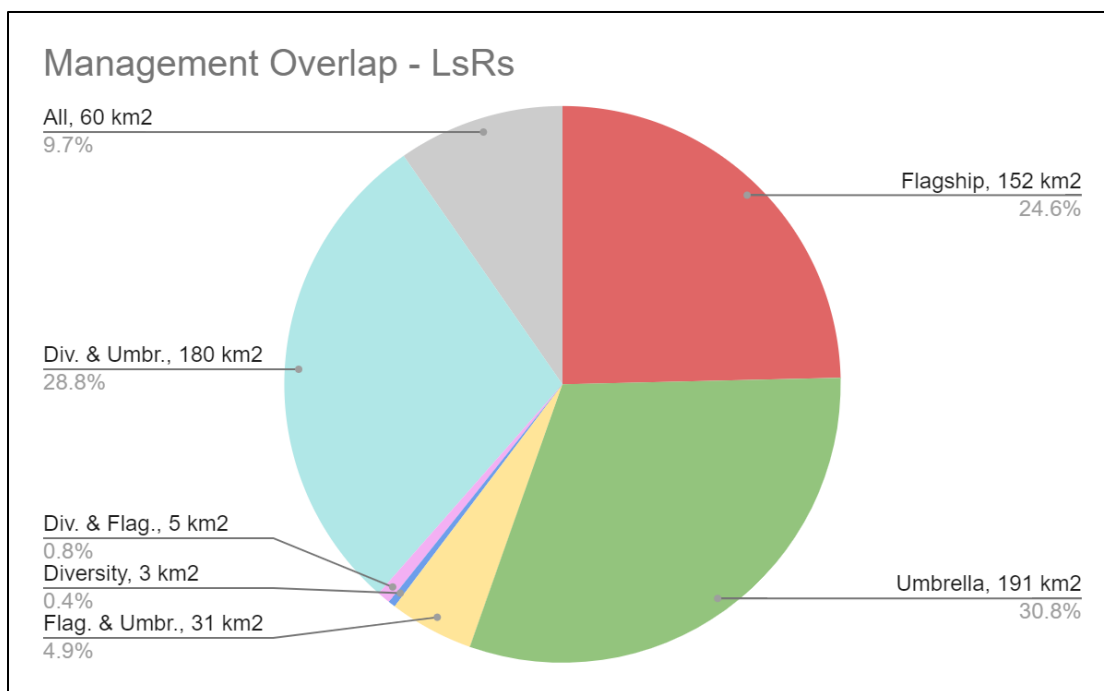


Figure 3.2: Relative composition of the 621 km² of the sum total of intertidal area designated by the different management approaches using the landscape-remote sensing based models. The most common area were areas solely designated as habitat by the umbrella approach (30.8%), followed by areas designated as important by both biodiversity and umbrella (28.8%) and finally flagship (24.6%). Only 9.7% of habitat was considered important by all three approaches to management decision making.

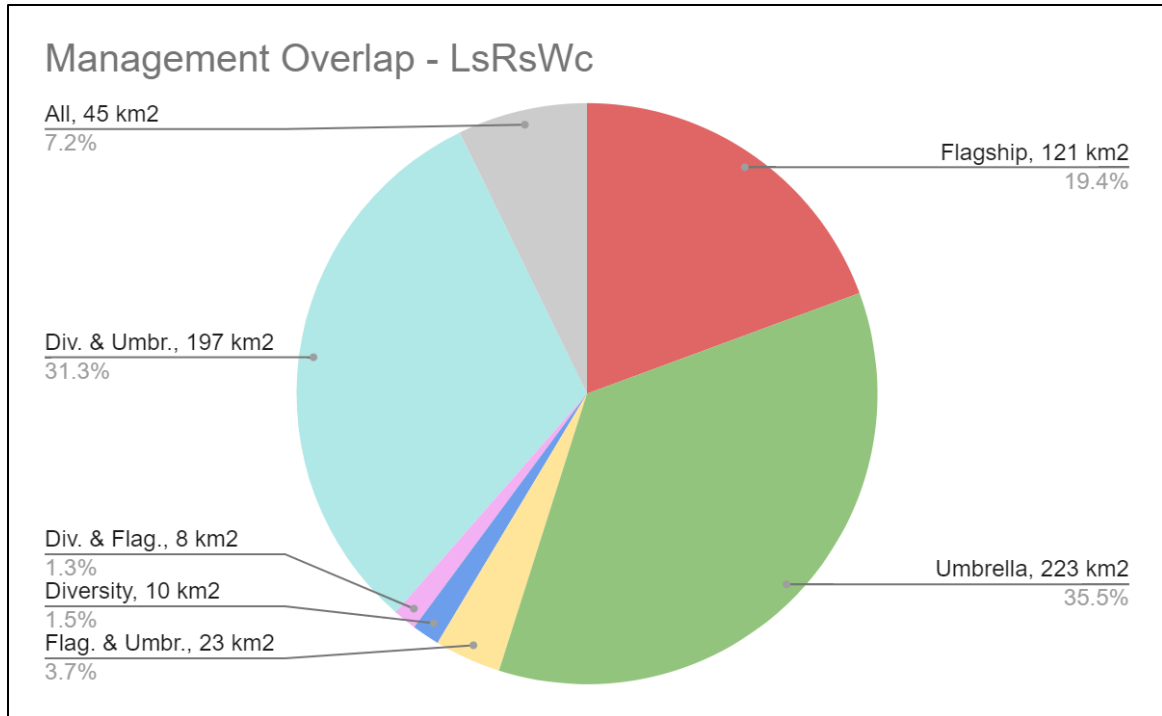


Figure 3.3: Relative composition of the 628 km² of the sum total of intertidal area designated by the different management approaches using the landscape-remote sensing-WorldClim based models. The most common area were areas solely designated as habitat by the umbrella approach (35.5%), followed by areas designated as important by both biodiversity and umbrella (31.3%) and finally flagship (19.4%). Only 7.2% of habitat was considered important by all three approaches to management decision making.

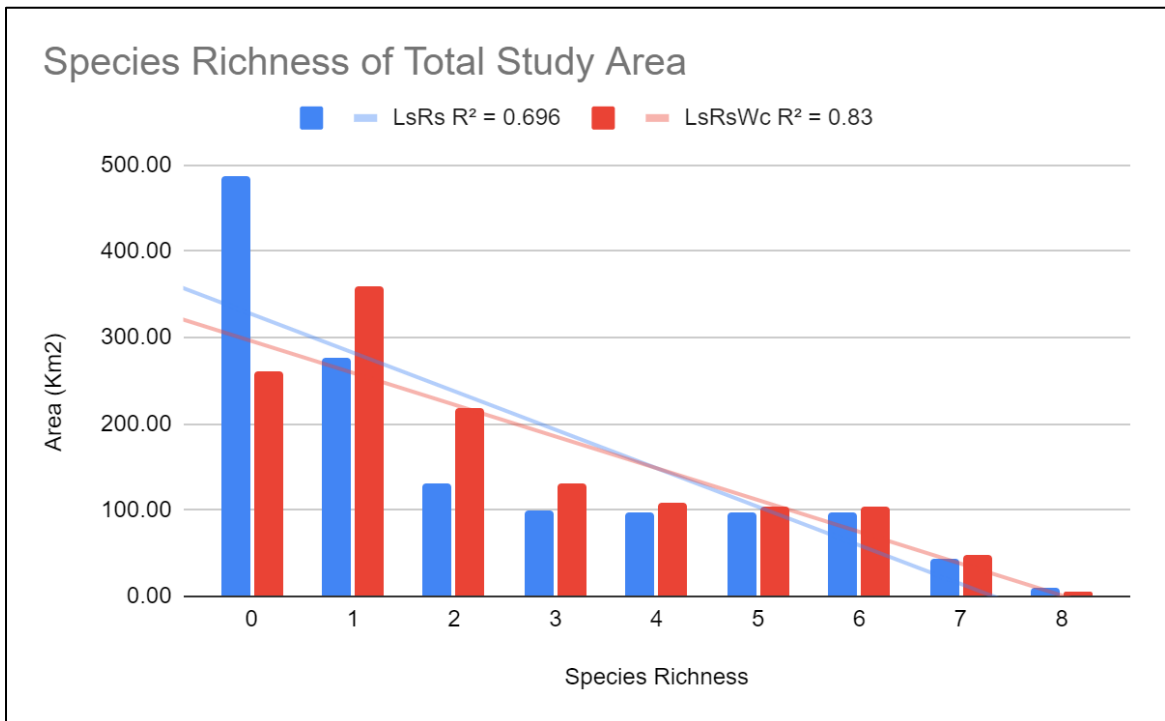


Figure 3.4. Area in square kilometers across the entirety of the landscape that is encompassed by each species richness value. Species richness was determined by overlaying binary presence rasters, delineated from Maxent models for eight shorebird species using environmental metrics of either landscape and remote sensing (blue) or landscape, remote sensing, and WorldClim climatic variables (red).

Table 3.4: Species richness derived from Maxent models of eight shorebirds species using only landscape and remote sensing variables. Model outputs were converted to binary rasters using equal training and specificity as a threshold, adding them together, approximating species richness for each pixel. 0 indicates that zero species had the pixel designated as habitat, while 8 indicates eight species had the pixel designated as habitat. Richness was weighted by area for each category to more accurately compare the relative species richness found under each scenario. Two weighted richness values were calculated for the total intertidal area and area within Marine Extractive Reserves (MER), since the total landscape and marine extractive reserves both had pixels where no species was located (richness = 0) and the management scenarios did not.

Landscape and Remote Sensing Models										
Species Richness	Total Intertidal		Within MER		Protected by Flagship, REKN		Protected by Umbrella, SESA		Protected by Biodiversity	
	Area (km ²)	% of Total	Area (km ²)	% of Category	Area (km ²)	% of Category	Area (km ²)	% of Category	Area (km ²)	% of Category
0	487.04	36.42%	156.32	32.10%	NA		NA		NA	
1	276.06	20.65%	66.14	23.96%	103.59	37.53%	22.52	8.16%	0	0%
2	130.80	9.78%	30.41	23.25%	39.80	30.43%	50.35	38.49%	0	0%
3	100.50	7.52%	20.51	20.40%	23.20	23.09%	67.42	67.08%	0	0%
4	96.30	7.20%	19.32	20.07%	16.74	17.39%	81.33	84.45%	0	0%
5	96.86	7.24%	18.93	19.54%	16.23	16.76%	91.49	94.45%	96.86	100%
6	96.41	7.21%	20.12	20.87%	16.42	17.03%	94.74	98.27%	96.41	100%
7	43.94	3.29%	12.23	27.83%	22.97	52.27%	43.65	99.33%	43.94	100%
8	9.21	0.69%	3.10	33.67%	9.21	100.00%	9.21	100.00%	9.21	100%
Weighted richness	With 0: 1.99 Without 0: 3.14		With 0: 1.7 Without 0: 3.1		Without 0: 2.96		Without 0: 4.46		Without 0: 5.86	

Table 3.5: Species richness derived from Maxent models of eight shorebirds species using either all landscape, remote sensing, and WorldClim variables. Model outputs were converted to binary rasters using equal training and specificity as a threshold, adding them together, and approximating species richness for each pixel. 0 indicates that zero species had the pixel designated as habitat, while 8 indicates eight species had the pixel designated as habitat. Richness was weighted by area for each category to more accurately compare the relative species richness found under each scenario. Two weighted richness values were calculated for the total intertidal area and area within Marine Extractive Reserves (MER), since the total landscape and marine extractive reserves both had pixels where no species was located (richness = 0) and the management scenarios did not.

Landscape, Remote Sensing, and WorldClim Models										
Species Richness	Total Intertidal		Within MER		Protected by Flagship, REKN		Protected by Umbrella, SESA		Protected by Biodiversity	
	Area (km ²)	% of Total	Area (km ²)	% of Category	Area (km ²)	% of Category	Area (km ²)	% of Category	Area (km ²)	% of Category
0	261.10	19.53%	83.25	31.89%	NA		NA		NA	
1	358.57	26.82%	85.33	23.80%	45.04	12.56%	27.68	7.72%	0	0%
2	217.52	16.27%	59.65	27.42%	55.42	25.48%	62.17	28.58%	0	0%
3	131.28	9.82%	33.24	25.32%	26.47	20.16%	75.58	57.57%	0	0%
4	108.89	8.14%	27.85	25.58%	17.89	16.43%	80.76	74.17%	0	0%
5	103.19	7.72%	20.84	20.20%	15.14	14.68%	89.22	86.46%	103.19	100%
6	103.41	7.73%	19.20	18.57%	15.70	15.18%	99.94	96.64%	103.41	100%
7	47.78	3.57%	14.58	30.52%	17.24	36.09%	47.41	99.23%	47.78	100%
8	5.41	0.40%	3.13	57.76%	5.41	100.00%	5.41	100.00%	5.41	100%
Weighted richness	With 0: 1.61 Without 0: 1.89		With 0: 1.68 Without 0: 2.89		Without 0: 3.23		Without 0: 4.35		Without 0: 5.83	

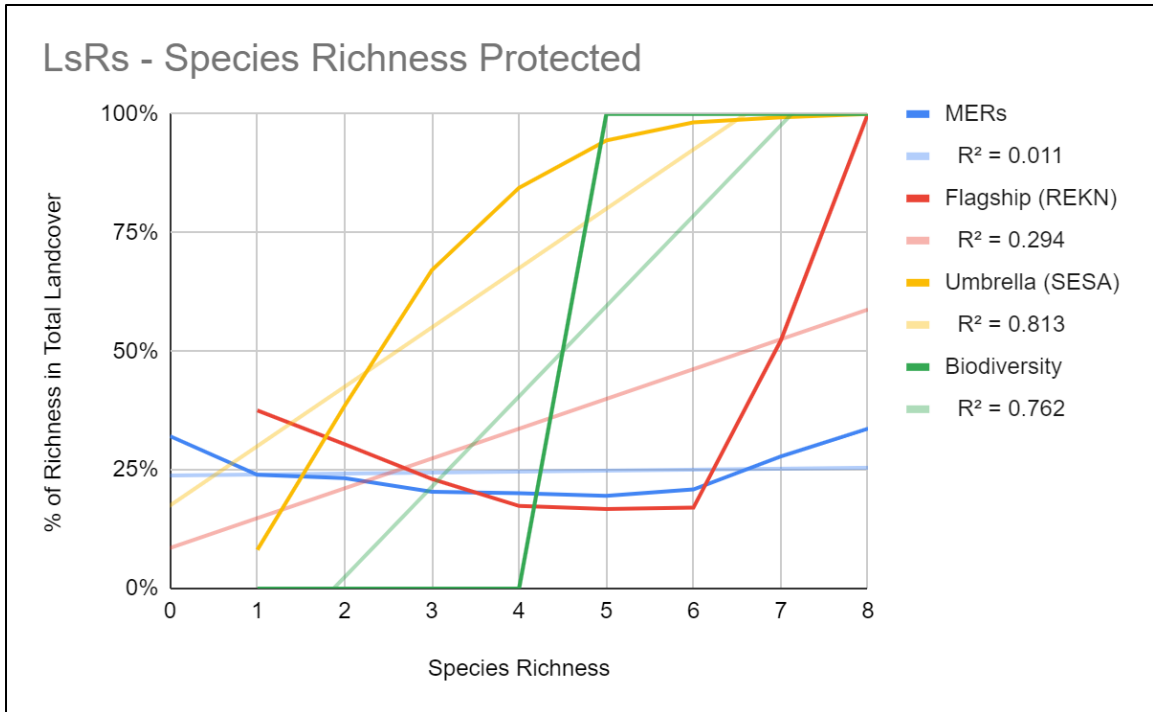


Figure 3.5: Percentage of area of each species richness value found across the landscape that is protected under each management scenario. Species richness was determined by overlaying Maxent models and summing the total number of species that would designate each pixel as potential habitat. Trend lines, in faded colors, represent the approximate linear relationship between species richness and percent of area protected under each scenario.

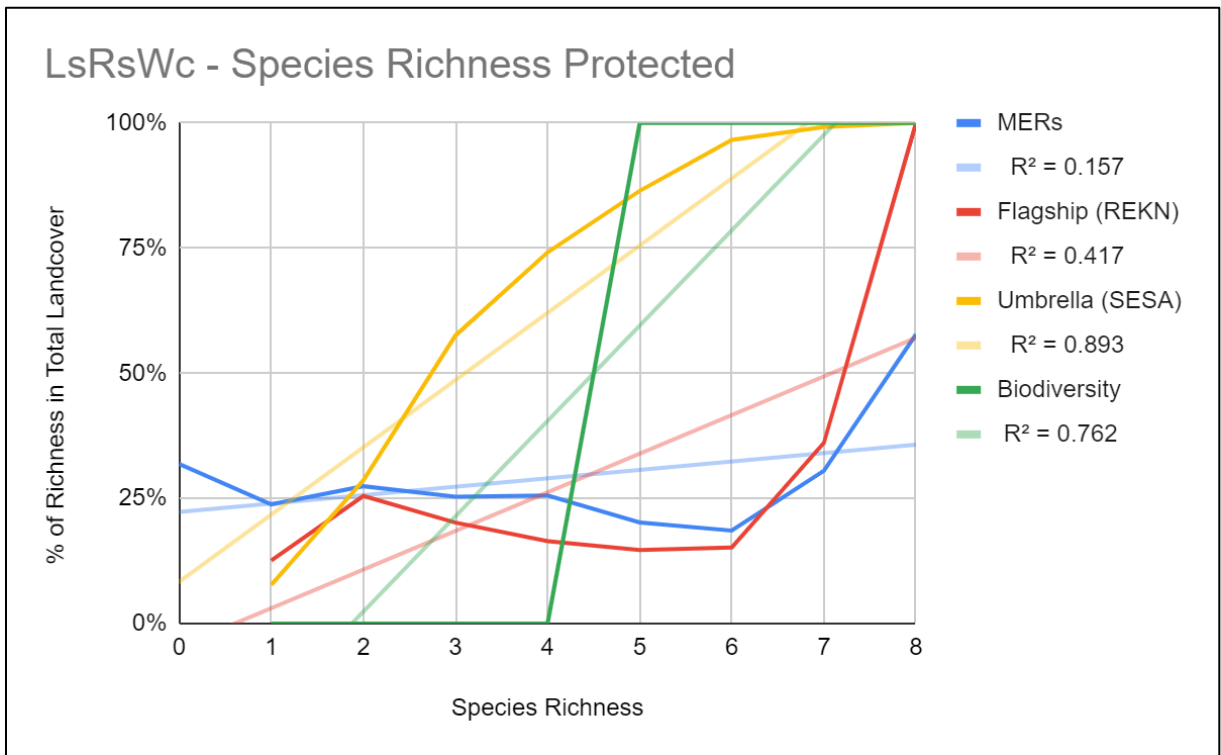


Figure 3.6: Percentage of area of each species richness value found across the landscape that is protected under each management scenario. Species richness was determined by overlaying Maxent models and summing the total number of species that would designate each pixel as potential habitat. Trend lines, in faded colors, represent the approximate linear relationship between species richness and percent of area protected under each scenario.

Table 3.6: The ten most common species assemblages (“Asmbl.”) based on area across the whole landscape (All), within Marine Extractive Reserves, and protected by the three different management regimes (flagship, umbrella, and diversity). Assemblages are based on overlapping Maxent model outputs, generated using survey data and landscape and remote sensing metrics as environmental variables.

Landscape and Remote Sensing Models														
All			Marine Extractive Reserves			Flagship (REKN)			Umbrella (SESA)			Diversity (Richness > 4)		
Asmbl.	Area (km ²)	Sp. Rich.	Asmbl.	Area (km ²)	Sp. Rich.	Asmbl.	Area (km ²)	Sp. Rich.	Asmbl.	Area (km ²)	Sp. Rich.	Asmbl.	Area (km ²)	Sp. Rich.
REKN	103.6	1	REKN	36.8	1	REKN	103.6	1	BBPL RUTU SEPL SESA WILL WHIM	61.9	6	BBPL RUTU SEPL SESA WILL WHIM	61.9	6
BBPL RUTU SEPL SESA WILL WHIM	61.9	6	SAND	11.7	1	REKN SAND	20.4	2	BBPL SEPL SESA WILL WHIM	29.8	5	BBPL SEPL SESA WILL WHIM	29.8	5
SAND	55.7	1	BBPL RUTU SEPL SESA WILL WHIM	11.4	6	BBPL REKN RUTU SEPL SESA WILL WHIM	16.5	7	SESA WILL	24.5	2	BBPL RUTU SESA WILL WHIM	22.8	5
RUTU	33.1	1	REKN SAND	8.2	2	BBPL REKN RUTU SAND SEPL SESA WILL WHIM	9.2	8	BBPL SESA WILL WHIM	24.0	4	BBPL RUTU SAND SEPL SESA WILL WHIM	21.0	7
WHIM	31.0	1	RUTU	6.9	1	REKN SESA	6.8	2	BBPL RUTU SESA WILL WHIM	22.8	4	BBPL REKN RUTU SEPL SESA WILL WHIM	16.5	7
BBPL SEPL SESA WILL WHIM	29.8	5	BBPL RUTU SAND SEPL SESA WILL WHIM	6.1	7	REKN SESA WILL	6.7	3	SESA	22.5	1	BBPL REKN RUTU SAND SEPL SESA WILL WHIM	9.2	8
SESA WHIM	24.5	2	BBPL SEPL SESA WILL WHIM	4.9	5	REKN RUTU	5.7	2	SESA WILL WHIM	21.2	3	BBPL SAND SEPL SESA WILL WHIM	9.1	6

BBPL SESA WILL WHIM	24.0	4	WILL	4.7	1	BBPL REKN RUTU SAND SEPL SESA WILL	4.2	7	BBPL RUTU SAND SEPL SESA WILL WHIM	21.0	7	BBPL RUTU SEPL SESA WILL	5.7	5
BBPL RUTU SESA WILL WHIM	22.8	5	BBPL SESA WILL WHIM	4.4	4	REKN SAND SESA	3.4	3	BBPL REKN RUTU SEPL SESA WILL WHIM	16.5	7	SAND SEPL SESA WILL WHIM	4.4	5
SESA	22.5	1	BBPL REKN RUTU SEPL SESA WILL WHIM	3.8	7	BBPL REKN RUTU SEPL SESA WILL	3.4	6	SEPL SESA WILL WHIM	12.4	4	BBPL REKN RUTU SAND SEPL SESA WILL	4.2	7
Total	409		Total	99		Total	179.9		Total	256.7		Total	184.6	

Table 3.7: The ten most common species assemblages (“Asmbl.”) based on area across the whole landscape (All), within Marine Extractive Reserves, and protected by the three different management regimes (flagship, umbrella, and diversity). Assemblages are based on overlapping Maxent model outputs, generated using survey data and landscape, remote sensing, and WorldClim metrics as environmental variables.

Landscape, Remote Sensing and WorldClim Models														
All			Marine Extractive Reserves			Flagship (REKN)			Umbrella (SESA)			Diversity (Richness > 4)		
Asmbl.	Area (km ²)	Sp. Rich.	Asmbl.	Area (km ²)	Sp. Rich.	Asmbl.	Area (km ²)	Sp. Rich.	Asmbl.	Area (km ²)	Sp. Rich.	Asmbl.	Area (km ²)	Sp. Rich.
RUTU	229.1	1	RUTU	56.2	1	REKN	45.0	1	BBPL RUTU SEPL SESA WILL WHIM	61.0	6	BBPL RUTU SEPL SESA WILL WHIM	61.0	6
BBPL RUTU SEPL SESA WILL WHIM	61.0	6	RUTU SAND	20.9	2	REKN RUTU	41.2	2	BBPL SEPL SESA WILL WHIM	37.2	5	BBPL SEPL SESA WILL WHIM	37.2	5
REKN	45.0	1	REKN	18.8	1	BBPL REKN RUTU SEPL SESA WILL WHIM	11.9	7	BBPL RUTU SAND SEPL SESA WILL WHIM	30.5	7	BBPL RUTU SAND SEPL SESA WILL WHIM	30.5	7
RUTU SAND	41.4	2	REKN RUTU	15.1	2	REKN RUTU SAND	10.5	3	SESA	27.7	1	BBPL SAND SEPL SESA WILL WHIM	15.5	6
REKN, RUTU	41.2	2	BBPL RUTU	7.8	2	REKN SAND	7.0	2	SESA WHIM	26.0	2	BBPL REKN RUTU SEPL SESA WILL WHIM	11.9	7
BBPL SEPL SESA WILL WHIM	37.2	5	BBPL RUTU SAND SEPL SESA WILL WHIM	7.5	7	BBPL REKN RUTU SAND SEPL SESA WILL WHIM	5.4	8	BBPL SAND SEPL SESA WILL WHIM	15.5	6	BBPL RUTU SESA WILL WHIM	10.1	5
BBPL RUTU SAND SEPL SESA WILL WHIM	30.5	7	BBPL RUTU SEPL SESA WILL WHIM	7.0	6	REKN RUTU SESA	4.8	3	RUTU SESA	14.4	2	RUTU SEPL SESA WILL WHIM	7.5	5

SESA	27.7	1	REKN RUTU SAND	6.3	3	REKN SESA	4.6	2	BBPL REKN RUTU SEPL SESA WILL WHIM	11.9	7	BBPL RUTU SEPL SESA WILL	6.4	5
WHIM, SESA	26.0	2	BBPL RUTU SAND	5.4	3	BBPL REKN RUTU SEPL SESA WILL	3.7	6	RUTU SESA WHIM	11.7	3	BBPL RUTU SEPL WILL WHIM	5.7	5
SAND	23.5	1	BBPL REKN RUTU SEPL SESA WILL WHIM	4.3	7	REKN RUTU SESA WILL	3.7	4	BBPL SESA WILL WHIM	10.8	4	BBPL REKN RUTU SAND SEPL SESA WILL WHIM	5.4	8
Total	562.8		Total	149.3		Total	137.9		Total	246.8		Total	191.2	

Potential Conservation Zone - Baía do Cumã

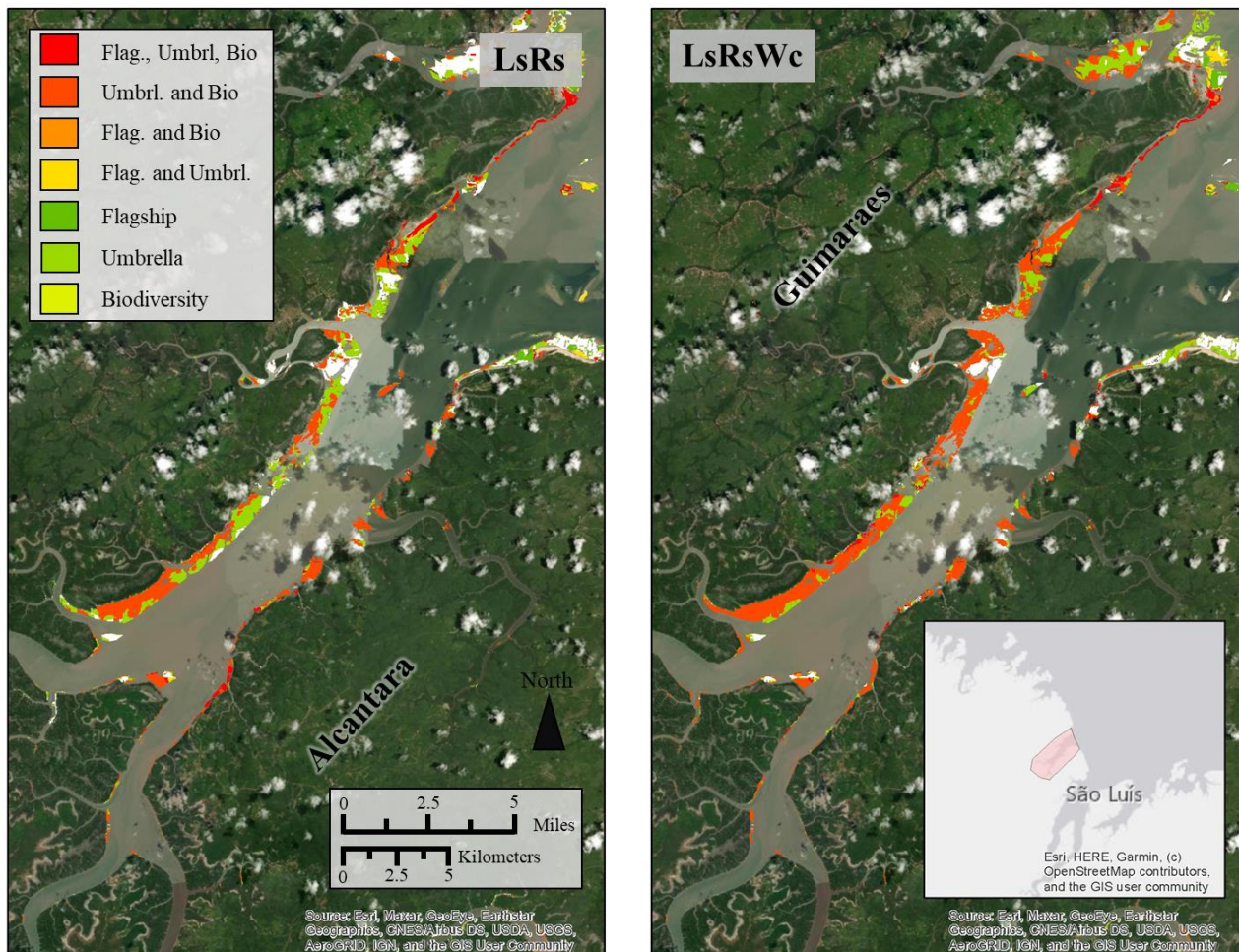


Figure 3.7: The potential conservation zone, Baía do Cumã, located between the municipalities of Guimaraes and Alcantara in the state of Maranhão. Conservation zones were identified by visual interpretation of overlaid coverage of flagship, umbrella, and biodiversity approaches to conservation. Areas in red are designated by flagship (“flag”), umbrella (“umbrl”), and biodiversity (bio) approaches. Dark orange are umbrella and biodiversity, light orange is flagship and biodiversity, and yellow is flagship and umbrella. Dark green, light green, and green-yellow represent pixels only designated as important by flagship, umbrella, and biodiversity approaches, respectively. Inset map in the bottom right shows approximate location of Baía do Cumã relative to the Maranhão state capital, Sao Luis.

Potential Conservation Zone - Baía de São José

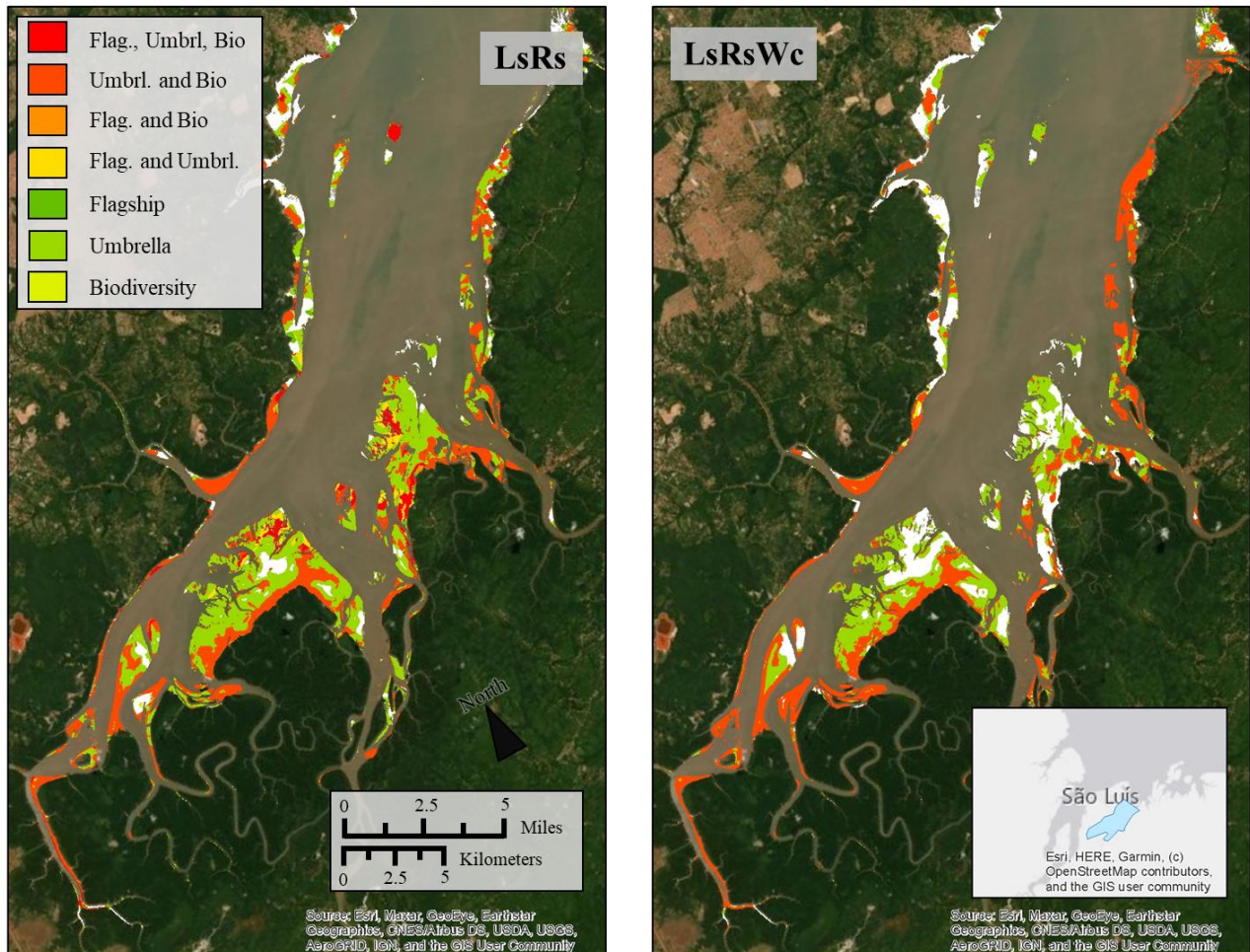


Figure 3.8: The potential conservation zone, Baía de São José, located to the south east of the state capital of Maranhão, São Luís. Conservation zones were identified by visual interpretation of overlaid coverage of flagship, umbrella, and biodiversity approaches to conservation. Areas in red are designated by flagship (“flag”), umbrella (“umbrl”), and biodiversity (bio) approaches. Dark orange are umbrella and biodiversity, light orange is flagship and biodiversity, and yellow is flagship and umbrella. Dark green, light green, and green-yellow represent pixels only designated as important by flagship, umbrella, and biodiversity approaches, respectively. Inset map in the bottom right shows approximate location of Baía de São José relative to Sao Luis.

Potential Conservation Zone – West of Resex Cururupu

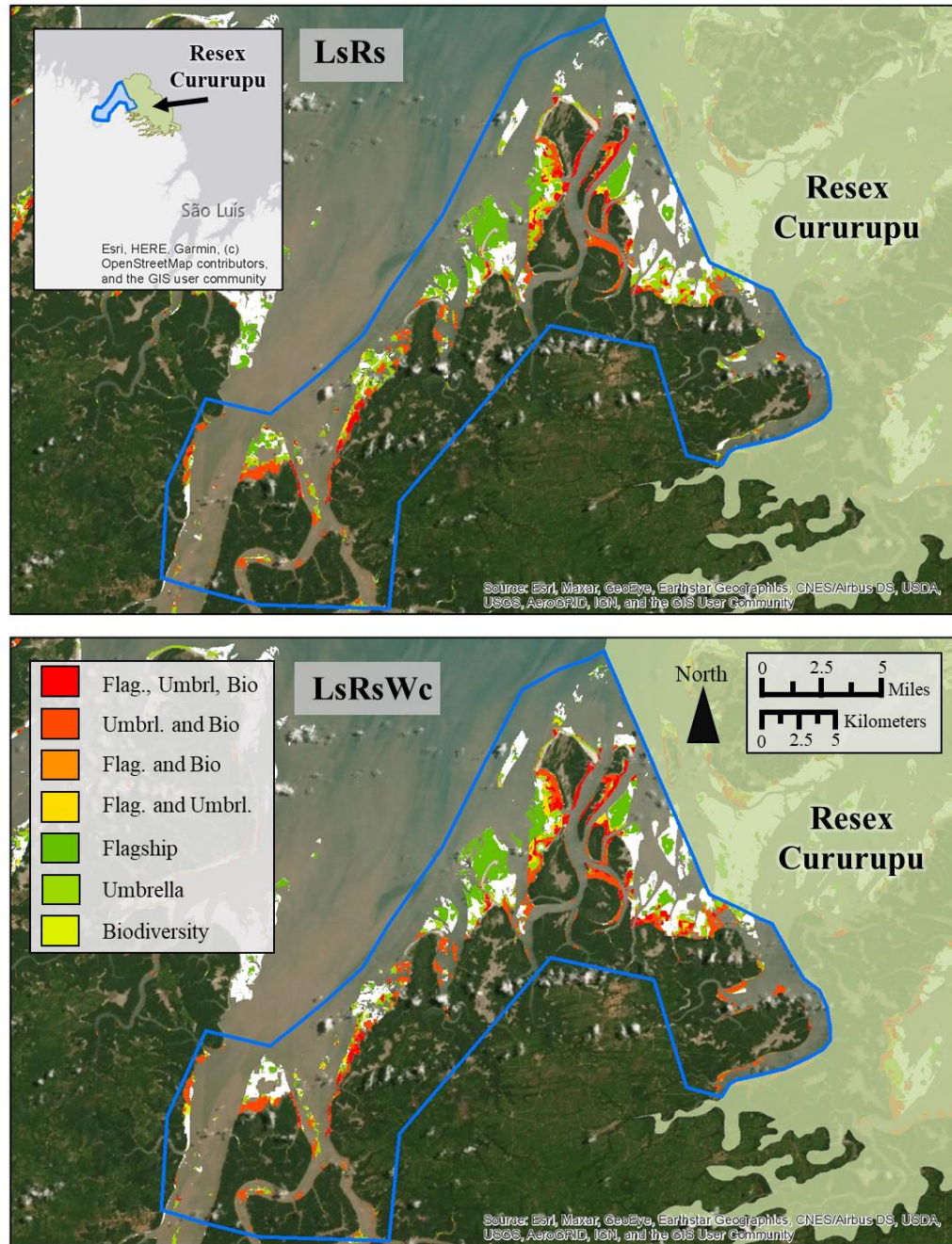


Figure 3.9: The potential conservation zone adjacent to the existing marine extractive reserve, Resex Cururupu, northeast of the state capital of Maranhão, São Luís. Conservation zones were identified by visual interpretation of overlaid coverage of flagship, umbrella, and biodiversity approaches to conservation. Areas in red are designated by flagship (“flag”), umbrella (“umbrl”), and biodiversity (bio) approaches. Dark orange are umbrella and biodiversity, light orange is flagship and biodiversity, and yellow is flagship and umbrella. Dark green, light green, and green-yellow represent pixels only designated as important by flagship, umbrella, and biodiversity approaches, respectively. Inset map in the bottom right shows approximate location of the conservation zone and Resex Cururupu.

Table 3.8: The top metric, area designated by flagship, is the breakdown of how much area of each potential conservation zone is considered habitat for the flagship red knot species by no models (None), landscape and remote sensing models only (LsRs), landscape, remote sensing, and WorldClim models only (LsRsWc), and by both models (Both). Area weighted richness is the species richness weighted by the area that each richness value occupies across the potential conservation zone. Species richness for each pixel was determined by overlaying the extent of species distributions based on either landscape and remote sensing models (LsRs), or landscape, remote sensing, and WorldClim models, then masking that coverage by the respective conservation zones.

		Baía do Cumã	Baía de São José	Resex Cururupu
Area Designated by Flagship (REKN)		Km ²	Km ²	Km ²
	None	29.96	81.28	62.93
	LsRs	3.34	8.86	3.97
	LsRsWc	0.97	0.00	5.12
	Both	1.21	0.04	25.85
Area Designated by Umbrella (SESA)	None	3.91	10.48	47.04
	LsRs	0.82	14.48	6.72
	LsRsWc	5.89	2.47	2.28
	Both	24.85	62.75	41.83
Area Designated by Biodiversity (Richness)	None	11.74	44.58	65.31
	LsRs	1.05	9.52	2.56
	LsRsWc	8.54	10.38	7.01
	Both	14.16	25.70	22.98
Area Weighted Richness	LsRs	3.84	3.81	2.65
	LsRsWc	4.71	3.55	2.95

Table 3.9: Percent of each potential conservation zone delineated by either model of each management scenario.

	Flagship	Umbrella	Biodiversity
Baía do Cumã	15.56%	88.97%	66.91%
Baía de São José	9.87%	88.38%	50.57%
Resex Cururupu	35.70%	51.93%	33.26%

Table 3.10: Co-occurrence matrix of species based on in-situ surveys. Numbers below represent how many presence points exist where both species were recorded, as well as how many points where *only* that species was recorded, what percentage of total presence points that consists of, and the total presence points for that species recorded during the field surveys. Data below includes both calibration data, and reserved validation data used in model development and evaluation.

All Surveys	BBPL	REKN	RUTU	SAND	SEPL	SESA	WHIM	WILL
BBPL	X	22	83	66	106	126	173	124
REKN	22	X	15	10	16	25	23	16
RUTU	83	15	X	22	64	68	104	58
SAND	66	10	22	X	42	46	39	15
SEPL	106	16	64	42	X	124	133	96
SESA	126	25	68	46	124	X	161	124
WHIM	173	23	104	39	133	161	X	169
WILL	124	16	58	15	96	124	169	X
Solo Presence Points	16	1	12	18	9	10	25	2
Percent Solo	7.4%	3.4%	8.8%	18.9%	5.0%	4.6%	8.4%	1.1%
Total Presence Points	216	29	136	95	179	216	299	184

Table 3.11: Presence records of each species associated with either mangroves or fiddler crabs. Associations were determined using qualitative habitat notes taken during surveys which indicated whether or not fiddler crab colonies or mangroves were adjacent to or incorporated in the survey area. Percent of each category represents what percent of the total number of recorded presence points were associated with either mangroves or crabs.

Mangroves	BBPL	REKN	RUTU	SAND	SEPL	SESA	WHIM	WILL
Mangrove Presences	32	2	24	10	16	22	49	22
Mangrove Percent	14.8%	6.9%	17.6%	10.5%	8.9%	10.2%	16.4%	12.0%
Crab Presences	28	2	11	3	13	30	40	35
Crab Percent	13.0%	6.9%	8.1%	3.2%	7.3%	13.9%	13.4%	19.0%
Total Presence Points	216	29	136	95	179	216	299	184

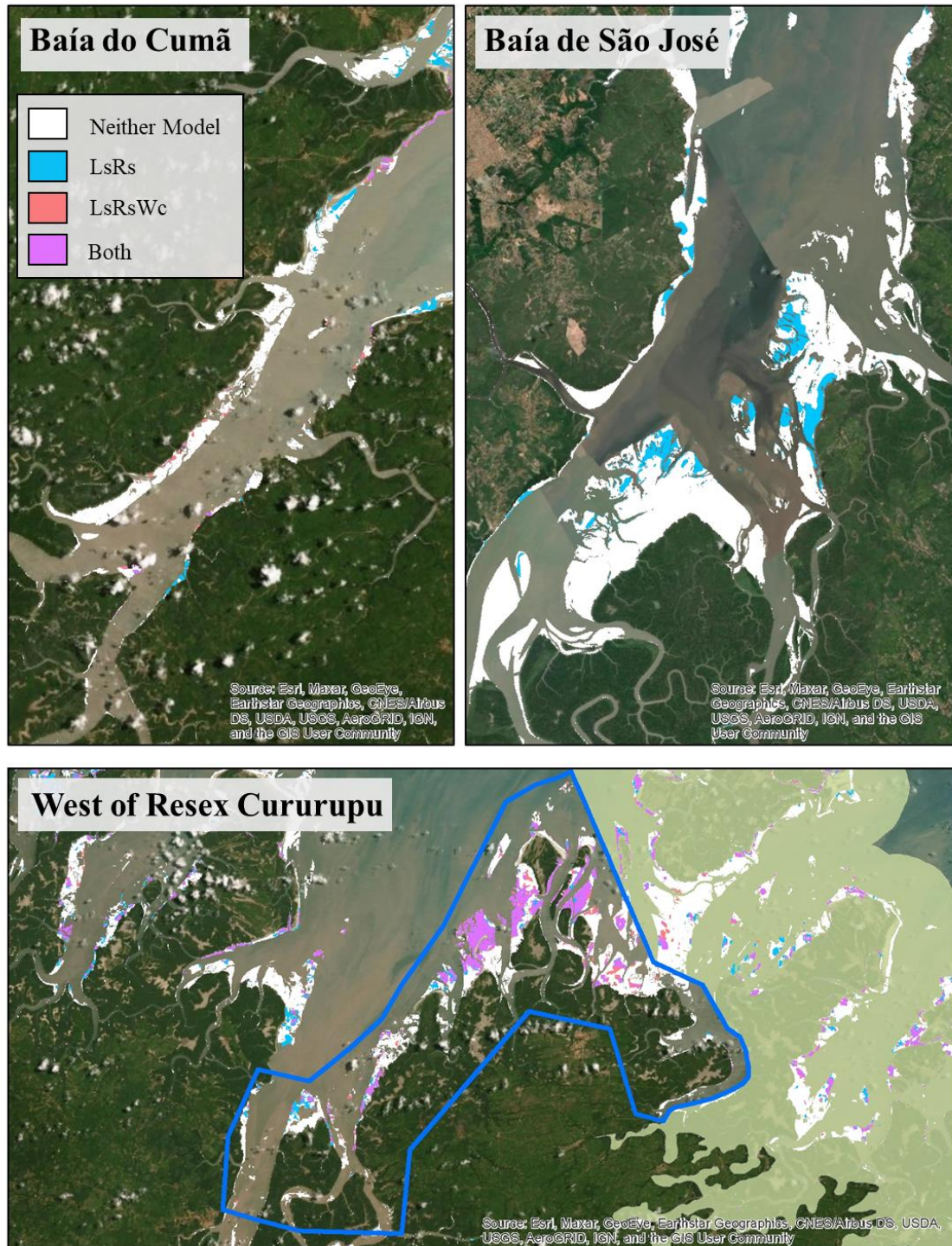


Figure 3.10: Extent of flagship red knot habitat predicted by neither model (white), LsRs models only (blue), LsRsWc models only (pink), and both models (purple).

Table 3.12: Coverage of species richness classes based on a hybrid flagship-biodiversity approach across the whole landscape. Weighted richness was calculated by multiplying the area of each richness category by the richness value, and dividing by the total intertidal area.

	Landscape	Hybrid (Flagship and Bio)	
Richness	Km ²	Km ²	Percent of Landscape
0	487.04		
1	276.06	103.59	38%
2	130.80	39.80	30%
3	100.50	23.20	23%
4	96.30	16.74	17%
5	96.86	96.86	100%
6	96.41	96.41	100%
7	43.94	43.94	100%
8	9.21	9.21	100%
Total	850.10	429.77	
Weighted Richness	1.99	4.10	

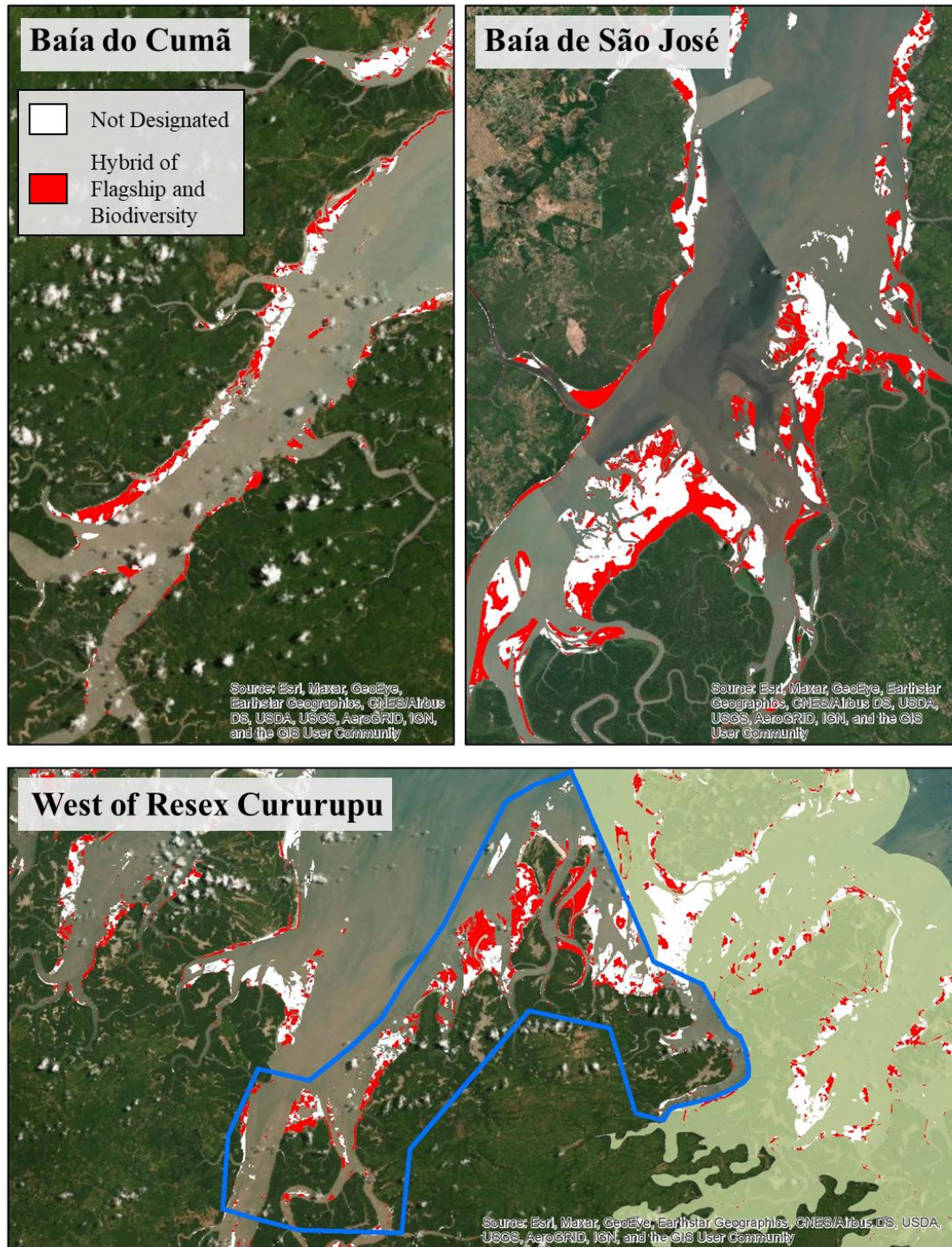


Figure 3.11: Coverage of prioritized habitat based on a hybrid flagship-biodiversity approach within selected potential conservation zones.

CONCLUSIONS

Previous research identified relationships between remote sensing metrics and intertidal sediment, while other work delineated broad extents of intertidal zone. I successfully accomplished both, delineating broad regions of intertidal habitat and characterizing the sediment within that habitat. Similar to previous research on remote sensing and intertidal sediment, I found that remote sensing consistently characterizes intertidal habitat within a location. Unlike previous research, I also found that the relationships between intertidal sediment and remote sensing response are not universal. One site's mud may be another site's sand, and, while we have some suggestions on why this may occur, more research is likely needed to fully understand this relationship. These results can inform future research and management of intertidal habitat across broad scales, from identifying changes in sediment due to beach filling, to utilization in habitat modeling.

Identifying which intertidal habitat characteristics predict shorebird distributions, and thus, where shorebirds can be found, is critical for conservation efforts across a migratory stop location, like northern Brazil. Based on the findings in Chapter 1, remote sensing metrics were successfully leveraged as proxies for intertidal sediment composition in Maxent species distribution models for eight shorebird species of conservation interest. The models, while not always demonstrating favorable internal metrics of modeling success, did consistently predict significantly different probabilities of presence when comparing presence and absence validation data. This discrepancy between internal metrics of model performance and external validation likely needs further investigation. Remote sensing variables contributed significantly to model performance, and models responded to the remote sensing metrics in ways consistent with known biology of the different shorebird species. Landscape variables often contributed significantly, but the biological significance of model response was sometimes vague. Climatic variables, often found to be highly influential in other studies, did have significant impacts on model function. However, the biological relevance of, for example, a few tenths of a degree difference is

somewhat suspect, particularly for such a climatically homogenous location like equatorial northern Brazil. Ultimately, novel remote sensing metrics, in conjunction with other conventional environmental variables, successfully distinguished between habitat (presence) and non-habitat for eight migratory shorebird species of conservation concern across a large, geographically complex region of intertidal habitat. The distributions models are useful for both identifying important habitat at a crucial stopover along the Western Atlantic Flyway, but also demonstrated methods that are easily transferable to other migratory locations and flyways.

Identifying the extent of habitat is informative, but conservation efforts across such a large region need to be focused and directed. The lens that is used to guide that decision making can influence what conclusions are drawn and which areas are targeted for conservation. Northern Brazil already has an extensive Marine Extractive Reserve network, but how those reserves protect shorebird habitat was unclear. In Chapter 3, the distribution models developed and vetted during Chapter 2 were used to investigate the effect of changing conservation priorities, effectiveness of current protections, and identify important regions of shorebird habitat currently unprotected. Three planning approaches were used: flagship species using red knots, umbrella species using semipalmated plovers, and biodiversity prioritizing areas with relatively high species richness. In this context, the more parsimonious distribution models had similar results to those that used the questionable climatic variables. Each conservation approach had its strengths, with flagship species protecting the relatively rare red knots, umbrella species casting a wide shadow that protected a diverse community, and a biodiversity approach protecting just the species rich areas. However, the flagship approach failed to prioritize particularly diverse communities, and the umbrella and biodiversity perspectives did not sufficiently protect the relatively rare and red knots. A hybrid approach that used both flagship and biodiversity approaches ensured that both red knots and diverse communities could be sheltered. Based on these results, three distinct regions for potential conservation efforts were located outside of existing protected areas.

Results presented in this dissertation are designed to inform and direct shorebird conservation efforts within Northern Brazil, a critical link in the Western Atlantic Flyway (Niles and Cooper Ornithological Society 2008, Colwell 2010), though their applications are not geographically limited. With shorebird populations declining across the North American (Bart et al. 2007, Morrison et al. 2012), European (Stroud et al. 2004), and the Asian-Australasian flyways (Clemens et al. 2016), identifying critical shorebird habitat within stopover locations is a key step to protecting the at-risk species that use these flyways. The methods developed here can act as a framework for future conservation at these other locations, identifying important habitat and gaps in existing protections, using readily available or easily developed remote sensing and landscape environmental metrics at broad spatial scales. Shaping conservation decision making at key stopover locations, focusing flagship species while protecting biodiversity, can help prioritize the wellbeing of the particularly vulnerable species, like red knots and other shorebirds. With these species serving as indicators of global change (Piersma and Lindstrom 2004), it is important to develop management decision making tools that can address the breadth of threats to their critical intertidal foraging habitat; from hunting (Andres et al. 2011) to coastal development (Murray et al. 2015), to sea level rise (Galbraith et al. 2002).

APPENDICES

Below is a rough outline for running the Maxent distribution modeling package via the Amarel Computing Clusters at Rutgers University.

Access Amarel

- Amarel info: <https://oarc.rutgers.edu/resources/amarel/>
- GUI access: <https://ondemand.hpc.rutgers.edu>
 - Interactive access for starting Amarel desktop session and managing files

Load Maxent into Amarel

- Via OnDemand GUI, file folder transferred to “home/[username]/Maxent/App”

Load files into Amarel

- Input Tables
 - Via OnDemand GUI, new folder added, “home/[username]/Maxent/InputTables”
- Envi Rasters
 - Via OnDemand GUI, new folder added, “home/[username]/Maxent/Envi”
 - Note: rasters need to be in .ascii format to run on Maxent

Run Maxent

- Run an Amarel Desktop (interactive gui version) session
 - Interactive Apps → Amarel Desktop → Hours 12, Num cores 4, Gig of mem, 8, Partition (nothing)
- Once GUI is open, click on black box at top (MATE terminal) to open command line input
- Load Java
 - module load java/11.0.7
- Set working directory
 - cd Maxent/App/
- Run Maxent
 - ./maxent.sh
 - ****note**, it is possible to configure the Maxent package to run using more resources including RAM. That configuration process was done by someone other than myself. I would suggest contacting either your IT professional or the folks over at Amarel for help in this process if you want to maximize the run-speed of your models.
- Access outputs
 - Outputs will go to folder designated by use
 - Results must be downloaded to native drive to access results
 - Download via OnDemand GUI

BIBLIOGRAPHY

- Amici, V., M. Marcantonio, N. La Porta, and D. Rocchini. 2017. A multi-temporal approach in MaxEnt modelling: A new frontier for land use/land cover change detection. *Ecological Informatics* 40:40–49.
- Andelman, S. J., and W. F. Fagan. 2000. Umbrellas and flagships: Efficient conservation surrogates or expensive mistakes? *Proceedings of the National Academy of Sciences* 97:5954–5959.
- Anderson, A. M., S. Duijns, P. A. Smith, C. Friis, and E. Nol. 2019. Migration distance and body condition influence shorebird migration strategies and stopover decisions during southbound migration. *Frontiers in Ecology and Evolution* 7:251.
- Andrade, L. P., H. M. L. Silva-Andrade, R. M. Lyra-Neves, U. P. Albuquerque, and W. R. Telino-Júnior. 2016. Do artisanal fishers perceive declining migratory shorebird populations? *Journal of Ethnobiology and Ethnomedicine* 12.
- Andres, B. A., C. Gratto-Trevor, P. Hicklin, D. Mizrahi, R. G. Morrison, and P. A. Smith. 2012. Status of the semipalmated sandpiper. *Waterbirds* 35:146–148.
- Andres, B., P. Smith, R. I. G. Morrison, C. L. Gratto-Trevor, S. Brown, and C. Friis. 1 December 12. Population estimates of North American shorebirds, 2012. *Wader Study Group Bulletin* 119:178–194.
- Andres, B., R. C. Ydenberg, and D. B. Lank. 2011. Shorebird hunting in the Caribbean. Pages 11–15 *Western Hemisphere Shorebird Group: Fourth meeting*.
- Araujo, M., and M. New. 2007. Ensemble forecasting of species distributions. *Trends in Ecology & Evolution* 22:42–47.

- Backwell, P. R. Y., P. D. O'Hara, and J. H. Christy. 1998. Prey availability and selective foraging in shorebirds. *Animal Behaviour* 55:1659–1667.
- Baker, A. J., P. M. Gonzalez, T. Piersma, L. J. Niles, I. de Lima Serrano do Nascimento, P. W. Atkinson, N. A. Clark, C. D. T. Minton, M. K. Peck, and G. Aarts. 2004. Rapid population decline in red knots: fitness consequences of decreased refuelling rates and late arrival in Delaware Bay. *Proceedings of the Royal Society B: Biological Sciences* 271:875–882.
- Baker, M. C., and A. E. M. Baker. 1973. Niche Relationships Among Six Species of Shorebirds on Their Wintering and Breeding Ranges. *Ecological Monographs* 43:193–212.
- Bart, J., S. Brown, B. Harrington, and R. I. Guy Morrison. 2007. Survey trends of North American shorebirds: population declines or shifting distributions? *Journal of Avian Biology* 38:73–82.
- Bocher, P., F. Robin, J. Kojadinovic, P. Delaporte, P. Rousseau, C. Dupuy, and P. Bustamante. 2014. Trophic resource partitioning within a shorebird community feeding on intertidal mudflat habitats. *Journal of Sea Research* 92:115–124.
- Bouma, T. J., J. van Belzen, T. Balke, Z. Zhu, L. Airoidi, A. J. Blight, A. J. Davies, C. Galvan, S. J. Hawkins, S. P. G. Hoggart, J. L. Lara, I. J. Losada, M. Maza, B. Ondiviela, M. W. Skov, E. M. Strain, R. C. Thompson, S. Yang, B. Zanuttigh, L. Zhang, and P. M. J. Herman. 2014. Identifying knowledge gaps hampering application of intertidal habitats in coastal protection: Opportunities & steps to take. *Coastal Engineering* 87:147–157.
- Bradie, J., and B. Leung. 2017. A quantitative synthesis of the importance of variables used in MaxEnt species distribution models. *Journal of Biogeography* 44:1344–1361.

- Brown, S., C. Gratto-Trevor, R. Porter, E. L. Weiser, D. Mizrahi, R. Bentzen, M. Boldenow, R. Clay, S. Freeman, M.-A. Giroux, E. Kwon, D. B. Lank, N. Lecomte, J. Liebezeit, V. Loverti, J. Rausch, B. K. Sandercock, S. Schulte, P. Smith, A. Taylor, B. Winn, S. Yezerinac, and R. B. Lanctot. 2017. Migratory connectivity of Semipalmated Sandpipers and implications for conservation. *The Condor* 119:207–224.
- Burger, J. 1986. The Effect of Human Activity on Shorebirds in Two Coastal Bays in Northeastern United States. *Environmental Conservation* 13:123.
- Burger, J., S. A. Carlucci, C. W. Jeitner, and L. Niles. 2007. Habitat Choice, Disturbance, and Management of Foraging Shorebirds and Gulls at a Migratory Stopover. *Journal of Coastal Research* 23:1159.
- Burger, J., M. A. Howe, D. C. Hahn, and J. Chase. 1977. Effects of Tide Cycles on Habitat Selection and Habitat Partitioning by Migrating Shorebirds. *The Auk* 94:743–758.
- Burger, J., L. Niles, and K. E. Clark. 1997. Importance of beach, mudflat and marsh habitats to migrant shorebirds on Delaware Bay. *Biological Conservation* 79:283–292.
- Burger, J., and L. Niles. 2013. Shorebirds and stakeholders: Effects of beach closure and human activities on shorebirds at a New Jersey coastal beach. *Urban Ecosystems* 16:657–673.
- Burger, J., and L. Niles. 2017. Shorebirds, Stakeholders, and Competing Claims to the Beach and Intertidal Habitat in Delaware Bay, New Jersey, USA. *Natural Science* 09:181–205.
- Burger, J., L. J. Niles, R. R. Porter, A. D. Dey, S. Koch, and C. Gordon. 2012. Migration and Over-Wintering of Red Knots (*Calidris canutus rufa*) along the Atlantic Coast of the United States. *The Condor* 114:302–313.

- Burger, J., L. Niles, C. Jeitner, and M. Gochfeld. 2018. Habitat risk: Use of intertidal flats by foraging red knots (*Calidris canutus rufa*), ruddy turnstones, (*Arenaria interpres*), semipalmated sandpipers (*Calidris pusilla*), and sanderling (*Calidris alba*) on Delaware Bay beaches. *Environmental Research* 165:237–246.
- Cao, Y., R. E. DeWalt, J. L. Robinson, T. Tweddale, L. Hinz, and M. Pessino. 2013. Using Maxent to model the historic distributions of stonefly species in Illinois streams: The effects of regularization and threshold selections. *Ecological Modelling* 259:30–39.
- Caro, T. M., and G. O’Doherty. 1999. On the Use of Surrogate Species in Conservation Biology. *Conservation Biology* 13:805–814.
- Clemens, R., D. I. Rogers, B. D. Hansen, K. Gosbell, C. D. T. Minton, P. Straw, M. Bamford, E. J. Woehler, D. A. Milton, M. A. Weston, B. Venables, D. Wellet, C. Hassell, B. Rutherford, K. Onton, A. Herrod, C. E. Studds, C.-Y. Choi, K. L. Dhanjal-Adams, N. J. Murray, G. A. Skilleter, and R. A. Fuller. 2016. Continental-scale decreases in shorebird populations in Australia. *Emu - Austral Ornithology* 116:119–135.
- Colwell, M. A. 2010. *Shorebird ecology, conservation, and management*. University of California Press, Berkeley.
- Colwell, M. A., and S. L. Landrum. 1993. Nonrandom Shorebird Distribution and Fine-Scale Variation in Prey Abundance. *The Condor* 95:94–103.
- D.A. Stroud, N. C. Davidson, R. West, D. A. Scott, L. Haanstra, O. Thorup, B. Ganter, and S. Delany. 2004. Status of migratory wader populations in Africa and Western Eurasia in the 1990s. *International Wader Studies* 15:1–259.
- De Moura, R. L., C. V. Minte-Vera, I. B. Curado, R. B. Francini-Filho, H. D. C. L. Rodrigues, G. F. Dutra, D. C. Alves, and F. J. B. Souto. 2009. Challenges and Prospects of Fisheries

- Co-Management under a Marine Extractive Reserve Framework in Northeastern Brazil. *Coastal Management* 37:617–632.
- Dhanjal-Adams, K. L., J. O. Hanson, N. J. Murray, S. R. Phinn, V. R. Wingate, K. Mustin, J. R. Lee, J. R. Allan, J. L. Cappadonna, C. E. Studds, R. S. Clemens, C. M. Roelfsema, and R. A. Fuller. 2016. The distribution and protection of intertidal habitats in Australia. *Emu* 116:208.
- Diefenbach, D. R., D. W. Brauning, and J. A. Mattice. 2003. VARIABILITY IN GRASSLAND BIRD COUNTS RELATED TO OBSERVER DIFFERENCES AND SPECIES DETECTION RATES. *The Auk* 120:1168.
- Dube, T. 2012. Primary productivity of intertidal mudflats in the Wadden Sea: a remote sensing method. University of Twente.
- Egbert, G. D., and S. Y. Erofeeva. 2002. Efficient Inverse Modeling of Barotropic Ocean Tides. *Journal of Atmospheric and Oceanic Technology* 19:183–204.
- Elith, J., and J. R. Leathwick. 2009. Species Distribution Models: Ecological Explanation and Prediction Across Space and Time. *Annual Review of Ecology, Evolution, and Systematics* 40:677–697.
- Elith, J., S. J. Phillips, T. Hastie, M. Dudík, Y. E. Chee, and C. J. Yates. 2011. A statistical explanation of MaxEnt for ecologists: Statistical explanation of MaxEnt. *Diversity and Distributions* 17:43–57.
- Elith*, J., C. H. Graham*, R. P. Anderson, M. Dudík, S. Ferrier, A. Guisan, R. J. Hijmans, F. Huettmann, J. R. Leathwick, and A. Lehmann. 2006. Novel methods improve prediction of species' distributions from occurrence data. *Ecography* 29:129–151.

- Emlen, J. M. 1966. The Role of Time and Energy in Food Preference. *The American Naturalist* 100:611–617.
- Erwin, R. M. 1996. Dependence of Waterbirds and Shorebirds on Shallow-Water Habitats in the Mid-Atlantic Coastal Region: An Ecological Profile and Management Recommendations. *Estuaries* 19:213.
- Essink, K. 1999. Ecological effects of dumping of dredged sediments; options for management. *Journal of Coastal Conservation* 5:69–80.
- FAO. 2014. World reference base for soil resources 2014: international soil classification system for naming soils and creating legends for soil maps. FAO, Rome.
- Faria, F. A., E. F. Albertoni, and L. Bugoni. 2018. Trophic niches and feeding relationships of shorebirds in southern Brazil. *Aquatic Ecology* 52:281–296.
- Fick, S. E., and R. J. Hijmans. 2017. WorldClim 2: new 1-km spatial resolution climate surfaces for global land areas. *International Journal of Climatology* 37:4302–4315.
- Folmer, E. O., H. Olf, and T. Piersma. 2010. How well do food distributions predict spatial distributions of shorebirds with different degrees of self-organization? *Journal of Animal Ecology*.
- Franklin, J., and J. A. Miller. 2009. Mapping species distributions: spatial inference and prediction. Cambridge University Press, Cambridge ; New York.
- Gade, M., S. Melchionna, K. Stelzer, and J. Kohlus. 2014. Multi-frequency SAR data help improving the monitoring of intertidal flats on the German North Sea coast. *Estuarine, Coastal and Shelf Science* 140:32–42.
- Galbraith, H., D. W. DesRochers, S. Brown, and J. M. Reed. 2014. Predicting vulnerabilities of North American shorebirds to climate change. *PLoS One* 9:e108899.

- Galbraith, H., R. Jones, R. Park, J. Clough, S. Herrod-Julius, B. Harrington, and G. Page. 2002. Global Climate Change and Sea Level Rise: Potential Losses of Intertidal Habitat for Shorebirds. *Waterbirds* 25:173.
- Gavin, M., J. McCarter, F. Berkes, A. Mead, E. Sterling, R. Tang, and N. Turner. 2018. Effective Biodiversity Conservation Requires Dynamic, Pluralistic, Partnership-Based Approaches. *Sustainability* 10:1846.
- Golicher, D., A. Ford, L. Cayuela, and A. Newton. 2012. Pseudo-absences, pseudo-models and pseudo-niches: pitfalls of model selection based on the area under the curve. *International Journal of Geographical Information Science* 26:2049–2063.
- Gratto-Trevor, C., R. I. G. Morrison, D. Mizrahi, D. B. Lank, P. Hicklin, and A. L. Spaans. 2012. Migratory Connectivity of Semipalmated Sandpipers: Winter Distribution and Migration Routes of Breeding Populations. *Waterbirds* 35:83–95.
- Guisan, A., and N. E. Zimmermann. 2000. Predictive habitat distribution models in ecology. *Ecological Modelling* 135:147–186.
- Harris, I., P. D. Jones, T. J. Osborn, and D. H. Lister. 2014. Updated high-resolution grids of monthly climatic observations - the CRU TS3.10 Dataset: UPDATED HIGH-RESOLUTION GRIDS OF MONTHLY CLIMATIC OBSERVATIONS. *International Journal of Climatology* 34:623–642.
- Herman, P. M. J., J. J. Middelburg, J. Van De Koppel, and C. H. R. Heip. 1999. Ecology of Estuarine Macrobenthos. Pages 195–240 *Advances in Ecological Research*. Elsevier.
- Hirzel, A. H., and G. Le Lay. 2008. Habitat suitability modelling and niche theory. *Journal of Applied Ecology* 45:1372–1381.

- Holmes, I., K. McLaren, and B. Wilson. 2015. Niche modeling for management-ready information in little-studied, threatened frog species assemblages. *Journal for Nature Conservation* 28:26–34.
- Howell, C. A., and S. D. Veloz. (n.d.). Priority Areas for Breeding Birds within the Planning Area of the Desert Renewable Energy Conservation Plan.
- Illera, J. C., H. Von Wehrden, and J. Wehner. 2010. Nest site selection and the effects of land use in a multi-scale approach on the distribution of a passerine in an island arid environment. *Journal of Arid Environments* 74:1408–1412.
- Iwamura, T., H. P. Possingham, I. Chadès, C. Minton, N. J. Murray, D. I. Rogers, E. A. Treml, and R. A. Fuller. 2013. Migratory connectivity magnifies the consequences of habitat loss from sea-level rise for shorebird populations. *Proceedings of the Royal Society B: Biological Sciences* 280:20130325.
- Jaffe, B. E., R. E. Smith, and A. C. Foxgrover. 2007. Anthropogenic influence on sedimentation and intertidal mudflat change in San Pablo Bay, California: 1856–1983. *Estuarine, Coastal and Shelf Science* 73:175–187.
- Jensen, J. R. 2007. Remote sensing of the environment: an earth resource perspective. 2nd ed. Pearson Prentice Hall, Upper Saddle River, NJ.
- Jourdan, C., J. Fort, D. Pinaud, P. Delaporte, J. Gernigon, N. Lachaussée, J.-C. Lemesle, C. Pignon-Mussaud, P. Pineau, F. Robin, P. Rousseau, and P. Bocher. 2021. Nycthemeral Movements of Wintering Shorebirds Reveal Important Differences in Habitat Uses of Feeding Areas and Roosts. *Estuaries and Coasts*.

- Kéry, M., and J. A. Royle. 2016. Applied hierarchical modeling in ecology: analysis of distribution, abundance and species richness in R and BUGS. Elsevier/AP, Academic Press is an imprint of Elsevier, Amsterdam ; Boston.
- Kober, K., and F. Bairlein. 2006. Shorebirds of the Bragantinian Peninsula I. Prey Availability and Shorebird Consumption at a Tropical Site in Northern Brazil. *Ornitologia Neotropical* 17:531–548.
- Kober, K., and F. Bairlein. 2009. Habitat Choice and Niche Characteristics Under Poor Food Conditions. A Study on Migratory Nearctic Shorebirds in the Intertidal Flats of Brazil. *Ardea* 97:31–42.
- Lathrop, R. G., L. Niles, P. Smith, M. Peck, A. Dey, R. Sacatelli, and J. Bognar. 2018. Mapping and modeling the breeding habitat of the Western Atlantic Red Knot (*Calidris canutus rufa*) at local and regional scales. *The Condor* 120:650–665.
- Latif, Q. S., V. A. Saab, J. G. Dudley, and J. P. Hollenbeck. 2013. Ensemble modeling to predict habitat suitability for a large-scale disturbance specialist. *Ecology and evolution* 3:4348–4364.
- Leyrer, J., B. Spaans, M. Camara, and T. Piersma. 2006. Small home ranges and high site fidelity in red knots (*Calidris c. canutus*) wintering on the Banc d'Arguin, Mauritania. *Journal of Ornithology* 147:376–384.
- Lunardi, V. O., R. H. Macedo, J. P. Granadeiro, and J. M. Palmeirim. 2012. Migratory flows and foraging habitat selection by shorebirds along the northeastern coast of Brazil: The case of Baía de Todos os Santos. *Estuarine, Coastal and Shelf Science* 96:179–187.
- MacArthur, R. H., and E. R. Pianka. 1966. On Optimal Use of a Patchy Environment. *The American Naturalist* 100:603–609.

- MacIntyre, H. L., R. J. Geider, and D. C. Miller. 1996. Microphytobenthos: The Ecological Role of the “Secret Garden” of Unvegetated, Shallow-Water Marine Habitats. I. Distribution, Abundance and Primary Production. *Estuaries* 19:186.
- Martín, B., S. Delgado, A. De la Cruz, S. Tirado, and M. Ferrer. 2015. Effects of human presence on the long-term trends of migrant and resident shorebirds: evidence of local population declines. *Animal Conservation* 18:73–81.
- Martinuzzi, S., W. A. Gould, and O. M. Ramos Gonzalez. 2007. Creating Cloud-Free Landsat ETM+ Data Sets In Tropical Landscapes: Cloud and Cloud-Shadow Removal. U.S. Department of Agriculture, Forest Service, International Institute of Tropical Forestry.
- Meir, E., S. Andelman, and H. P. Possingham. 2004. Does conservation planning matter in a dynamic and uncertain world? *Ecology Letters* 7:615–622.
- Mikhail, E. M., J. S. Bethel, and J. C. McGlone. 2001. Introduction to modern photogrammetry. John Wiley & Sons, New York.
- Millennium Ecosystem Assessment (Program), editor. 2005. Ecosystems and human well-being: synthesis. Island Press, Washington, DC.
- Mizrahi, D. S., K. A. Peters, and P. A. Hodgetts. 2012. Energetic Condition of Semipalmated and Least Sandpipers during Northbound Migration Staging Periods in Delaware Bay. *Waterbirds* 35:135–145.
- Morrison, R. I. G., D. S. Mizrahi, R. K. Ross, O. H. Ottema, N. de Pracontal, and A. Narine. 2012. Dramatic Declines of Semipalmated Sandpipers on their Major Wintering Areas in the Guianas, Northern South America. *Waterbirds: The International Journal of Waterbird Biology* 35:120–134.

- Mu, T., and D. S. Wilcove. 2020. Upper tidal flats are disproportionately important for the conservation of migratory shorebirds. *Proceedings of the Royal Society B: Biological Sciences* 287:20200278.
- Murray, N. J., R. S. Clemens, S. R. Phinn, H. P. Possingham, and R. A. Fuller. 2014. Tracking the rapid loss of tidal wetlands in the Yellow Sea. *Frontiers in Ecology and the Environment* 12:267–272.
- Murray, N. J., and R. A. Fuller. 2015. Protecting stopover habitat for migratory shorebirds in East Asia. *Journal of Ornithology* 156:217–225.
- Murray, N. J., Z. Ma, and R. A. Fuller. 2015. Tidal flats of the Yellow Sea: A review of ecosystem status and anthropogenic threats: Status of Yellow Sea tidal flats. *Austral Ecology* 40:472–481.
- Murray, N. J., S. R. Phinn, M. DeWitt, R. Ferrari, R. Johnston, M. B. Lyons, N. Clinton, D. Thau, and R. A. Fuller. 2019. The global distribution and trajectory of tidal flats. *Nature* 565:222–225.
- Murray, N., S. Phinn, R. Clemens, C. Roelfsema, and R. Fuller. 2012. Continental Scale Mapping of Tidal Flats across East Asia Using the Landsat Archive. *Remote Sensing* 4:3417–3426.
- Myers, N., R. A. Mittermeier, C. G. Mittermeier, G. A. B. da Fonseca, and J. Kent. 2000. Biodiversity hotspots for conservation priorities. *Nature* 403:853–858.
- Nagendra, H., R. Lucas, J. P. Honrado, R. H. G. Jongman, C. Tarantino, M. Adamo, and P. Mairota. 2013. Remote sensing for conservation monitoring: Assessing protected areas, habitat extent, habitat condition, species diversity, and threats. *Ecological Indicators* 33:45–59.

- Navedo, J. G., C. Verdugo, I. A. Rodríguez-Jorquera, J. M. Abad-Gómez, C. G. Suazo, L. E. Castañeda, V. Araya, J. Ruiz, and J. S. Gutiérrez. 2019. Assessing the effects of human activities on the foraging opportunities of migratory shorebirds in Austral high-latitude bays. *PLOS ONE* 14:e0212441.
- Niles, L. and Cooper Ornithological Society, editors. 2008. Status of the red knot (*Calidris canutus rufa*) in the Western Hemisphere. Cooper Ornithological Society, Camarillo, CA.
- Niles, L. J., J. Burger, R. R. Porter, A. D. Dey, C. D. Minton, P. M. González, A. J. Baker, J. W. Fox, and C. Gordon. 2010. First results using light level geolocators to track Red Knots in the Western Hemisphere show rapid and long intercontinental flights and new details of migration pathways. *Wader Study Group Bulletin* 117:123–130.
- Niles, L. J., J. A. M. Smith, D. F. Daly, T. Dillingham, W. Shadel, A. D. Dey, M. S. Danihel, S. Hafner, and D. Wheeler. 2013. Restoration of Horseshoe Crab and Migratory Shorebird Habitat on Five Delaware Bay Beaches Damaged by Superstorm Sandy.
- von Numers, S., M. Öst, and M. von Numers. 2020. Population changes in the declining Turnstone (*Arenaria interpres*) and other waders in the northern Baltic Sea based on past and current breeding observations. *Ornis Fennica* 97:149–164.
- Nybakken, J. W., and M. D. Bertness. 2005. *Marine biology: an ecological approach*. 6th ed. Pearson/Benjamin Cummings, San Francisco.
- Ottema, O. H., and A. L. Spaans. 2008. Challenges and advances in shorebird conservation in the Guianas, with a focus on Suriname. *Ornitologia Neotropical* 19:339–346.
- Peterson, C. H., M. J. Bishop, G. A. Johnson, L. M. D’Anna, and L. M. Manning. 2006. Exploiting beach filling as an unaffordable experiment: Benthic intertidal impacts

- propagating upwards to shorebirds. *Journal of Experimental Marine Biology and Ecology* 338:205–221.
- Pfister, C., B. A. Harrington, and M. Lavine. 1992. The impact of human disturbance on shorebirds at a migration staging area. *Biological Conservation* 60:115–126.
- Philippe, A. S., D. Pinaud, M.-L. Cayatte, C. Goulevant, N. Lachaussée, P. Pineau, M. Karpytchev, and P. Bocher. 2016. Influence of environmental gradients on the distribution of benthic resources available for shorebirds on intertidal mudflats of Yves Bay, France. *Estuarine, Coastal and Shelf Science* 174:71–81.
- Phillips, S. J., M. Dudík, and R. E. Schapire. 2004. A maximum entropy approach to species distribution modeling. Page 83. ACM Press.
- Phillips, S. J., R. P. Anderson, and R. E. Schapire. 2006. Maximum entropy modeling of species geographic distributions. *Ecological Modelling* 190:231–259.
- Phillips, S. J., and M. Dudík. 2008. Modeling of species distributions with Maxent: new extensions and a comprehensive evaluation. *Ecography* 31:161–175.
- Phillips, S. J., M. Dudík, J. Elith, C. H. Graham, A. Lehmann, J. Leathwick, and S. Ferrier. 2009. Sample selection bias and presence-only distribution models: implications for background and pseudo-absence data. *Ecological Applications* 19:181–197.
- Piersma, T., and Å. Lindström. 2004. Migrating shorebirds as integrative sentinels of global environmental change: Shorebirds integrate global environmental information. *Ibis* 146:61–69.
- Pollock, L. J., R. Tingley, W. K. Morris, N. Golding, R. B. O’Hara, K. M. Parris, P. A. Vesk, and M. A. McCarthy. 2014. Understanding co-occurrence by modelling species

- simultaneously with a Joint Species Distribution Model (JSDM). *Methods in Ecology and Evolution* 5:397–406.
- Rainey, M. P., A. N. Tyler, D. J. Gilvear, R. G. Bryant, and P. McDonald. 2003. Mapping intertidal estuarine sediment grain size distributions through airborne remote sensing. *Remote Sensing of Environment* 86:480–490.
- Rodrigues, A. A. F. 2000. SEASONAL ABUNDANCE OF NEARTIC SHOREBIRDS IN THE GULF OF MARANHÃO, BRAZIL. *Journal of Field Ornithology* 71:665–675.
- Riera, P., L. J. Stal, and J. Nieuwenhuize. 2000. Heavy $\delta^{15}\text{N}$ in Intertidal Benthic Algae and Invertebrates in the Scheldt Estuary (The Netherlands): Effect of River Nitrogen Inputs. *Estuarine, Coastal and Shelf Science* 51:365–372.
- Santos, C. Z., and A. Schiavetti. 2014. Assessment of the management in Brazilian Marine Extractive Reserves. *Ocean & Coastal Management* 93:26–36.
- Sheaves, M., L. Dingle, and C. Mattone. 2016. Biotic hotspots in mangrove-dominated estuaries: macro-invertebrate aggregation in unvegetated lower intertidal flats. *Marine Ecology Progress Series* 556:31–43.
- Shrader-Frechette, K. S., and E. D. McCoy. 1993. *Method in ecology: strategies for conservation*. Cambridge University Press, Cambridge [England] ; New York, NY, USA.
- Simberloff, D. 1998. Flagships, umbrellas, and keystones: Is single-species management passé in the landscape era? *Biological Conservation* 83:247–257.
- Smith, J. A. M., K. Regan, N. W. Cooper, L. Johnson, E. Olson, A. Green, J. Tash, D. C. Evers, and P. P. Marra. 2020. A green wave of saltmarsh productivity predicts the timing of the annual cycle in a long-distance migratory shorebird. *Scientific Reports* 10:20658.

- Stabach, J. A., N. Laporte, and W. Olupot. 2009. Modeling habitat suitability for Grey Crowned-cranes (*Balearica regulorum gibbericeps*) throughout Uganda. *International Journal of Biodiversity and Conservation* 1:177–186.
- Studds, C. E., B. E. Kendall, N. J. Murray, H. B. Wilson, D. I. Rogers, R. S. Clemens, K. Gosbell, C. J. Hassell, R. Jessop, D. S. Melville, D. A. Milton, C. D. T. Minton, H. P. Possingham, A. C. Riegen, P. Straw, E. J. Woehler, and R. A. Fuller. 2017. Rapid population decline in migratory shorebirds relying on Yellow Sea tidal mudflats as stopover sites. *Nature Communications* 8:14895.
- Tarr, N. M., T. R. Simons, and K. H. Pollock. 2010. An Experimental Assessment of Vehicle Disturbance Effects on Migratory Shorebirds. *Journal of Wildlife Management* 74:1776–1783.
- Thien, S. J. 1979. A flow diagram for teaching texture-by-feel analysis. *Journal of Agronomic Education* 8:54–55.
- Thrush, S., J. Hewitt, A. Norkko, P. Nicholls, G. Funnell, and J. Ellis. 2003. Habitat change in estuaries: predicting broad-scale responses of intertidal macrofauna to sediment mud content. *Marine Ecology Progress Series* 263:101–112.
- van der Wal, D., P. Herman, R. Forster, T. Ysebaert, F. Rossi, E. Knaeps, Y. Plancke, and S. Ides. 2008. Distribution and dynamics of intertidal macrobenthos predicted from remote sensing: response to microphytobenthos and environment. *Marine Ecology Progress Series* 367:57–72.
- van der Wal, D., and P. M. J. Herman. 2007. Regression-based synergy of optical, shortwave infrared and microwave remote sensing for monitoring the grain-size of intertidal sediments. *Remote Sensing of Environment* 111:89–106.

- van der Wal, D., P. M. J. Herman, and A. Wielemaker-van den Dool. 2005. Characterisation of surface roughness and sediment texture of intertidal flats using ERS SAR imagery. *Remote Sensing of Environment* 98:96–109.
- van Maren, D. S., T. van Kessel, K. Cronin, and L. Sittoni. 2015. The impact of channel deepening and dredging on estuarine sediment concentration. *Continental Shelf Research* 95:1–14.
- Warnock, N. 2010. Stopping vs. staging: the difference between a hop and a jump. *Journal of Avian Biology* 41:621–626.
- Warnock, S. E., and J. Y. Takekawa. 2008. Wintering site fidelity and movement patterns of Western Sandpipers *Calidris mauri* in the San Francisco Bay estuary. *Ibis* 138:160–167.
- Wickham, H. 2016. *ggplot2: Elegant Graphics for Data Analysis*. 2nd ed. 2016. Springer International Publishing : Imprint: Springer, Cham.
- Widdows, J., S. Brown, M. D. Brinsley, P. N. Salkeld, and M. Elliott. 2000. Temporal changes in intertidal sediment erodability: influence of biological and climatic factors. *Continental Shelf Research* 20:1275–1289.
- Wilcove, D. 1993. Getting Ahead of the Extinction Curve. *Ecological Applications* 3:218–220.
- Williams, K. K., and R. Greeley. 2004. Laboratory and field measurements of the modification of radar backscatter by sand. *Remote Sensing of Environment* 89:29–40.
- Yackulic, C. B., R. Chandler, E. F. Zipkin, J. A. Royle, J. D. Nichols, E. H. Campbell Grant, and S. Veran. 2013. Presence-only modelling using MAXENT: when can we trust the inferences? *Methods in Ecology and Evolution* 4:236–243.

- Yamada, F., N. Kobayashi, Y. Shirakawa, Y. Watabe, S. Sassa, and A. Tamaki. 2012. Effects of Tide and River Discharge on Mud Transport on Intertidal Flat.
- Yates, M. G., A. R. Jones, S. McGroarty, and J. D. Goss-Custard. 1993. The Use of Satellite Imagery to Determine the Distribution of Intertidal Surface Sediments of The Wash, England. *Estuarine, Coastal and Shelf Science* 36:333–344.
- Zadrozny, B. 2004. Learning and evaluating classifiers under sample selection bias. Page 114 Twenty-first international conference on Machine learning - ICML '04. ACM Press, Banff, Alberta, Canada.
- Zwarts, L. 1988. Numbers and distribution of coastal waders in Guinea-Bissau. *Ardea* 76:42–55.
- Zwarts, L., and J. H. Wanink. 1993. How the food supply harvestable by waders in the Wadden Sea depends on the variation in energy density, body weight, biomass, burying depth and behaviour of tidal-flat invertebrates. *Netherlands Journal of Sea Research* 31:441–476.